In compliance with the
Canadian Privacy Legislation
some supporting forms
may have been removed from
this dissertation.

While these forms may be included
in the document page count,
their removal does not represent
any loss of content from the dissertation.

University of Alberta

Mismatch repair protein Msh2 protects mouse embryonic fibroblasts from UVB-induced DNA damage by facilitating apoptosis and p53 activation.

by

Anthea Carmen Peters

©

A thesis submitted to the Faculty of Graduate Studies and Research in partial fulfillment of the requirements for the degree of *Master of Science*

in

Medical Sciences – Medical Genetics

Edmonton, Alberta
Fall 2003

National Library of Canada
Acquisitions and Bibliographic Services
395 Wellington Street
Ottawa ON K1A 0N4
Canada

Bibliothèque nationale du Canada
Acquisisitons et services bibliographiques
395, rue Wellington
Ottawa ON K1A 0N4
Canada

Your file Votre référence
ISBN: 0-612-87860-0
Our file Notre référence
ISBN: 0-612-87860-0

The author has granted a non-exclusive licence allowing the National Library of Canada to reproduce, loan, distribute or sell copies of this thesis in microform, paper or electronic formats.

The author retains ownership of the copyright in this thesis. Neither the thesis nor substantial extracts from it may be printed or otherwise reproduced without the author's permission.

L'auteur a accordé une licence non exclusive permettant à la Bibliothèque nationale du Canada de reproduire, prêter, distribuer ou vendre des copies de cette thèse sous la forme de microfiche/film, de reproduction sur papier ou sur format électronique.

L'auteur conserve la propriété du droit d'auteur qui protège cette thèse. Ni la thèse ni des extraits substantiels de celle-ci ne doivent être imprimés ou aturement reproduits sans son autorisation.

Canadä

University of Alberta

Library Release Form

Name of Author: *Anthea Carmen Peters*

Title of Thesis: *Mismatch repair protein Msh2 protects mouse embryonic fibroblasts from UVB-induced DNA damage by facilitating apoptosis and p53 activation.*

Degree: *Master of Science*[1]

Year this Degree Granted: *2003*

Permission is hereby granted to the University of Alberta Library to reproduce single copies of this thesis and to lend or sell such copies for private, scholarly or scientific research purposes only.

The author reserves all other publication and other rights in association with the copyright in the thesis, and except as herein before provided, neither the thesis nor any substantial portion thereof may be printed or otherwise reproduced in any material form whatever without the author's prior written permission.

June 20, 2003

University of Alberta

Faculty of Graduate Studies and Research

The undersigned certify that they have read, and recommend to the Faculty of Graduate Studies and Research for acceptance, a thesis entitled **Mismatch repair protein Msh2 protects mouse embryonic fibroblasts from UVB-induced DNA damage by facilitating apoptosis and p53 activation** submitted by **Anthea Carmen Peters** in partial fulfillment of the requirements for the degree of **Master of Science in Medical Sciences - Medical Genetics**.

June 20, 2003
Date

Abstract

The DNA mismatch repair system, known for repairing DNA replication errors, has been recognized for performing an independent tumour suppressive role of facilitating apoptotic and cell cycle responses to several DNA adducts. Although not involved in post-UVB DNA repair, the MMR protein Msh2 binds directly to photoproducts, suggesting that it does play a role in post-UVB responses. Therefore I hypothesized that Msh2 is involved in facilitating post-UVB apoptosis. By comparing the responses of *Msh2*$^{+/+}$ and *Msh2*$^{-/-}$ mouse embryonic fibroblasts to UVB irradiation, I determined that Msh2 deficiency results in increased viability, increased clonogenic survival, and significantly reduced UVB-induced apoptosis. Furthermore, p53 phosphorylation on serine 15 is delayed or diminished in Msh2-deficient cells. *In vivo*, the absence of Msh2 results in increased rates of UVB-induced skin tumorigenesis. These data support a role for Msh2 in activating the apoptotic response to UVB-induced DNA damage and implicates MMR as a protector against UV-induced tumorigenesis.

Acknowledgements

I wish to thank Le Luong, Melanie Boskill, Gabi Constantinescu, Eugene Chomey, Kim Williams, and Dorothy Rutkowksi for their technical assistance, Brenda Roszell and the staff at HSLAS for their maintenance of the mouse colony, and the Andrew Lab for their collegiality and relaxed work environment. I also wish to thank Dr. Tomoko Maeda, Dr. Victor Tron, and Dr. Leah Young for their expertise and encouragement. Finally, I wish to thank Dr. Susan Andrew, for her support and her commitment to helping me finish my thesis, and for providing a strong female role model for myself and other young aspiring scientists.

Table of Contents

Introduction.....1

DNA Mismatch Repair.....6

MMR and apoptosis.....11

MMR and cell cycle.....19

The role of p53 in apoptosis facilitated by MMR.....20

The role of p73 in apoptosis facilitated by MMR.....23

UV Radiation.....24

UV-induced apoptosis.....29

The role of p53 in post-UVB apoptosis.....34

The role of MMR in post-UVB apoptosis.....35

Materials and Methods.....**43**

Msh2 Mouse Colony.....43

Cell Culture.....45

UV Irradiation.....45

Cell Viability Assay.....46

Colony Formation Assay.....47

Annexin V-FITC/PI Assay for Apoptosis.....47

SDS/PAGE gels / Western Blots.....48

DNA Photoproduct Slot Blot Southwestern.....49

Results.....**51**

Msh2 and Msh6 accumulate in response to UVB.....51

Msh2-deficient MEFs are capable of photoproduct repair.....53

Table of Contents continued

Msh2-deficiency in primary and transformed MEFs enhances cell survival post-UVB.....55

MEFs deficient in Msh2 undergo less post-UVB apoptosis than those that express Msh2.....57

Msh2-deficient primary and transformed MEFs display less caspase 3 and PARP cleavage than Msh2-proficient MEFs.....66

p53 activated by phosphorylation at serine 15 is more abundant in the presence than in the absence of Msh2.....68

p21 accumulates less in Msh2-deficient primary MEFs.....70

Msh2-deficient mice develop UVB-induced skin tumours more quickly than wild-type mice.....72

Discussion.....75

Future Directions.....111

References.....114

List of Tables

Table 1: Effects of MMR-deficiency on cytoxicity, apoptosis, and cell cycle arrest in response to various DNA damaging agents.....14

Table 2: DNA adducts to which MutSα specifically binds.....17

List of Figures

Figure 1: Outline of the DNA damage response signal transduction pathway.....2

Figure 2: Diagrams of the morphologies of a normal cell dying by either apoptosis or necrosis.....4

Figure 3: Two major pathways of apoptosis.....5

Figure 4: MMR functional heterodimers.....7

Figure 5: Biochemical pathway of human MMR 8

Figure 6: The role of p53 in cellular responses to DNA damage.....22

Figure 7: Ultraviolet light spectrum.....25

Figure 8: Structural models of the DNA adducts induced by UVB irradiation..26

Figure 9: Biochemical steps in the NER pathway.....28

Figure 10: Histological layers of human epidermal cells, stained with hematoxylin and eosin.....30

Figure 11: Three distinct pathways of UV-induced apoptosis.....32

Figure 12: Proposed model of MMR as general DNA damage sensor.....41

Figure 13: Sample PCR showing all possible genotypes of Msh2 mice.....44

Figure 14: Msh2 and Msh6 are upregulated in response to UVB in Msh2-proficient primary and transformed MEFs.....52

Figure 15: Both wild-type and Msh2-deficient MEFs are capable of repairing UVB-induced thymidine dimers.....54

Figure 16: Msh2-deficient primary MEFs exhibit increased survival post-UVB.....56

Figure 17: The absence of Msh2 in transformed MEFs enhances post-UVB clonogenic survival.....58

Figure 18: Msh2-deficient primary MEFs undergo less apoptosis than wild-type.....59

List of Figures continued

Figure 19: Msh2-deficiency confers significant resistance to UVB-induced apoptosis in primary MEFs.....61

Figure 20: Msh2-deficient transformed MEFs undergo less apoptosis than wild-type.....63

Figure 21: Msh2-deficiency confers significant resistance to UVB-induced apoptosis in transformed MEFs.....64

Figure 22: Msh2-deficient MEFs express less cleaved caspase 3 and less cleaved PARP than wild-type 67

Figure 23: p53 expression and activation by phosphorylation of serine 15 in primary and transformed MEFs post-UVB.....69

Figure 24: p21 expression in primary and transformed MEFs.....71

Figure 25: Kaplan-Meier survival curve showing skin tumour development for *Msh2*$^{+/+}$ and *Msh2*$^{-/-}$ mice after chronic doses of UVB.....73

List of Abbreviations

5-FU – 5-fluorouracil

6-4PP – 6-4 photoproduct

6-TG – 6-thioguanine

8-oxo-G – 8-oxoguanine

A - adenine

ATM – Ataxia Telangiectasia Mutated

ATR – AT - related

BCC – basal cell carcinoma

BCNU - 1,3-bis(2-chloro-ethyl)-1-nitrosourea

bp – base pair

C - cytosine

CS – Cockayne's Syndrome

CPD – cyclobutane pyrimidine dimer

FACScan – fluorescence activated cell scan

FBS – fetal bovine serum

G – guanine

GGR – global genome repair

HPV16 – human papilloma virus 16

HNPCC – hereditary non-polyposis colorectal cancer

IDL – insertion/deletion loop

IR – ionizing radiation

List of Abbreviations continued

J – Joules

kDa - kilodaltons

MED – minimum erythema dose

MEF – mouse embryonic fibroblast

MGMT - O^6-methylguanine-DNA methyltransferase

MMR – mismatch repair

MNNG - *N*-methyl-*N'*-nitro-*N*-nitrosoguanidine

MNU - *N*-methyl-*N*-nitrosourea

MSI – microsatellite instability

NER – nucleotide excision repair

NMSC – nonmelanoma skin cancer

O^6-meG - O^6-methylguanine

PAGE – polyacrylamide gel electrophoresis

PBS – phosphate buffered saline

PCR – polymerase chain reaction

PhIP - 2-amino-1-methyl-6-phenylimidazo [4,5-b] pyridine

PI – propidium iodide

ROS – reactive oxygen species

SBC – sunburn cells

SCC – squamous cell carcinoma

SDS – sodium dodecyl sulphate

ser – serine

List of Abbreviations continued

SV40 – simian virus 40

T – thymidine

TAg – T Antigen

TCR – transcription coupled repair

UV - ultraviolet

XP – xeroderma pigmentosum

Introduction

The maintenance of the integrity of a cell's genome is of the utmost importance to the cell's ability to maintain normal function and to accurately propagate. DNA damage may result from DNA polymerase errors, endogenous chemical changes of bases, such as spontaneous free radical damage and deaminations, as well as exogenous insults, therefore cells require a stringent DNA damage surveillance mechanism. When DNA damage is incurred, it activates a tightly regulated defense program that involves sensing the damage, growth cycle arrest to allow time for repair, or cell suicide to prevent propagation of mutagenic cells. The suicide mechanism, called apoptosis or programmed cell death, is presumably activated when the damage is extensive, and therefore is of vital importance to a multicellular organism in preventing the uncontrolled growth of a mutagenic cell and its tumorigenic progression. Although a reduction in DNA repair ability may create a high level of persistent damage and may therefore render a cell sensitive to apoptotic death, the loss or reduction in a cell's ability to apoptose in addition to a deficiency in DNA repair could lead to the persistence of cells accumulating DNA damage. Reduction in both DNA repair and apoptosis simultaneously would drastically accelerate the tumorigenic phenotype and inevitably lead to cancer (Bernstein et al., 2002; Rich et al., 2000) (Figure 1).

Apoptosis, an active mode of programmed cell death, allows an organism to safely eliminate unwanted or damaged cells; in contrast, necrosis, the alternate passive type of cell death, occurs only under pathological conditions. In normal

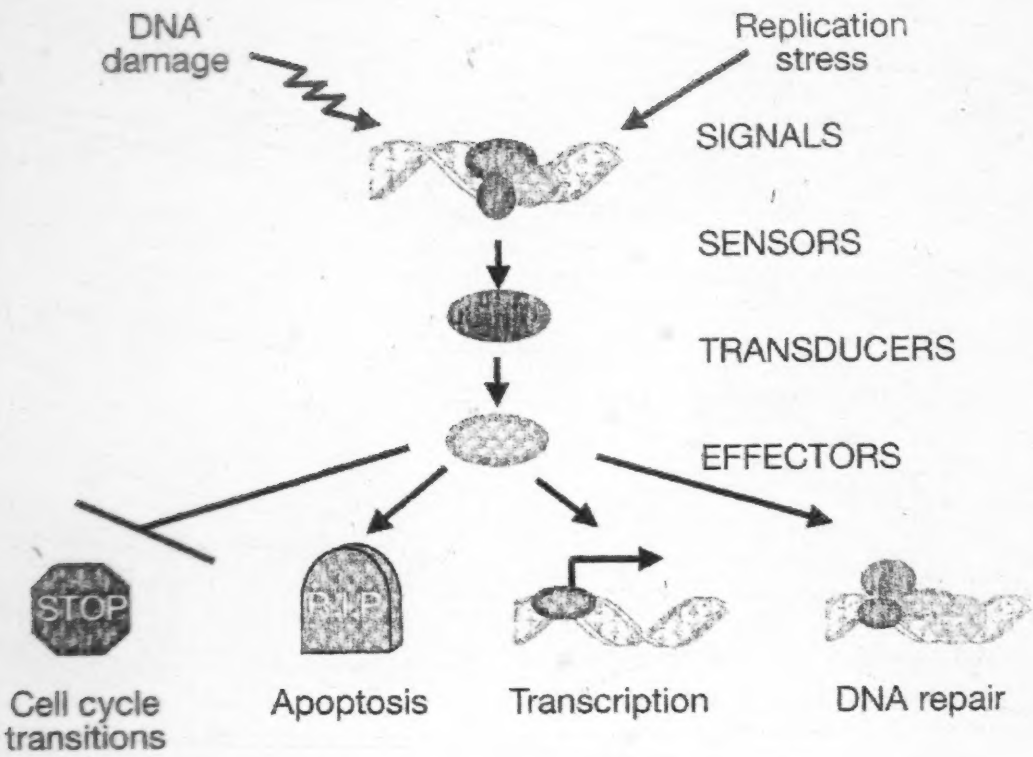

Figure 1. Outline of the DNA damage response signal transduction pathway (Zhou and Elledge, 2000).

cells a homeostatic balance exists between mitosis and apoptosis, and this balance may be disrupted in damaged tissue and malignancy. Because the process of apoptosis is under molecular control, its occurrence may be actively modulated; for this reason, it has captured the attention of many scientists, particularly in the field of cancer biology, since its discovery in 1972. Apoptosis is characterized by membrane blebbing, the condensation of chromatin and the progressive endonucleolytic cleavage of chromosomal DNA ultimately to approximately 200 base pair (bp) fragments, resulting in cell shrinkage and condensation into multiple small membrane-bound apoptotic bodies which are targets for phagocytosis (Gobé, 2000; Wu, 1999) (Figure 2).

Mammalian cells undergo two major pathways of apoptosis, depending on the stimulus (Figure 3). The death-receptor pathway is triggered by the binding of a specific ligand to a membrane-bound receptor of the death-receptor superfamily (such as CD95 and tumor necrosis factor receptor 1) (left pathway in Figure 3). Internal stress such as DNA damage stimulates the mitochondrial pathway (right pathway of Figure 3), which results in activation of a pro-apoptotic member of the Bcl-2 family; pro- and anti-apoptotic Bcl-2 family members form heterodimers in various combinations, where the ratio of pro- to anti-apoptotic members determines the amount of release of pro-apoptotic factors, such as cytochrome *c*, from the intermembrane space of the mitochondria. Cytochrome *c* then associates with Apaf-1 and procaspase-9 to form an apoptosome. Caspases are a highly conserved family of cysteine proteases considered to be the central executioners of apoptosis. They are synthesized in zymogen form and are activated by

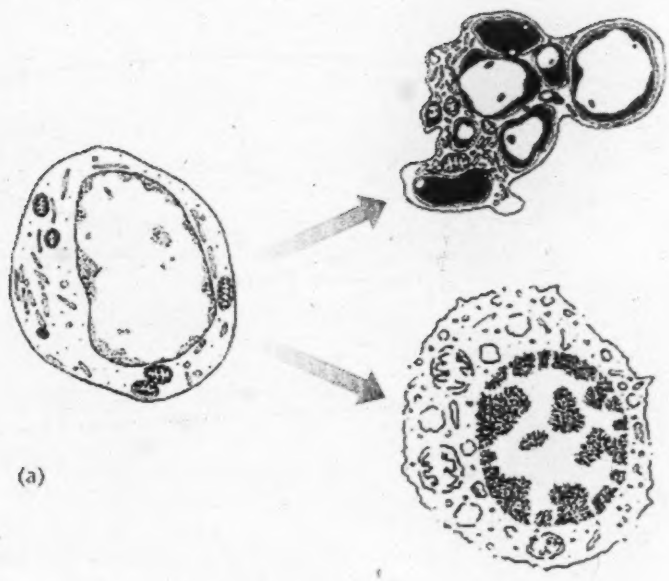

Figure 2. Morphologies of a normal cell (left) dying by either apoptosis (top right) or necrosis (bottom right). While the apoptotic cells undergoes shrinkage, blebbing, condensation of heterochromatin, maintenance of organelles, and development of membrane-bound apoptotic bodies, the necrotic cell displays swelling, disrupted organelles irregularly clumped heterochromatin and densities in the mitochondria (printed with permission from (Gobé, 2000)).

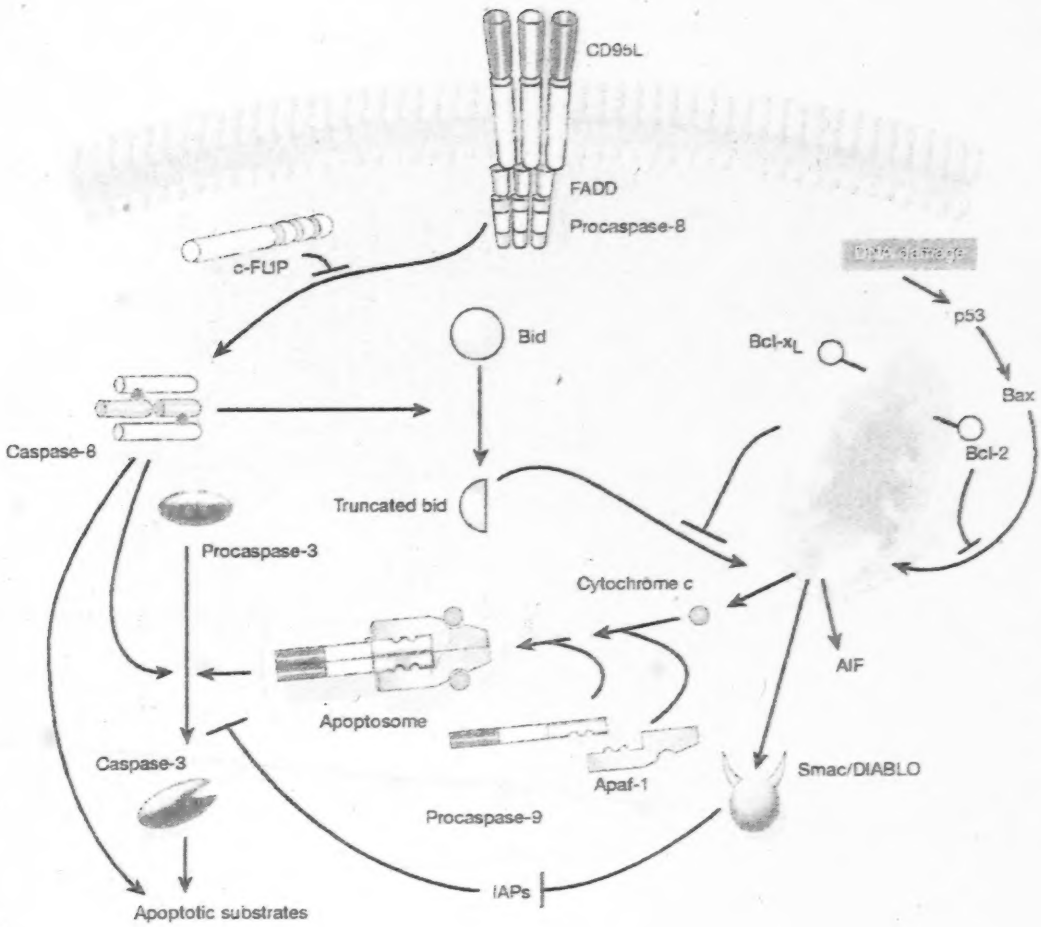

Figure 3. Two major pathways of apoptosis (Hengartner, 2000).

proteolytic cleavage, usually by a previously activated caspase upstream in the apoptotic pathway. Indeed, the apoptosome, which includes caspase 9, as well as caspase 8 of the death-receptor pathway, activate caspase 3, representing the convergence of the two pathways. Caspase 3 in turn activates effectors of apoptosis, such as caspase-activated DNase (CAD), the nuclease that fragments chromosomal DNA, resulting in the characteristic endpoints of apoptosis mentioned previously, such as nucleosomal fragmentation and formation of apoptotic bodies (Hengartner, 2000; Wu, 1999).

DNA Mismatch Repair. The mammalian DNA mismatch repair (MMR) system is well-known for its ability to repair mispaired bases and insertion/deletion loops (IDLs) during DNA replication and heteroduplexes during recombination. MMR consists of heterodimers hMutSα or hMutSβ (involving MSH2 paired with MSH3 or 6 respectively) that bind to mispairs and recruit hMutL (MLH1 paired with PMS2, PMS1, or MLH3) (Figure 4). The hMutS heterodimer that recognizes the mismatches depends on the nature of the mismatch, with MSH6 primarily recognizing base-base mismatches and 1-bp IDLs, and MSH3 recognizing and binding to IDLs larger than 1-bp but smaller than 12-bps, although their roles are partially redundant in the recognition of IDLs (Bellacosa, 2001; Peltomaki, 2001). Following mismatch recognition are less defined steps that involve the recruitment of exonucleases, helicases and PCNA for excision of the strand containing the mismatch, and finally resynthesis and ligation (Buermeyer et al., 1999) (Figure 5).

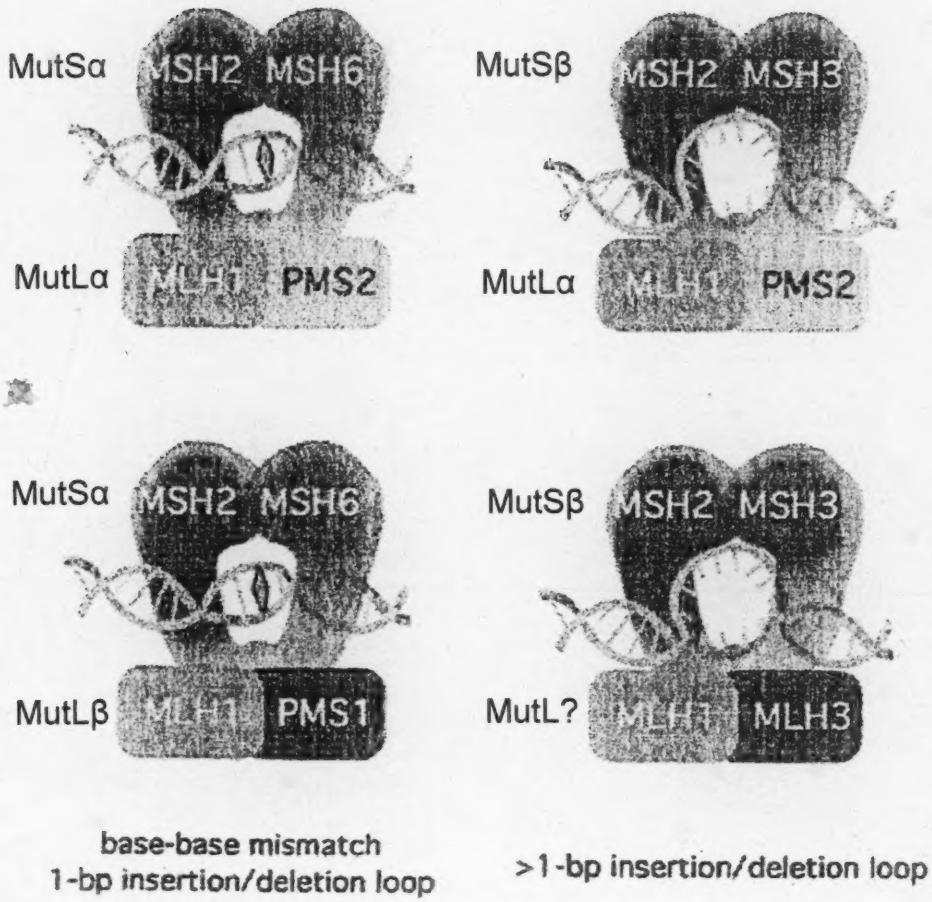

Figure 4. MMR functional heterodimers (adapted from (Bellacosa, 2001)).

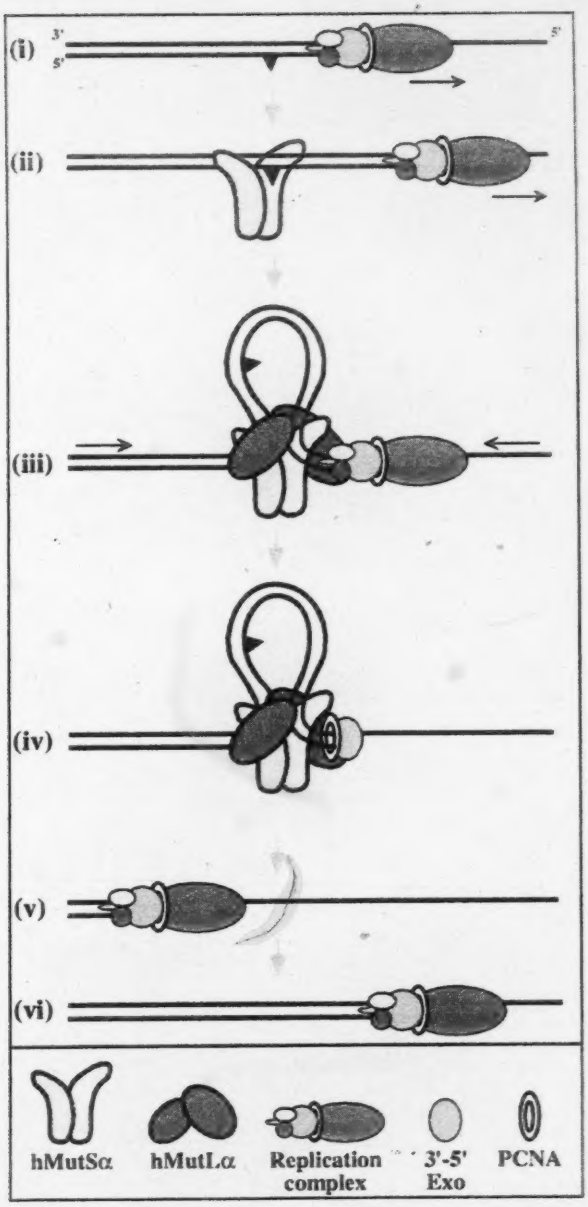

Figure 5. Biochemical pathway of human MMR (Jiricny, 1998). (i) The post-replicative mismatch, represented by a black triangle, has escaped proofreading by the replication complex. (ii) The mismatch is recognized by hMutSα, (iii) hMutLα is recruited, and the MMR complex is assembled in the presence of ATP, leading to replication arrest and dissociation of DNA polymerase. (iv) Exonucleolytic degradation of the strand containing the error occurs, (v) the MMR complex dissociates, PCNA recruits the replication complex, (vi) and DNA synthesis is re-initiated.

Testimony to the value of the MMR system in tumor suppression lies in the cancer-prone phenotype of individuals with Hereditary Non-Polyposis Colorectal Cancer (HNPCC), who carry heterozygous germline mutations of a component of the MMR machinery. Upon eventual loss of the second wild-type allele, individuals with such mutations develop colorectal cancers and adenocarcinoma of the endometrium, and less frequently cancers of the stomach, ovary, small bowel, pancreas, ureter and renal pelvis (Reitmair et al., 1996). Mutations in *MSH2* and *MLH1* are responsible for most HNPCC cases, while *MSH6*, *PMS2*, and *PMS1* are mutated less frequently, possibly indicating redundancy of their function (Peltomaki, 2001). Muir-Torr syndrome, characterized by skin neoplasms, particularly sebaceous tumors and keratoacanthomas, as well as internal malignancies (Reitmair et al., 1996), is also associated with mutations in *MSH2* or *MLH1*. In both HNPCC and Muir-Torr syndrome, it is thought that the loss of the second wild-type allele of an MMR gene (loss of heterozygosity) occurs as an early mutational event in tumor development, and the resultant lack of mismatch repair drives a rapid accumulation of mutations that, if situated within key oncogenes, tumor suppressor genes or growth regulation genes, result in tumorigenesis. Evidence to support this hypothesis has come from mutational studies demonstrating a 100-1000-fold hypermutability in the absence of MMR (Peltomaki, 2001). Secondary mutations have been identified in HNPCC colorectal tumours in key genes important in regulating cell growth, including those recognized as being involved in the multi-step pathway of colon tumorigenesis (e.g. *p53*, *KRAS*, and

adenomatous polyposis coli (*APC*)) (Peltomaki, 2001). Tumours arising from HNPCC and Muir-Torr patients as well as some sporadic tumors that lack expression of MSH2, MLH1, and other MMR genes, are characterized by microsatellite instability (MSI), the expansion or contraction of repetitive sequences in their DNA that is a hallmark of DNA polymerase slippage and lack of repair (Bocker et al., 1999). As a result, genes with mononucleotide repeats in their coding regions such as transforming growth factor β receptor II (*TGFβRII*), insulin-like growth factor II receptor (*IGFIIR*), the proapoptotic gene *BAX*, and the MMR genes *MSH3* and *MSH6*, are particularly susceptible to mutation with an MMR-deficient genotype (Peltomaki, 2001). For example, over 90% of HNPCC colorectal cancers carry an insertion or deletion mutation in the 10 bp polyadenine repeat within *TGFβRII*, suggesting that it is a critical mutational event in the etiology of colorectal cancer (Myeroff, 1995).

Mouse models bearing knockout mutations in MMR genes have proven to be a useful model for studying MMR defects and tumorigenesis. Unlike the human HNPCC disease phenotype, mice with heterozygous deficiencies in MMR genes are not predisposed to tumors and do not show decreased survival or fertility (Reitmair et al., 1995). However, mice bearing homozygous deficiencies of the mismatch repair genes *Msh2* or *Mlh1* are prone to MSI-positive intestinal tumours, lymphomas, skin tumours, and sarcomas (Marti et al., 2002). *Msh2*$^{-/-}$ mice are viable and fertile but almost invariably succumb to thymic lymphoma tumours between 2 and 12 months (Reitmair et al., 1995). There is an increased rate of intestinal carcinomas in mice that live past 8 months (Reitmair et al.,

1996). The MMR deficient mice are also susceptible to spontaneous skin neoplasms (about 7%), analogous to the human Muir-Torr syndrome (Reitmair et al., 1995). *Mlh1* deficiency in mice results in a phenotype very similar to that of *Msh2* deficiency, whereas *Msh6*$^{-/-}$ and *Pms2*$^{-/-}$ mice display lymphomas and epithelial tumors but are not prone to intestinal tumors and *Msh3*$^{-/-}$ are not cancer prone (Marti et al., 2002). *Msh3/Msh6* double knockout mice, however, do exhibit susceptibility to intestinal tumors (de Wind et al., 1999), confirming the partial functional redundancy of these two proteins (Marti et al., 2002).

Furthermore, mouse embryonic fibroblasts (MEFs) derived from the *Msh2*$^{-/-}$ and *Pms2*$^{-/-}$ mice develop a mutator phenotype, demonstrated as an elevated mutation rate both at the *HPRT* locus and using *lacI* and *supF* transgenes as reporter genes, similar to MMR-deficient human tumor cell lines (Andrew et al., 1997; Narayanan et al., 1997; Reitmair et al., 1997). Therefore, both increased mutation frequency and increased tumour susceptibility make mouse models of HNPCC extremely valuable tools for scientific investigation.

MMR and apoptosis. Current progress in cancer research is revealing several tumor suppressor proteins with dual roles in both DNA repair and apoptosis (Bernstein et al., 2002). MMR is gaining recognition for its role in signaling the presence of DNA damage to effectors of apoptosis and cell cycle arrest (Bellacosa, 2001). The use of DNA damaging agents for cancer chemotherapy often results in the emergence of a tumor cell population that is resistant to the cytotoxicity of the drug, a characteristic that is often associated

with the inactivation of MMR. Therefore, the role of MMR in the signaling of apoptosis is of great clinical interest because the effectiveness of chemotherapeutic and radiological treatment of tumors can depend significantly on the MMR status of the tumor, and the acquisition of MMR deficiency in the tumor can lead to the ineffectiveness of chemotherapeutic drugs (Fink et al., 1998).

Common chemotherapeutic agents are S_N1 DNA methylators, including *N*-methyl-*N*-nitrosourea (MNU), *N*-methyl-*N*'-nitro-*N*-nitrosoguanidine (MNNG), and temozolomide, which produce DNA adducts such as O^6-methylguanine (O^6-meG). O^6-meG can be directly reversed by O^6-methylguanine-DNA methyltransferase (MGMT); however, if MGMT is overwhelmed or debilitated, the O^6-meG is usually mispaired with a thymine upon DNA replication, thus creating GC→AT transition mutations in subsequent rounds of replication (Kawate et al., 1998). MMR recognizes O^6-meG – T mispaired bases, but does not contribute to overall repair of these adducts, as DNA polymerase repeats the mispairing with thymine during resynthesis unless the methyl group is removed by MGMT. However, although MGMT-deficient cells are very sensitive to the cytotoxic effects of DNA alkylating agents that induce O^6-meG, the subsequent inactivation of MMR on the MGMT-deficient background confers complete resistance to the cytotoxicity of O^6-meG (de Wind et al., 1995; Kawate et al., 1998; Reitmair et al., 1997). Thus when exposed to alkylating agents, this population of MGMT- and MMR-deficient cells are highly mutagenic, because they lack the primary DNA repair mechanism for alkylated bases, and they are

still capable of growth and replication as MMR-deficiency confers resistance to cell death. Indeed, Hickman and Samson (1999) have shown that MutSα heterodimer is required in the apoptotic response to DNA alkylator damage, meaning that cell tolerance for DNA alkylators results from a failure to engage or to signal apoptosis. Therefore, MMR prevents neoplastic transformation by facilitating cell death in the face of extensive mutation, even when it is not specifically involved in the repair of the DNA damage incurred.

In addition to alkylating agents, MMR facilitates cell survival in response to a wide variety of DNA damaging agents (Table 1). This important tumor suppressive role of MMR is evident when MMR-deficient cells experience diminished cell death in response to cytotoxic agents, usually corresponding to a failure to engage apoptosis. However, in contrast to alkylation damage, MMR-deficiency confers only partial resistance to apoptosis in response to other DNA damaging agents. MMR deficient cells exhibit partial resistance to several DNA adducts, including environmental carcinogens N-acetoxy-acetylaminofluorine (AAAF) and benzo[a]pyrene dihydrodiaol epoxide (BPDE) (Wu et al., 1999), chemotherapeutic drugs cisplatin (Gong et al., 1999), methotrexate (Frouin et al., 2001), 5-fluorouracil (5-FU) and 5-fluoro-2'-deoxyuridine (FdUrd) (Meyers et al., 2001), as well as hydrogen peroxide (Hardman et al., 2001) and low doses of ionizing radiation (IR) (DeWeese et al., 1998), both of which induce oxidation damage. Partial resistance to cytotoxicity of these DNA damaging agents exhibited in MMR-deficient cells also corresponds with a partial failure to

Agent	Cytotoxicity	Apoptosis	Cell Cycle
MNNG	↓↓ (Kat et al., 1993; Koi et al., 1994)).	↓↓ (Hickman and Samson, 1999; Zhang et al., 1999)).	↓ G_2-M arrest (D'Atri et al., 1998; Hawn et al., 1995)).
MNU	↓↓ (Friedman et al., 1997)).	↓↓ (Kawate et al., 1998)).	
Temozolomide (TMZ)	↓↓ (D'Atri et al., 1998; Friedman et al., 1997)).	↓↓ (D'Atri et al., 1998)).	↓ G_2-M arrest (D'Atri et al., 1998)).
Hydrogen peroxide	↓ (Hardman et al., 2001)).	↓ (Hardman et al., 2001)).	No effect (Hardman et al., 2001)).
AAAF and BPDE	↓ (Wu et al., 1999)).	↓ (Wu et al., 1999)).	
Cisplatin	↓ (Fink et al., 1996; Gong et al., 1999)).	↓ (Gong et al., 1999; Toft et al., 1999)).	↓ G_1-S arrest (Lan et al., 2002)).
5FU and FdUrd	↓ (Meyers et al., 2001)).	↓ (Meyers et al., 2001)).	↓ G_2-M arrest (Meyers et al., 2001)).
IR	↓ (DeWeese et al., 1998; Fritzell et al., 1997)).	↓ (DeWeese et al., 1998; Zhang et al., 1999)).	↓ G_2-M arrest(Davis et al., 1998)).
6-Thioguanine	↓ (Hawn et al., 1995; Swann et al., 1996)).		↓ G_2-M arrest (Hawn et al., 1995)).
Methotrexate	↓ (Frouin et al., 2001)).	↓ (Frouin et al., 2001)).	↓ G_2-M arrest (Frouin et al., 2001)).
BCNU	No effect (Hickman and Samson, 1999)).	↓ (Hickman and Samson, 1999)).	
PhIP	No effect (Duc and Leong-Morgenthaler, 2001)).	↓ (Duc and Leong-Morgenthaler, 2001)).	
Camptothecin	↑ (Jacob et al., 2001)).		No effect (Jacob et al., 2001)).
Etoposide	↑ (Jacob et al., 2001)}.; no effect (D'Atri et al., 1998)).	No effect (D'Atri et al., 1998)}.	No effect (D'Atri et al., 1998; Jacob et al., 2001)).
Iododeoxyuridine (IdUrd)	↑ (Berry et al., 2000)).		No effect (Berry et al., 2000)).

Table 1. Effects of MMR-deficiency on cytotoxicity, apoptosis, and cell cycle arrest in response to various DNA damaging agents.

apoptose in response to DNA damage (Gong et al., 1999; Hardman et al., 2001; Meyers et al., 2001; Toft et al., 1999).

Resistance to cytotoxicity in the absence of MMR does not always correspond with a deficient apoptotic response. In response to chemotherapeutic agent 1,3-bis(2-chloro-ethyl)-1-nitrosourea (BCNU) (Hickman and Samson, 1999) and food-borne heterocyclic amine 2-amino-1-methyl-6-phenylimidazo [4,5-b]pyridine (PhIP) (Duc and Leong-Morgenthaler, 2001), MMR-deficient cells display reduced apoptosis; however the cytotoxicity of these agents is not affected by their MMR status. Although not yet explained by biochemical evidence, this disparity may result from a lack of participation of MMR in growth arrest in response to BCNU and PhIP; in contrast, most other DNA adducts may utilize MMR to conduct both cell cycle arrest and apoptosis (Table 1).

One final possibility for the effect of MMR status on the response of cells to DNA damage involves increased cytotoxicity of MMR-deficient cells, as may be the case with topoisomerase inhibitors camptothecin and etoposide (Jacob et al., 2001). This increase in sensitivity in the absence of MMR may result from the possible involvement of MMR in reversing DNA adducts that result from topoisomerase inhibitors, including double strand breaks, due to the role of MMR in recombinational repair and repair of double strand breaks (Jacob et al., 2001). Thus in the absence of a mechanism of DNA repair, MMR-deficient cells may be increasingly susceptible to a high level of DNA damage with camptothecin and etoposide. However, several previous studies reported the opposite effect of MMR-deficiency, namely an increase in cellular resistance, for topoisomerase II

inhibitors etoposide and doxorubicin (Fink et al., 1998; Lage and Dietel, 1999), thus the literature is unclear.

Although it is known that recognition of various types of DNA damage by MutSα or MutLα can influence a signaling cascade that leads to apoptosis or cell cycle arrest, the molecular events have not yet been clearly established (Li, 1999). For example, in normal cells, alkylating agents induce an apoptotic signaling pathway following G_2M arrest (Tominaga et al., 1997) that involves reduction in anti-apoptotic protein Bcl-2 and subsequent activation of caspase 9 followed by caspase 3, a protease that represents a final effector of apoptosis (Figure 3) (Ochs and Kaina, 2000); however, how this pathway is initiated and why it requires MMR is unclear. Two possible mechanisms have been proposed for the signaling of apoptosis by MMR, primarily from studies using alkylation treatment: adducted bases leading to mispairs upon replication induce futile cycles of repair by MMR that may provide a signal to downstream kinases, or the binding of MutSα/MutLα to DNA adducts may block transcription, replication, or repair and is somehow recognized as a signal that activates apoptosis (Li, 1999). In support of the latter, a study by Zhang et al. (1999) directly implicated hMSH2 and hMLH1 in the activation of apoptosis by showing that overexpression of either of these two proteins, but not of hMSH3, hMSH6, or hPMS2, induced apoptosis in either repair-proficient or –deficient cells. MutSα is known to bind specifically and directly to many adducts such as O^6-meG (Duckett et al., 1996), cisplatin-induced 1,2-intrastrand purine-purine crosslinks (Yamada et al., 1997), and oxidation-induced 8-oxo-guanine (8-oxo-G) (Mazurek et al., 2002) (Table 2), thus

DNA Adduct	Source	Reference
O^6-meG	Alkylating agents	(Duckett et al., 1996)).
Aminofluorine (AF)	Environmental carcinogens	(Li et al., 1996b)).
Acetylaminofluorine (AAF)	Environmental carcinogens	(Li et al., 1996b)).
Benzo[a]pyrene dihydrodiaol epoxide (BPDE)	Environmental carcinogens	(Wu et al., 1999)).
S^6-methylthioguanine	6-thioguanine (6-TG)	(Swann et al., 1996)).
1,2-intrastrand purine-purine crosslink	Cisplatin	(Duckett et al., 1996; Mu et al., 1997; Yamada et al., 1997)).
6-4 photoproducts	UV	(Mu et al., 1997; Wang et al., 1999)).
Cyclobutane pyrimidine dimers	UV	(Mu et al., 1997; Wang et al., 1999)).
8-oxo-guanine (8-oxo-G)	Oxidation	(Mazurek et al., 2002; Ni et al., 1999)).
Propanodeoxyguanosine (PdG)	Malionaldehyde	(Johnson et al., 1999)).
Pyrimido[1,2-α]purin-10(3H)-one (M(1)G)	Malionaldehyde	(Johnson et al., 1999)).

Table 2. DNA Adducts to which MutS specifically binds (adapted from (Li, 1999)).

it is conceivable that MutSα directly senses DNA damage and signals to effectors of apoptosis. Furthermore, as discussed later, p53 phosphorylation, an important step in many DNA damage-induced apoptotic pathways, requires MutSα and MutLα in response to methylation damage (Duckett et al., 1999). On the other hand, Ochs et al. (2000) found that nondividing cells treated with MNNG do not respond by inducing apoptosis, suggesting that the presence of O^6-meG adducts is not sufficient for eliciting an apoptotic signal, and that a cycle of DNA replication is required for MMR to exert its effect.

Christmann et al. (2000) found that treatment with alkylating agents elevates the levels of MSH2 and MSH6 and results in their translocation from the cytoplasm to the nucleus only in the absence of MGMT. Furthermore, MSH2 and MSH6 have been found to be phosphorylated by protein kinase C (PKC) and casein kinase II but not protein kinase A *in vitro* and this phosphorylation enhances the nuclear translocation of MutSα and its ability to bind to DNA adducts (Christmann et al., 2002). Interestingly, PKC, a serine-threonine kinase, has also recently been implicated in directly and indirectly regulating expression of hMSH2 and, to a lesser extent, hMSH6 and hPMS2 in myeloid leukemia cells treated with 6-thioguanine (6-TG) (Humbert et al., 2002), but whether the interaction of MMR with PKC facilitates repair, apoptosis, or both is unclear. Therefore, MMR has been associated with several possible pathways of transmitting a signal for the presence of DNA damage, but the precise mechanism of signal transmission is an important question that remains unresolved.

The proposed role of MMR in sensing damage and signaling apoptosis may also be integrated with its involvement with other tumor suppressors. Interestingly, Wang et al. (2000) identified a large complex of proteins that physically associate with BRCA1 by mass spectroscopy and co-immunoprecipitation and that may provide the key to the coordination of repair and apoptosis events. This complex, called BASC (BRCA1-associated genome surveillance complex), is hypothesized to be a DNA structure surveillance device; it includes proteins with the ability to bind abnormal DNA structures, such as MSH2, MSH6, MLH1, ATM, BLM, and the RAD50-MRE11-NBS1 complex, as well as signal transducers, such as the kinases ATM and ATR, and also several scaffolding proteins, such as BRCA1 itself. Thus BASC theoretically could sense the presence of DNA damage and respond rapidly with the signal transducers' phosphorylation of BASC components to activate repair, checkpoints, or apoptosis (Wang et al., 2000).

MMR and cell cycle. MMR has also been shown to facilitate cell cycle arrest in the G_2-M transition in response to DNA damage, supporting its proposed role in signal transduction pathways that inhibit the propogation of damaged cells. Indeed, a lack of MMR confers deficiency in the G_2-M cell cycle checkpoint in response to O^6-meG (D'Atri et al., 1998; Hawn et al., 1995), 6-TG (Hawn et al., 1995) and IR (Davis et al., 1998), all of which elicit apoptotic pathways fully or partially dependent on MMR (DeWeese et al., 1998; Hawn et al., 1995); however, they are competent in G_1 arrest and the G_1-S transition (Davis et al., 1998) (Table

1). In contrast, recent data indicate that MMR is required for inducing the G_1-S checkpoint, but not the G_2-M cell cycle checkpoint, in response to cisplatin, and that the mechanism for this role involves coupling DNA damage with cyclin D1 degradation and attenuation of CDK2 activity (Lan et al., 2002). Thus if MMR is defective, cells may assume a precarious combination of increased mutagenesis, loss of cell cycle control, and resistance to apoptosis in response to DNA damage, all of which promote neoplastic transformation (Bellacosa, 2001).

The role of p53 in apoptosis facilitated by MMR. Several studies suggest that another downstream effector in the DNA damage response mediated by MMR may be p53. p53 is a critical coordinator of cell cycle arrest and apoptosis in response to many types of DNA damage and cellular stresses. Indeed, it is the most commonly mutated gene in human cancers (Li et al., 1998) and is a common target for the development of many novel cancer therapies. It is a transcription factor with an N-terminal transcriptional activation domain and a central sequence-specific DNA binding domain (Janus et al., 1999). In response to DNA damage and other cellular stresses the levels and DNA-binding abilities of p53 are substantially increased, both of these events being primarily due to post-translational modifications such as phosphorylations and acetylations (Appella and Anderson, 2001; Janus et al., 1999). Its activation involves stabilization by phosphorylation at several amino acid residues including serines 15 and 392, thereby prolonging its half-life by preventing association with MDM2, which targets it for degradation (Appella and Anderson, 2001; Ashcroft and Vousden,

1999). Its ability to transactivate target genes such as *p21, GADD45, MDM2*, and *BAX*, some of which in turn activate DNA repair, cell cycle arrest, or apoptosis, is consequently induced with cellular stress (Appella and Anderson, 2001) (Figure 6).

Although p53 is a strong candidate for participation in MMR-dependent apoptosis, its role in this process remains controversial. Studies have found that in response to O^6MeG, p53 (and p21) expression increase only in the presence of MutSα (in human lymphoblastoid cell lines) (D'Atri et al., 1998), and that the phosphorylation of serines 15 and 392 on p53 seems to require functional MutLα and MutSα components of MMR (Duckett et al., 1999). An *in vivo* study using an *Msh2*-deficient mouse model showed that MMR-mediated apoptosis induced by O^6MeG is mediated primarily through a p53-dependent mechanism, but that MMR also directed delayed p53-independent apoptosis (Toft et al., 1999). Furthermore, while some *in vitro* studies claim that apoptosis induced by O^6MeG occurs only in the presence of both p53 and MMR (Li, 1999; Wu et al., 1999), others show that this mechanism is largely p53-independent (Hickman and Samson, 1999). Similarly, MMR-dependent apoptosis induced by other agents such as PhIP (Duc and Leong-Morgenthaler, 2001), polycyclic aromatic hydrocarbons (Wu et al., 1999), and IR (Zeng et al., 2000), appears to be largely p53-independent, although p53-dependent mechanisms were also identified in response to polycyclic aromatic hydrocarbons (Wu et al., 1999). Thus the involvement of p53 in MMR-dependent apoptosis appears to vary depending on cell type and DNA damage type, and to add a further complication, p53 does not

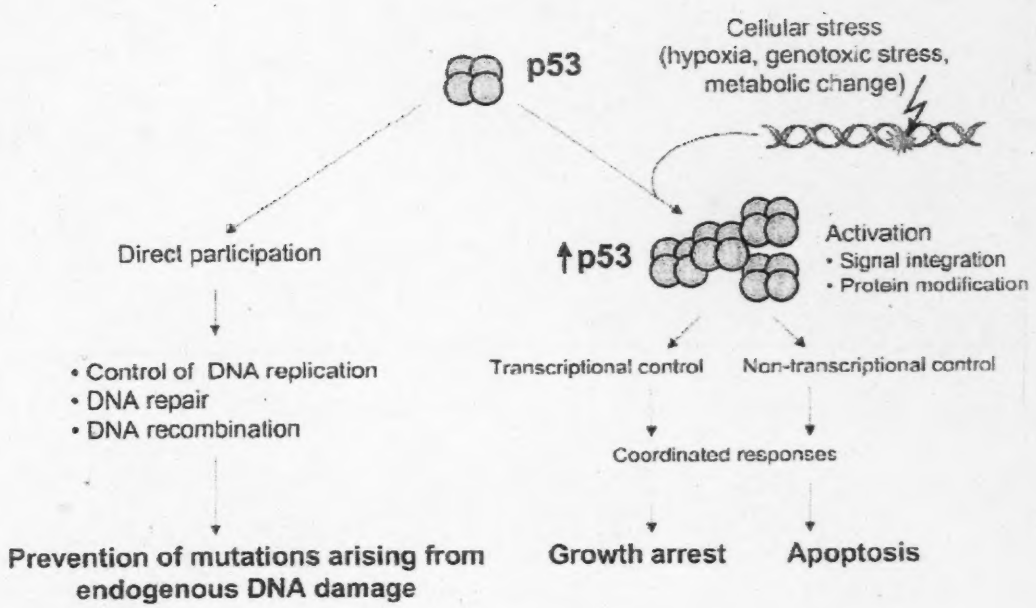

Figure 6. The role of p53 in cellular responses to DNA damage (Janus et al., 1999).

appear to be involved in an exclusive apoptotic pathway.

The role of p73 in apoptosis facilitated by MMR. Perhaps the only well-characterized MMR-dependent pathway of apoptosis involves p73, a structural relative of p53. Gong et al. (1999) showed that p73 and c-Abl tyrosine kinase are components of a MMR-dependent pathway of apoptosis induced by cisplatin, independent of the apoptotic pathway induced by p53 in response to cisplatin. Using human colorectal carcinoma (*MLH1*$^{-/-}$) and osteosarcoma cell lines, p73 protein was shown to be induced by cisplatin, due to protein stabilization rather than an increase in mRNA, only in the presence of both a functional MMR system and c-Abl tyrosine kinase activity; activation of c-Abl also required MMR proficiency. Conversely, the induction of p53 did not require MMR or c-Abl. Furthermore, MEFs deficient in MMR or c-Abl were less sensitive to cisplatin-induced apoptosis, which may be related to a lack of p73 accumulation. Additionally, a human neuroblastoma cell line lacking p73 expression was found to be less sensitive to cisplatin than its p73-expressing counterpart. Indeed p53-deficient MEFs were also less sensitive to cisplatin than wild-type cells, but the apoptosis occurring in *p53*$^{-/-}$ MEFs may be due to the intact MMR/p73/c-Abl apoptotic pathway (Gong et al., 1999).

UV Radiation. One carcinogen that has not yet been investigated as a substrate for MMR-mediated apoptosis is ultraviolet (UV) light, an environmental carcinogen of increasing concern globally. The spectrum of UV is divided into three wavelength ranges: UVC (200-290 nm) is absorbed by the ozone layer and

therefore, unlike UVA (320-400 nm) and UVB (290-320 nm), does not reach the earth (Figure 7). UVA creates mostly reactive oxygen species (ROS) that contribute to the aging of skin, but UVB penetrates the epidermal layer of skin to induce mainly bulky intrastrand DNA cross-links called cyclobutane pyrimidine dimers (CPDs) and 6-4 photoproducts (6-4 PP), which are the major etiological factors of non-melanoma skin cancer (NMSC) by leading to mutations in critical genes (Jost et al., 2001; Li and Ho, 1998) (Figure 8).

In 2001, 70,000 Canadians were diagnosed with NMSC, equivalent to over 50% of all other cancer diagnoses combined (National Cancer Institute of Canada: Canadian Cancer Statistics 2001). Indeed, as the protective ozone layer in the earth's atmosphere progressively diminishes, an increasing amount of UV radiation reaches the earth, contributing to a rapidly increasing incidence world-wide, particularly in Caucasian populations (Li et al., 1998). NMSC includes both cutaneous squamous cell carcinoma (SCC) and basal cell carcinoma (BCC), both of which arise from cells in the epidermis, called keratinocytes, and are hastened by sun exposure (Wikonkal and Brash, 1999). SCCs are generally invasive, as over 10% metastasize, and result in approximately 1500 deaths per year in the US; in contrast, BCCs are rarely fatal, but can be locally invasive and cause significant morbidity (Stratton et al., 2000). Therefore, although mortality of NMSC is much lower than that of melanoma, NMSC does impose a significant cost to the health care system in terms of diagnosis and minor surgeries.

The enormous task of repairing base damage caused by UV-induced adducts CPDs and 6-4PPs, as well as other helix-distorting adducts such as

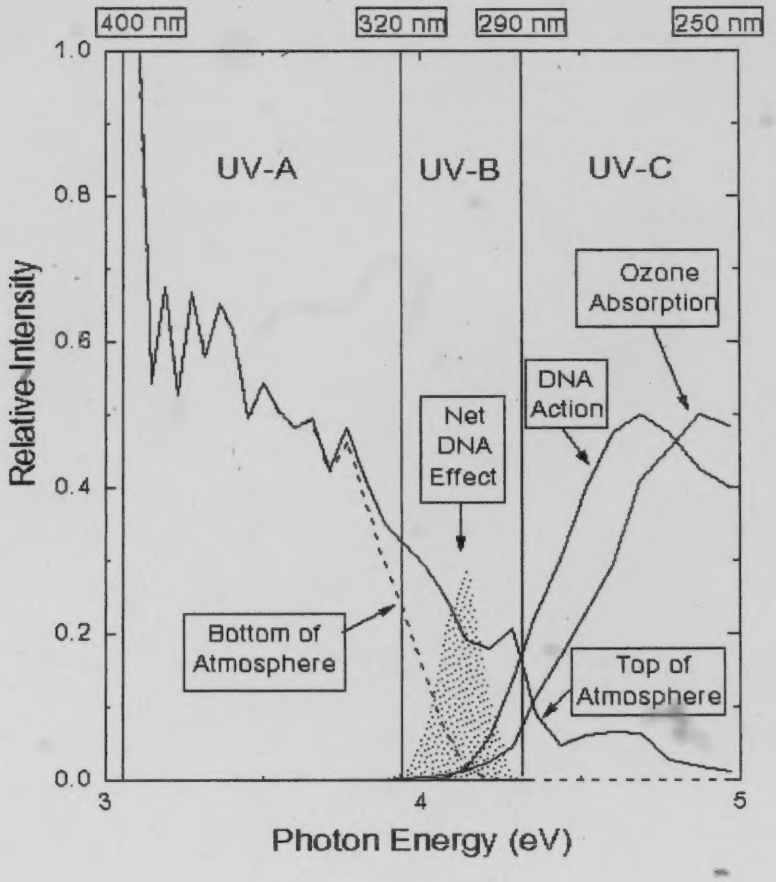

Figure 7. Ultraviolet light spectrum (http://www.phys.ksu.edu/gene/e3f3.html).

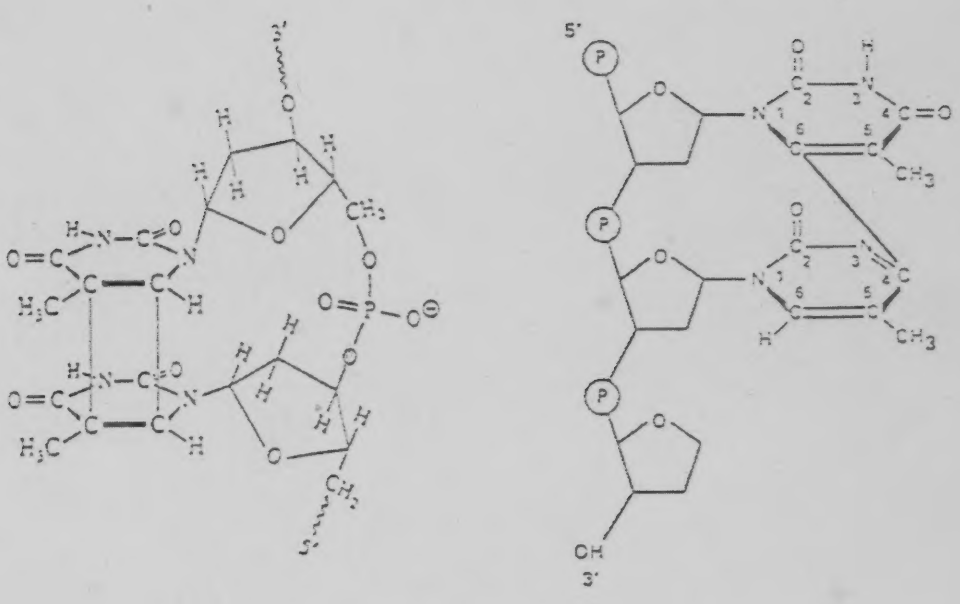

A

B

Figure 8. Structural models of the DNA adducts induced by UVB irradiation. A. Cyclobutane pyrimidine dimer. B. 6-4 Photoproduct.

those induced by polycyclic aromatic hydrocarbons and intrastrand cross-links induced by cisplatin, rests upon the nucleotide excision repair (NER) pathway (McKay et al., 2001). NER can be divided into the transcription coupled repair (TCR) pathway, which collaborates with RNA polymerase to preferentially remove adducts in actively transcribed DNA, and the global genome repair (GGR) pathway, which removes adducts from the bulk genomic DNA (de Boer and Hoeijmakers, 2000). In GGR, DNA damage is recognized by Xeroderma pigmentosum C (XPC), and repair occurs with help from XPA, RPA, transcription factor IIH (TFIIH), XPG endonuclease, helicases XPB and XPD, excision cross-complementing 1 (ERCC1)-XPF heterodimeric subcomplex, DNA polymerase δ or ε, accessory proteins PCNA, RFC, and DNA ligase (mechanism described in Figure 9). In TCR, damage is thought to be recognized by the arrested RNA polymerase II transcription machinery, which includes two proteins, Cockayne syndrome A (CSA) and Cockayne syndrome (CSB); the ensuing events following this recognition step, which does not require XPC, are the same as those for GGR (Friedberg, 2001).

The importance of the NER system in maintaining the integrity of the genome in the skin is exemplified in individuals with a rare (1/250,000 in Western countries) autosomal recessive hereditary disease, xeroderma pigmentosum (XP), characterized by severe predisposition to skin tumours, mainly SCCs and BCCs (Friedberg, 2001). Complementation groups XPA-G correspond to the NER proteins affected (Friedberg, 2001). Mouse models of XP accurately mimic the predisposition to UV-induced skin cancer, providing useful tools with which

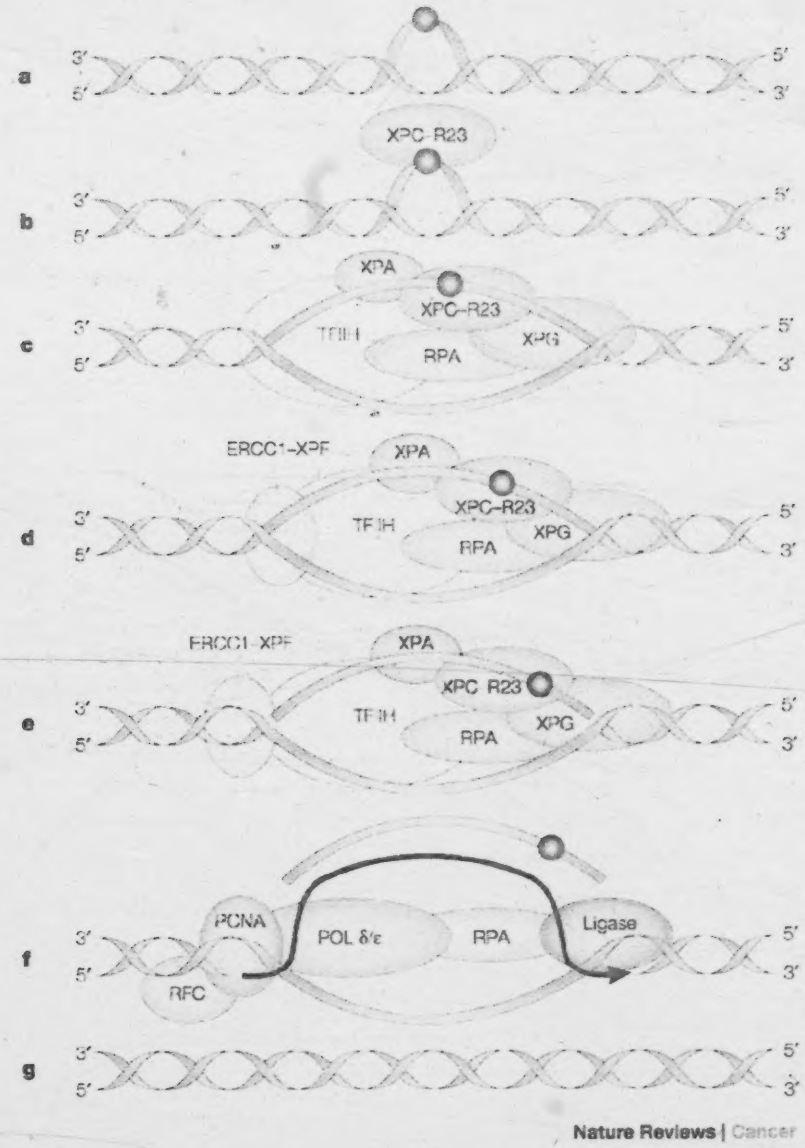

Figure 9. Biochemical steps in the NER pathway. In GGR (a) DNA damage (b) is recognized by Xeroderma pigmentosum C (XPC), (c) and subsequently several other proteins bind, including XPA and RPA, which facilitate recognition of adducts, transcription factor IIH (TFIIH), a subcomplex of RNA polymerase II transcription initiation machinery, and XPG, an endonuclease. TFIIH contains XPB and XPD, two helicases that unwind the duplex near the base damage. Finally, (d) the excision repair cross-complementing 1 (ERCC1)-XPF heterodimeric subcomplex binds. (e) ERCC1-XPF and XPG cut 5' and 3' to the damage site respectively, (f) allowing repair synthesis to ensue, which involves DNA polymerase δ or ϵ, accessory proteins PCNA, RPA, and RFC, and DNA ligase (Friedberg, 2001).

to study the complexities of NER (Friedberg, 2001). Deficiencies in CSA or B result in the more severe Cockayne's syndrome (CS), characterized by early mortality, as well as photosensitivity without a propensity for skin cancer due to compromised transcription and repair (Friedberg, 2001). Trichothiodystrophy (TTD), characterized by photosensitivity, brittle hair and nails, physical and mental retardation, and ichthyosis (scaly skin), is caused by deficiency in XPD or XPB, resulting in compromised transcription and repair (Friedberg, 2001). The phenotypes of complementation groups have revealed the fact that GGR is more important than TCR for cancer prevention because it does not discriminate repair based on the location of damage; indeed, XPC patients have a defect only in GGR, XPA and XPB patients have defective GGR and TCR, and CSA and CSB patients that are not cancer-prone have a defect only in TCR (de Boer and Hoeijmakers, 2000; McKay et al., 2001).

UV-induced apoptosis. Epidermal cells called keratinocytes (Figure 10) constantly deal with UV-induced DNA damage; a common effect of excessive exposure to UVR is erythema or sunburn, characterized by skin redness and sometimes peeling. The UV exposure needed to induce erythema is called the minimum erythema dose (MED). Keratinocytes are continually sloughed from the surface and renewal of the cell population occurs in the basal epidermal layer, with new cells pushing the cells above to the surface; differentiation occurs as cells move from basal layer to the surface, a cycle that normally takes 20 to 30 days (Gartner and Hiatt, 2001). UV exposure that exceeds the MED induces the

Figure 10. Histological slide of human epidermis, stained with hematoxylin and eosin. SC, stratum corneum; SG, stratum granulosum; SS, stratum spinosum; BL, basal layer (Bernerd, 2001).

formation of sunburn cells (SBC), which are keratinocytes undergoing apoptosis. SBC are induced as a protective mechanism for actively eliminating damaged cells at risk for malignant transformation (Murphy et al., 2001). SBCs are distinguishable on tissue sections stained with hematoxylin and eosin as isolated epidermal cells with pyknotic nuclei as well as shrunken and eosinophilic cytoplasm, which are characteristics of apoptosis (Murphy et al., 2001). As discussed previously, in contrast to necrosis, apoptosis is an active process that occurs without potentially damaging inflammation in adjacent tissues (Murphy et al., 2001). Apoptosis involves cell shrinkage and nuclear membrane blebbing, followed by condensation of chromatin and fragmentation of genomic DNA; SBCs are ultimately phagocytosed by macrophages (Murphy et al., 2001).

UVB irradiation induces apoptosis using three cellular signaling pathways independently: nuclear DNA damage, direct activation of death receptors, and formation of reactive oxygen species (ROS) (Figure 11). Because genomic DNA has a maximum absorption that matches the action spectra of some UVB effects it is regarded as the main cellular target for UVB, serving as the chromophore that transduces the energy from UVB into a biochemical signal. The induced DNA lesions (CPDs and 6-4 PP) are normally removed by NER, but lesion removal has also been shown to be greatly enhanced by bacterial-derived enzymes T4-endonuclease V (T4N5) and photolyase. In fact, these exogenous DNA repair enzymes contributed greatly to the elucidation of the mechanisms of UV-induced apoptosis (Kulms and Schwarz, 2002a). When photolyase or T4N5 enzymes encapsulated into liposomes were introduced *in vivo* (topical application) in

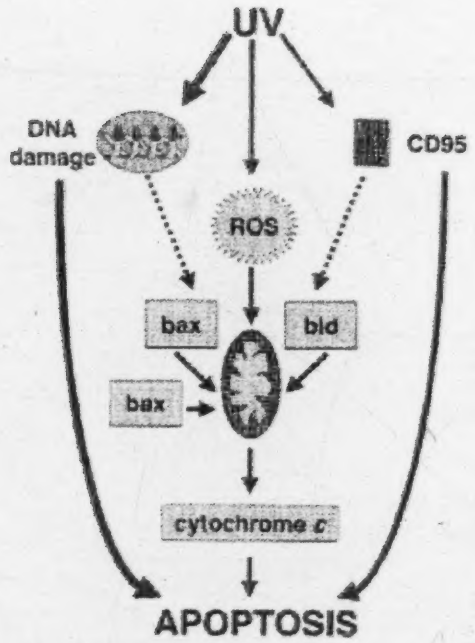

Figure 11. Three distinct pathways of UV-induced apoptosis (Kulms and Schwarz, 2002a).

human or mouse skin or *in vitro,* thereby enhancing repair of the DNA adducts, pronounced reduction of CPDs correlated with a significant inhibition of UVB-induced apoptosis (Kulms et al., 1999; Kulms and Schwarz, 2002a). These experiments demonstrated that DNA damage plays a crucial role in mediating UVB-induced apoptosis; however, apoptosis was not completely inhibited by enhanced DNA repair, indicating that extranuclear factors are responding to UVB.

Indeed, UVB also affects targets in the cytoplasm or at the cell membrane by activating membrane-bound death receptors, members of the tumor necrosis factor (TNF) receptor superfamily. One such receptor, CD95 (Fas, APO-1), is activated independently of its naturally activating ligand upon UVB exposure, forming functional clusters and binding its adaptor molecule FADD. Utilizing the fact that irradiation of cells at low temperatures inhibits receptor clustering, Kulms et al. (1999) demonstrated that inhibiting receptor clustering reduced apoptosis moderately, while enhancement of DNA repair reduced apoptosis even more substantially. Accordingly, combining both interventions resulted in almost complete blockage of UVB-induced apoptosis, proving an additive and independent contribution of nuclear and membrane mediated pathways of apoptosis, as well as the existence of a possible third mechanism.

A third effect of UVB on cells is the induction of reactive oxygen species (ROS), which cause cellular damage, such as membrane damage by lipid peroxidation. ROS induce apoptosis by damaging the inner mitochondrial membrane resulting in loss of membrane potential and release of cytochrome *c*, leading to activation of members of the Bcl-2 protein family (Figure 3). The

radical scavenger pyrrolidene-dithiocarbonate (PDTC) is used experimentally to eliminate ROS, and early application results in partial reduction of UVB-induced apoptosis. Complete suppression was indeed achieved by enhancing DNA repair, blocking death receptor signaling by blocking downstream effector caspase 8, and by eliminating ROS with PDTC (Kulms et al., 2002), thus demonstrating the independent contribution of three pathways during UVB-induced apoptosis. Furthermore, although these three mechanisms have mostly been tested in [redacted]thelial cell lines and primary keratinocytes, evidence does exist that the same holds true for other cell types (Kulms and Schwarz, 2002a).

The role of p53 in post-UVB apoptosis. Over 90% of human NMSCs display mutations in the *p53* gene, including skin tumours from XP patients (Li et al., 1998). Furthermore, most of these *p53* mutations display the distinctive characteristics of UV-induced DNA mutagenesis. Because photoproducts occur only where two pyrimidines are adjacent, dipyrimidine sites are common sites of mutation; either cytosine (C) is replaced by thymine (T) (C→T transition – 70%), or two adjacent C's are replaced by two T's (CC→TT base substitutions - 10%) (Wikonkal and Brash, 1999). Because these mutations are induced by UV and are rarely seen in internal tumours, they are a direct result of UV radiation, confirming that NMSC is induced by UV (Li et al., 1998).

The mutation of *p53* is thought to be an early event in the development of nonmelanoma skin cancer (NMSC), as most human NMSCs have mutated p53 (Wikonkal and Brash, 1999), and mice genetically deficient in p53 are

predisposed to UV-induced squamous cell carcinomas (Li et al., 1998). Therefore, p53 is a natural candidate for transmission of a signal from a molecule that senses UV-induced DNA damage. Activation of p53 occurs in response to UVB-induced DNA damage as early as 30 minutes after UV exposure (Wikonkal and Brash, 1999); protein induction occurs by the reduction in protein degradation by phosphorylation of serines 15 and 392, as previously discussed, among many other serine and tyrosine residues being targeted for phosphorylation for various purposes (Appella and Anderson, 2001). Several reports have shown that p53-deficient cells show reduced repair of UV-induced DNA adducts (Li et al., 1996a); it has been proposed that p53 regulates post-UV cell cycle arrest and NER (de Boer and Hoeijmakers, 2000), and may also play a direct role in NER (Janus et al., 1999). However, p53-deficient mice produce fewer SBCs than wild-type (Ziegler et al., 1994), emphasizing the importance of p53 in the apoptotic response to UV. Indeed, phosphorylation of serines 15 and 20 has been shown to be important for UV-induced apoptosis (Unger et al., 1999). However, many studies have found that UVB-induced apoptosis occurs through both p53-dependent and p53-independent pathways (Brash et al., 2001; Li and Ho, 1998; Li et al., 1996a; Tron et al., 1998). Therefore, p53 likely is an important effector of UV-induced apoptosis, however its role is not exclusive.

Role of MMR in post-UVB apoptosis. Intriguing evidence emerged several years ago that bacterial, yeast, and human MMR played a direct role in TCR of UV-induced DNA damage (Leadon and Avrutskaya, 1997; Mellon and Champe,

1996; Mellon et al., 1996). Although scientists have not been able to explain this phenomenon of interplay between repair systems biochemically, nor its significance evolutionarily, MMR proteins have often been postulated as accessory proteins in the TCR pathway without a precise role assigned (Friedberg, 2001). However, several studies, using *S. cerevisiae* (Sweder et al., 1996), mouse (Shin et al., 2002; Sonneveld et al., 2001), and human (Mu et al., 1997; Rochette et al., 2002) cell models, have since refuted the role of MMR in TCR and asserted that the pathways of repair for MMR and NER are distinct.

The discrepancies in the data addressing the role of MMR in TCR may have arisen from the differences in experimental methods used. The original study used a strand-specific Southern blot assay that quantified CPD excision at gene-level resolution (Mellon et al., 1996). Subsequently Leadon et al. (1997) confirmed the original results using a different type of strand-specific DNA repair assay that measures gap-filling steps of NER. However, several studies have also proven that TCR is equally efficient with or without functional MLH1 or MSH2 using the same DNA strand-specific assay in yeast (Sweder et al., 1996), mouse (Sonneveld et al., 2001), and human (Adimoolam et al., 2001) cells. Furthermore, the ligation-mediated polymerase chain reaction (LM-PCR), which measures CPD removal at nucleotide resolution, has been used by at least two recent studies to confirm that in the absence of MMR, TCR of CPDs is competent (Rochette et al., 2002; Therrien et al., 2001). Therefore, conflicting results were produced even with similar strand-specific assays, but the most recent evidence using the most precise TCR assay to date indicates that MMR does not facilitate TCR. Therefore

MMR is unlikely to be involved in the TCR pathway for the removal of UV-induced photoproducts.

However, several lines of evidence suggest that MMR is indeed involved in some other aspect of cellular response to UV light. MutSα, the component of MMR that recognizes and binds to post-replicative mispairs, also binds specifically to compound DNA lesions involving UV-induced CPDs and 6-4PPs (Mu et al., 1997; Wang et al., 1999), suggesting that MMR may be involved in responding to these adducts. Furthermore, several proteins of the NER pathway have been shown to interact specifically with MSH2, suggesting that some functional overlap does exist between the two repair systems (Bertrand et al., 1998). Bertrand et al. (1998) hypothesized in this study performed in *S. cerevisiae* that MSH2 may recognize UV damage and recruit XPG, the human homologue of RAD2, one of the NER proteins found to bind MSH2. But if MMR does not remove UV-induced photoproducts or their resultant mismatches, or assist the NER molecules with their repair, what is the purpose of their recognition by MutSα?

Despite the apparent lack of involvement of MMR in TCR of UV-induced DNA adducts, MMR does seem to affect the mutagenicity of these photoproducts. Indeed, Nara et al. (2001) found that UVC-induced mutagenesis associated with NER deficiency increases with the loss of MMR; however, MMR-deficiency alone does not increase mutagenesis at low UVC doses, verifying the lack of involvement of MMR in repair of UV-induced adducts. Furthermore, the efficiency of NER removal of photoproducts has been shown to be unaffected by

the absence of MMR (Mu et al., 1997). Therefore another question that arises is how MMR affects mutagenicity of photoproducts without being required for or affecting the efficiency of their repair.

MMR also appears to have a significant impact on UV-induced tumorigenesis. *Msh2*-deficiency accelerated the rate of skin tumour development above that of wild-type in chronically UVB-exposed skin of mice; furthermore, *Xpc*$^{-/-}$ mice, which are deficient in GGR but proficient in TCR, developed tumors faster than *Msh2*$^{-/-}$ mice, but a deficiency in both *Xpc* and *Msh2* resulted in an extremely rapid development of skin tumours (Meira et al., 2002; Meira et al., 2001). To confirm that the increased susceptibility of *Msh2*-deficient mice to skin tumours was not a result of increased cellular proliferation, Meira et al. (2002) combined UV-irradiation with topical application of cell division inducer 12-O-tetradecanoylphorbol 13-acetate (TPA), which does not induce DNA damage, and observed no further increase in tumorigenicity in the MMR-deficient background. Therefore, if MMR were in fact essential for TCR an attractive conclusion would ascribe the additive effect of Xpc and Msh2 in skin tumorigenesis to their separate essential roles in GGR and TCR respectively, meaning that the rate of tumorigenesis of the double mutant should represent that of a fully NER-deficient mouse. Indeed, *Xpa*$^{-/-}$ mice, in which NER activity is completely abolished, display a propensity for UVB-induced tumorigenesis that is comparable to the *Xpc*$^{-/-}$ *Msh2*$^{-/-}$ double mutants (Meira et al., 2002). However, *Xpa*$^{-/-}$ *Msh2*$^{-/-}$ double mutants manifest an even greater susceptibility to skin tumours than *Xpa*$^{-/-}$ mice, indicating that MMR has a role in tumour prevention beyond or exclusive from

the repair of UV adducts by NER (Yoshino et al., 2002). Furthermore, tumours arising from NER-deficient mice often acquire the loss of MMR at some point during their development (Tanaka et al., 2001), indicating that MMR provides some level of protection from UVB-induced tumorigenesis in the absence of NER. Therefore, tumorigenesis studies further suggest that MMR may not be essential to the repair of photoproducts, and also reveal a role for MMR in UV-induced tumorigenesis that may be independent of DNA repair.

Thus MMR may be involved in cellular responses to UV-induced DNA damage other than repair. I propose that its ability to recognize photoproducts as well as its role in tumor suppression point to a role for MMR in post-UVB apoptotic response. With a post-UVB apoptotic response compromised, DNA damage that exceeds the repair capacity of NER would fail to evoke apoptosis and would lead to mutagenesis and ultimately tumorigenesis. A role for MMR in detecting photoproducts and signaling apoptosis would support a proposed model for MMR as a universal DNA damage sensor, with the capability of sensing most base alterations and helix-distorting lesions, excluding double strand breaks (Figure 12).

The characterization of the role of MMR in post-UVB apoptosis holds significant implications for human health. An immunohistochemical screen of human SCCs recently reported aberrant expression of hMSH2 in a significant number of SCCs compared to tumors of three precancerous lesion types, suggesting that hMSH2 may indeed play a role in the development of human skin cancers (Liang et al., 2001) despite its lack of participation in DNA repair.

Furthermore, hMSH2 expression levels were significantly correlated with sun exposure in presumably normal skin, suggesting that hMSH2 may protect human skin during sun exposure (Liang et al., 2001). Therefore, individuals with germline mutations in MMR genes, currently recognized with manifestations of HNPCC or Muir-Torr syndrome as previously discussed, may further experience increased susceptibility to UV-induced NMSCs. Although the SCCs that are commonly associated with Muir-Torr syndrome have not yet been linked with exposure to UV, the connection is possible. Therefore, the establishment of a role for MMR in UV-induced apoptosis may allow the development of tools for molecular diagnosis of these cancer syndromes, and may also lead to the development of preventative and therapeutic strategies for NMSC.

In order to explore further the types of DNA damage that MMR is capable of sensing and responding to by activating apoptosis, I investigated the effects that deficiency in Msh2 had on the levels of apoptosis in response to UVB irradiation in primary and SV40-T Antigen (TAg) immortalized mouse embryonic fibroblasts (MEFs). The cytotoxic effects of UVB were significantly abrogated in the Msh2-deficient MEFs, and more markedly so in transformed cells. In support of the hypothesis that MMR facilitates an apoptotic response to UVB, the enhanced survival in the absence of Msh2 is in fact associated with a reduction in apoptotic response. The absence of Msh2 also resulted in a reduction in the phosphorylation of p53 on ser15. Furthermore, Msh2- deficient mice exposed to chronic doses of UVB irradiation experience an accelerated development of skin tumours compared to wild-type. Thus I propose that MMR, specifically Msh2,

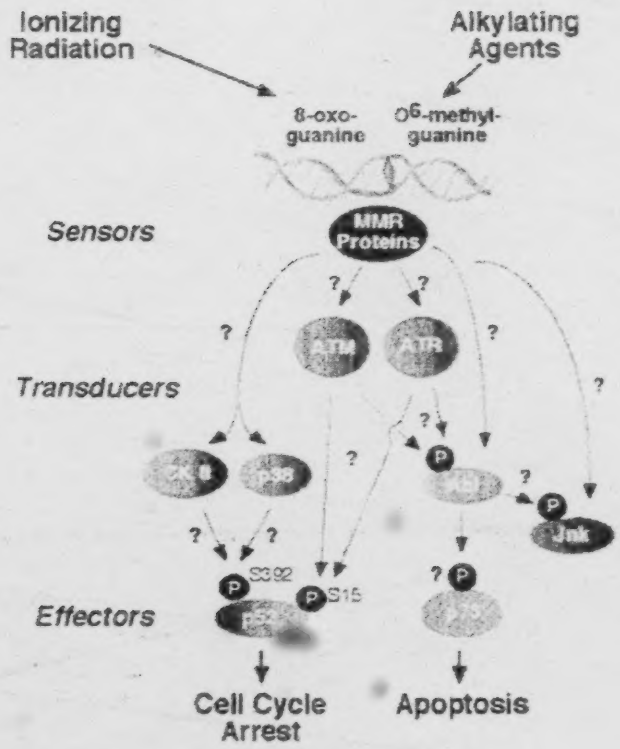

Figure 12. Proposed model of MMR as general DNA damage sensor (Bellacosa, 2001).

may function as a damage sensor in response to UVB by its role in apoptosis as well as p53 phosphorylation, which may or may not be a downstream effector in the pathway of MMR-mediated apoptosis.

Materials and Methods

Msh2 Mouse Colony: Mice deficient in Msh2, previously generated by gene targeting (Reitmair et al., 1995) were obtained from Dr. Tak Mak, AMGEN. Mouse ears were notched for identification at approximately 4 weeks of age. The ear biopsies were suspended in 150 µL STE buffer (50 mM Tris-HCl, 10 mM EDTA, 100 mM NaCl, 0.1% SDS) and 9 µL Proteinase K (180 µg) and digested for 1-2 hours at 55 °C followed by 10 minutes at 95 °C. Genotyping was performed as previously described (Reitmair et al., 1995) with the following modifications that I developed to increase the robustness of the PCR. The PCR reaction included the following reagents: 1X PCR buffer without Mg (Invitrogen), 15 mM $MgCl_2$, 1.25 mM dNTPs, 5 µL primer L926 (50 pmol), 3 µL primer U771 (30 pmol), 3 µL primer neo (30 pmol), 2.5 U Taq polymerase (Invitrogen), 3 µL of 3/100 dilution of tissue digestion, and H_20 to 50 µL. Primers U771 (5' GCT CAC TTA GAC GCC ATT GT 3') and L926 (5' AAA GTG CAC GTC ATT TGG A 3') amplify a 174 bp fragment of the wildtype allele, and primers U771 and neo (5' TGG AAG GAT TGG AGC TAC GG 3') amplify a 325 bp fragment identifying the neo gene. The PCR thermocycle conditions were as follows: 95 °C for 2 minutes; 40 cycles of 95 °C for 30 seconds, 58 °C for 1 minute, 72 °C for 30 seconds. PCR products were visualized on a 2% (w/v) agarose TAE gel with ethidium bromide for visualization with UV light (Figure 13).

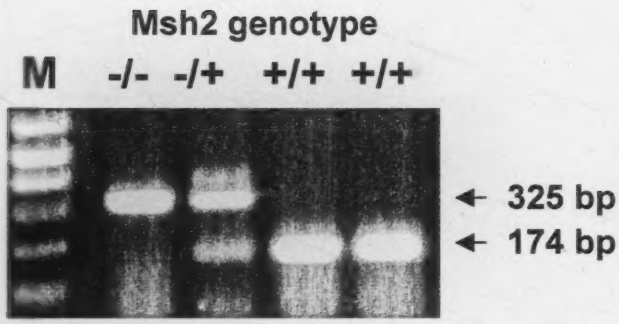

Figure 13. Sample PCR showing all possible genotypes of Msh2 mice. The negative control for PCR (no DNA template) lane is not shown.

Cell Culture: Primary mouse embryonic fibroblasts (MEFs) were cultured with Dulbucco's Minimal Essential Medium (DMEM) plus 20% Fetal Bovine Serum (FBS) (Gibco BRL). Embryos at E13.5 were obtained from pregnant females, rinsed with sterile phosphate-buffered saline (PBS), separated from the placental tissue, and rinsed again. Embryos were minced, suspended in 0.25% trypsin-EDTA, incubated at 37 °C for 5 minutes, and neutralized with DMEM + 20% FBS. The suspensions were passed through an 18 gauge syringe and the supernatant was plated for one passage and then frozen in liquid nitrogen with 10% DMSO. Cells were used for experiments at the fourth passage or sooner.

Transformed MEFs MS5-7 were derived from E13.5 Msh2-deficient mouse embryos and transformed MEFs BC1-6 from E13.5 Msh2-proficient mouse embryos, immortalized with TAg expression as previously described (Fritzell et al., 1997). Immortalized MEFs were cultured with DMEM plus 10% FBS, and cells were used for experiments no more than 4 passages from original frozen stock.

UV Irradiation: A custom-constructed metal UV-treatment apparatus with an adjustable platform and a bank of six unfiltered UVB bulbs (FS20T12/UVB-BP, Light Sources Inc., Orange CT) was employed for treating cultured cells with UVB. The intensity of UVB irradiation penetrating the culture dish lid was determined by placing a culture dish lid over the sensor of an IL1700 radiometer with a SED 240/UVB-1/W detector (International Light, Newburyport, MA) at the predicted height of the bottom of the culture dish during UVB treatment.

Culture dish lids filtered out contaminating UVC radiation (Maeda et al., 2001). Media was aspirated from 80% confluent cell cultures, cells were rinsed with PBS, cells were treated with UVB at a dose of 50 – 250 J/m^2, and culture media was replaced. Control cells were subjected to a mock UV treatment. Cells were then incubated for the desired length of recovery time. For cell pellet collection, floating cells were collected, plates were trypsinized (0.25%, Gibco BRL), culture media with FBS was added to neutralize; cell suspensions were then centrifuged, rinsed once with PBS and snap frozen at –80 °C.

For the UVB tumorigenesis study, the same bulbs as above were filtered using Kodacel sheeting (Kodak, Rochester, NY) and used to treat mice (with shaven backs) 4 weeks of age with 3 doses of 2000 J/m^2 per week until a tumour (approximately 1 cm diameter) developed. Animals with appropriate skin tumours were sacrificed and the skin tumours were biopsied and fixed in 10% formalin. If the mouse was not removed from treatment due to the development of a tumour, treatment was withdrawn after 37 weeks, for a total of 200,000 J/m^2 UVB.

Cell Viability Assay: Primary MEFs were plated in triplicate at 250,000 cells per 35 mm plate. Cells at 80% confluency were treated with UVB, as above, at doses of 0-250 J/m^2. After 48 hours recovery, the media was removed and the plates were washed twice with sterile PBS. Crystal violet in 20% methanol was applied and allowed to set for 25 minutes, then plates were gently washed with distilled water until they rinsed clear. Stained plates were scanned on a flat bed scanner (Epson) without their lids and subjected to densitometry (Quantity One,

Bio-Rad) to determine stain intensity. An empty plate was also scanned, and its density was subtracted from all other values. Cell viability was expressed as a percentage of viability of untreated cells.

Colony Formation Assay: BC1-6 and MS5-7 cells were plated in triplicate in 60 mm culture dishes at a low density (200-250 cells). Plates were irradiated within 6-12 hours as above, with doses of 0-50 J/m^2. Colonies were incubated at 37 °C for 7 days and then crystal violet stained as above. Colonies with >50 cells were then scored, and expressed as a percentage of the average number of colonies for the non-treated controls. The assay was repeated at least three times (with triplicates for each dose) and standard error of the mean was determined.

Annexin V-FITC/PI Assay for Apoptosis: Annexin V-FITC staining was performed using a commercial kit (Pharmingen). Cells were grown to 80% confluency and treated with UVB as described above. After the appropriate elapse of recovery, media was collected in 15 mL conical tubes. Plates were rinsed with PBS and the rinse was collected and added to the tube containing media. Plates were trypsinized (Gibco BRL, 0.125% v/v) and the reaction stopped with FBS immediately upon cell liberation, thus minimizing damage to cellular membranes. These cells were pooled with the floating cells already in the sample tubes and the total number of cells was counted. Tubes were centrifuged at 10,000 x g for 5 minutes and cell pellets were washed twice in ice cold PBS, then resuspended in 1 x binding buffer (Pharmingen) to a concentration of

approximately 2 X 10^6 cells/mL. In a FACscan tube (Falcon), 100 µL (2 x 10^5 cells) of cell suspension, 5 µL of AnnexinV-FITC and 5 µL of propidium iodide (Pharmingen) were mixed and incubated in the dark for 15 minutes. Assay controls included apoptotic cells with no stain, no propidium iodide, and no AnnexinV-FITC. After incubation, 400 µL of binding buffer was added to each sample and samples were read with a flow cytometer (Becton Dickinson) within 1 hour of staining. Results were analyzed with Cell Quest software.

SDS/PAGE gels / Western Blots: Cell pellets were sonicated in 200-400 µL lysis buffer (50 mM Tris pH 7.5, 10 mM $MgCl_2$, 1 x protease inhibitor (Complete Mini, Roche), 1% SDS). Protein concentrations were determined using a detergent compatible protein assay (BioRadDC). Cell lysates (typically 30 µg) were separated on SDS-PAGE gels (7.5% - 15%) using standard protocols and transferred to PVDF membrane. Membranes were blocked in 5% non-fat milk in TBST (20 mM Tris, 137 mM NaCl, 0.001% Tween 20, pH 7.6) at room temperature for 1 hour. Primary antibodies were diluted to the appropriate concentration in 5% milk/TBST and incubated with membranes for 1-2 hours at room temperature or overnight at 4 °C. Primary antibodies were used at the following dilutions: Msh2 (clone FE11/Ab-2, Oncogene Research Products, Boston, MA) 1:500, Msh6/GTBP (clone 44, BD Transduction Laboratories) 1:2000, cleaved caspase 3 (Asp175) (Cell Signaling Technology, Beverly, MA) 1:1000, PARP (clone C2-10, PharMingen International) 1:2000-1:1000, p53 (Ab-3, Oncogene Research Products) 1:200, phospho-p53 ser15 (#9284, Cell

Signaling Technology, Beverly, MA) 1:1000, p21 (clone SXM30, BD Pharmingen) 1:1000, p42 MAP Kinase 3A7/Erk2 (Cell Signaling Technology, Beverly, MA) 1:2000 – 1:4000. The Western blot protocol was modified slightly for phospho-p53 ser15 in that the primary antibody was diluted in 5% BSA/TBST and incubated with the membrane at 4 °C overnight. After rinsing three times for 5 minutes in TBST at room temperature, membranes were incubated with IgG HRP-conjugated secondary antibodies (anti-mouse: Transduction Laboratories; anti-rabbit: Cell Signaling Technology) in 5% milk/TBST for 1 hour at room temperature. Membranes were rinsed 5 times in TBST for 5 minutes, then incubated in ECL solution (Perkin Elmer) for 1 minute and exposed to autoradiography film for 1 sec to 5 minutes. Antibodies were stripped from the membranes with a 30 minute incubation in stripping solution (62.5 mM Tris HCl pH 6.8, 2% SDS, 100 mM 2-mercaptoethanol) at 50 °C for subsequent Western blots.

DNA Photoproduct Slot Blot SouthWestern: Cells were treated with UVB and cell pellets were collected as described, but the media was aspirated before collecting cells so as to include only viable cells attached to the plate. Samples were protected from direct sunlight with aluminum foil at all stages of the experiment. DNA was extracted using the Qiagen DNeasy kit; samples were eluted twice in 100 µL ddH_20 and were standardized at 5 ng/µL. 100 ng of DNA was mixed with 50 µL of 1M NaOH (0.4 M final concentration), 2 µL of 0.5 M EDTA pH 8.0 (10 mM final concentration), and ddH_20 to a final volume of 100

µL. Samples were heated to 95-100 °C for 10 minutes, 100 µL of ice-cold NH_4OAc pH7.0 was added, and samples were placed immediately on ice. A vacuum slot-blotting apparatus (Biorad) was assembled with nitrocellulose membrane (Biorad) soaked in 6XSSC for 10 minutes and 3 sheets of thick filter paper. After all wells were rinsed with 500 µL ddH20, samples were applied followed by a rinse of 2XSSC. The apparatus was then disassembled and the membrane was rinsed in 2XSSC for 1 minute, air dried and baked in a vacuum oven at 80 °C for 2 hours.

Thymidine dimers were detected on the membrane with a specific primary antibody (Kamiya Biomedical) following the protocol for immunoblot detection previously described. Following immunoblot analysis, the antibody was stripped from the membrane as described previously. To standardize DNA loading, southern blotting was performed using digested mouse genomic DNA as a probe. DNA (25 ng) was denatured by heating at 95-100 °C for 5 minutes and placed immediately on ice. A random primer labeling reaction produced ^{32}P-labelled oligonucleotides and hybridization performed as previously described (Otto, 2001). The membrane was then exposed to autoradiography film and densitometry was performed using Quantity One software.

Results

Figures 16, 17, 18, 19 (modified), 21 (modified), 22, and 23 from this thesis contributed to the following publication:

> Peters, A.C., Young, L.C., Maeda, T., Tron, V.A., Andrew, S.E. Mammalian DNA mismatch repair protects cells from UVB-induced DNA damage by facilitating apoptosis and p53 activation. 2003. *DNA Repair* **2**:427-435.

Msh2 and Msh6 accumulate in response to UVB. To investigate the possible responsiveness of Msh2 and Msh6, together comprising MutSα, an *in vitro* evaluation of their expression post-UVB was performed. Primary and transformed MEFs were exposed to 100 or 200 J/m^2 UVB and their whole-cell protein preparations analyzed by Western blot (Figure 14). In both primary and transformed cells, *Msh2*$^{-/-}$ cells expressed neither Msh2 nor Msh6 at detectable levels. Overall levels of Msh2 and Msh6 were much higher in transformed MEFs than primary MEFs (Figure 14A). In wild type cells, both Msh2 and Msh6 protein levels increased in response to UVB in primary and transformed MEFs, but the patterns differed with cell type and UVB dose. In primary MEFs, 100 J/m^2 induced a gradual accumulation over time of both Msh2 and Msh6 that persisted for at least 32 hours (Figure 14A). After 200 J/m^2, Msh6 levels peaked at 8 hours and began to gradually decline; however, Msh2 levels underwent a gradual increase for at least 32 hours, similar to but less pronounced than the response at 100 J/m^2 (Figure 14B). In transformed MEFs (BC1-6), however, 100 J/m^2 induced rapid accumulation of Msh6 by 8 hours post-UVB and levels declined gradually

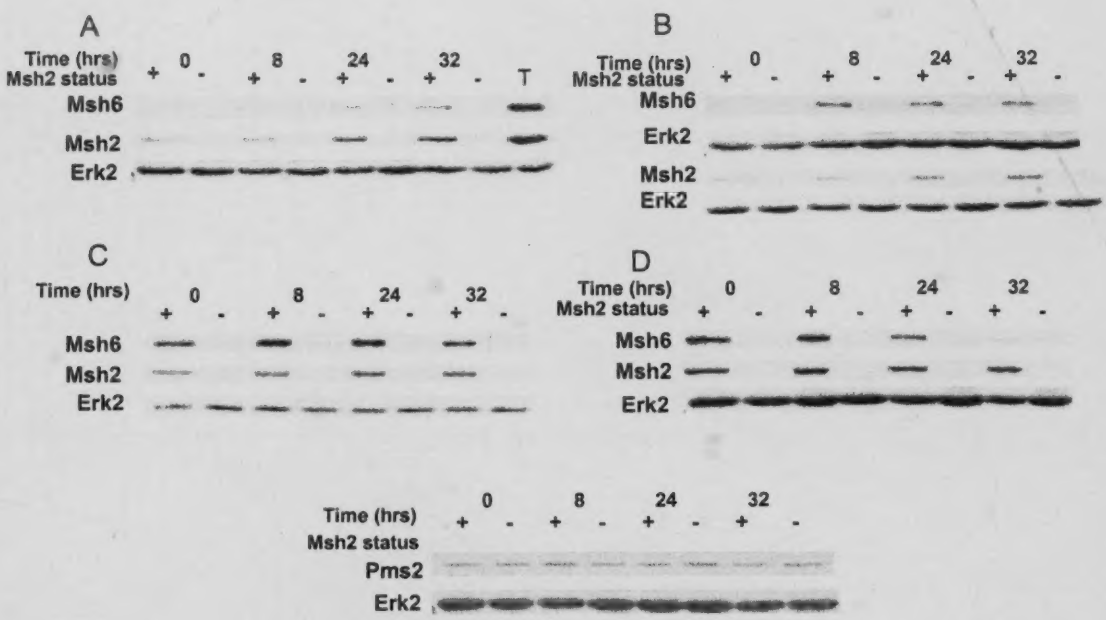

Figure 14. Msh2 and Msh6 are upregulated in response to UVB in Msh2-proficient primary and transformed MEFs. A) Primary MEFs derived from mice proficient (+) or deficient (-) for Msh2 were treated with 100J/m^2 UVB as described. Whole cell lysates were separated on 7.5% SDS-PAGE gels and probed with Msh2 and Msh6 antibodies. T indicates transformed BC1-6 wild-type cells treated with 100 J/m^2 and harvested at 24 hours to allow comparison of expression levels between primary and transformed MEFs. B) Treatment with 200 J/m^2 produced the same results. C) Transformed MEFs BC1-6 (+) and MS5-7 (-) whole cell lysates examined by western blot for Msh2 and Msh6 expression after treatment with 100 J/m^2 and D) 200 J/m2 UVB. E) Transformed MEFs BC1-6 (+) and MS5-7 (-) examined for Pms2 expression after treatment with 200 J/m^2 UVB.

after 24 hours, but only a slight increase in Msh2 levels was observed (Figure 14C). In response to 200 J/m^2, Msh2 and Msh6 levels increased only very slightly, followed by a gradual decline, more rapid in Msh6 (Figure 14D). In contrast, Pms2, another molecule involved in MMR, was stable in the absence of Msh2 expression and did not accumulate significantly in response to UVB (Figure 14E).

Msh2-deficient MEFs are capable of photoproduct repair. Although the literature appears to indicate that Msh2 is not involved in TCR of UV-induced CPDs and 6-4PPs, there are inconsistencies that may be influenced by factors such as cell type and UV dose. Prior to investigating post-UVB responses, I wanted to confirm that the Msh2-deficient MEFs used for my experiments were capable of repairing UVB-induced damage. Therefore transformed and primary MEFs were irradiated with a sub-apoptotic dose of 50 J/m^2 UVB and the amount of remaining DNA CPDs analyzed at 0, 8, 24, and 48 hours (Figure 15). In all experiments and cell types, the amount of CPDs progressively decreased after 0 hours and the amount of DNA damage at the last time point was significantly less than the first. There remained residual CPDs at the last time point in all experiments; experiments that included an extended 72 hours time point showed that CPDs were not completely removed even after extended periods of time (data not shown). Despite slightly higher levels of residual damage in the Msh2-deficient UVB-treated samples, there were no significant differences between the

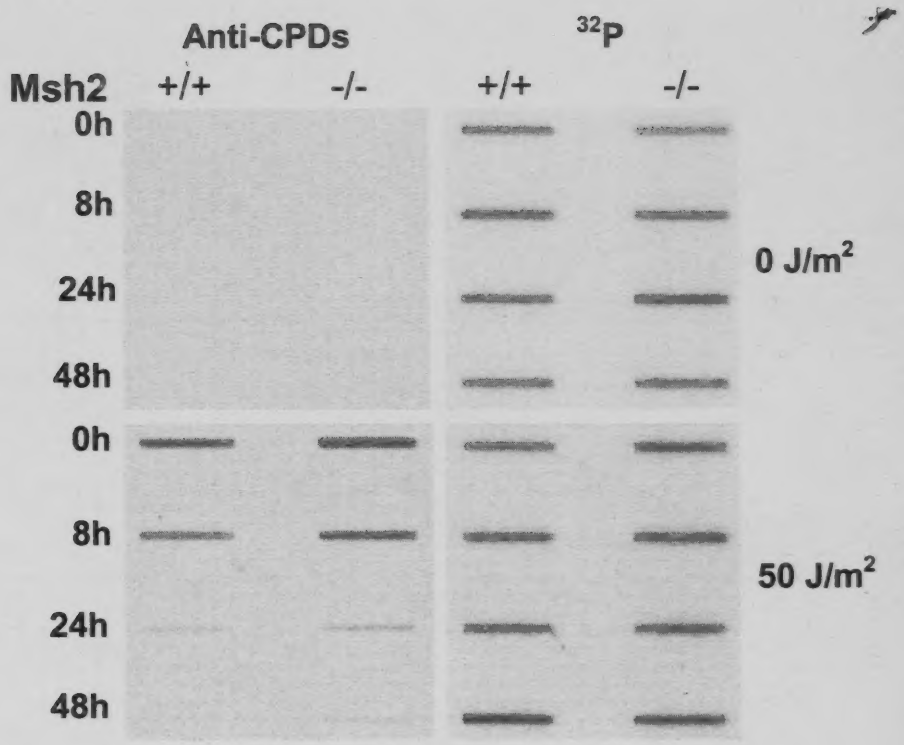

Figure 15. Both wild-type and Msh2-deficient MEFs are capable of repairing UVB-induced thymidine dimers. DNA from UVB-irradiated (lower left) and mock-irradiated (upper left) transformed MEFs was fixed to a membrane and probed with a thymidine dimer-specific antibody as described. The same membranes were later probed with radio-labeled genomic DNA to standardize the amount of DNA loaded in each slot (upper and lower right). The number of hours cells recovered after UVB treatment are indicated in the far left column, and the doses of UVB are indicated on the far right column. Experiments were done in triplicate for both primary and transformed MEFs.

rate of CPD removal of wild-type and Msh2-deficient cells, in both transformed and primary MEFs by densitometry, indicating that using this assay, Msh2 may not be essential for repair of CPDs. Therefore, this result suggests that Msh2-deficient cells used for subsequent experiments are not disadvantaged in terms of NER.

Msh2-deficiency in primary and transformed MEFs enhances cell survival post-UVB. One standard method of evaluating whether a molecule is essential for the cellular response to DNA damage (or any cellular stress), such as cell cycle arrest or apoptosis, is the assessment of cytotoxicity. The clonogenic survival assay measures cytotoxicity by counting only the cells that survive and are capable of reproduction. Unfortunately, primary MEFs are not capable of surviving on a standard tissue culture plate in the sparse quantities required for a clonogenic survival assay. Therefore, primary MEFs were subjected to a basic semi-quantitative cell survival assay that measured cell survival post-UVB but did not differentiate senescent cells from viable cells.

Primary MEFs were treated with 0 – 250 J/m^2 UVB and stained with crystal violet, which is retained by only live cells; the density of crystal violet stain minus the density of a blank culture plate was taken to reflect the number of cells that survived UVB irradiation (percentage survival compared to 0 J/m^2 control). *Msh2*$^{-/-}$ primary MEFs displayed significantly better survival post-UVB than *Msh2*$^{+/+}$ primary MEFs (Figure 16). The LD50 (the dose that 50% of cells survived) of UVB in *Msh2*$^{-/-}$ was 155 J/m^2, whereas that of *Msh2*$^{+/+}$ primary

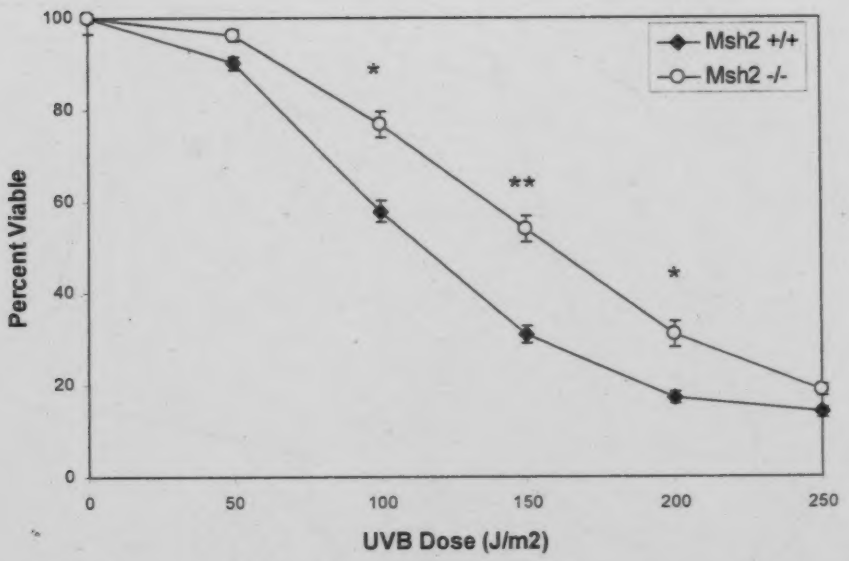

Figure 16. Msh2-deficient primary MEFs exhibit increased survival post-UVB. Msh2-deficient and -proficient primary MEFs were irradiated with 0 to 250 J/m2 of UVB and stained after 48 hours recovery for viability using crystal violet. Viability was defined as the density of stain as a percentage of untreated cells. Data, mean ± SE. Data are representative of at least two independent experiments with three plates for each dose. Comparison between *Msh2*$^{+/+}$ and *Msh2*$^{-/-}$ cells were made using the unpaired Student's *t* test. *, P<0.05; ** P<0.01.

MEFs was 110 J/m^2.

Transformed MEFs, on the other hand, are capable of clonogenic growth, and thus their viability post-UVB was tested using a clonogenic survival assay. The assay, which tests the individual cell's capacity to overcome DNA damage, demonstrated that transformed MEFs MS5-7 (*Msh2*$^{-/-}$) produced a slightly yet significantly ($P<0.05$) greater number of colonies post-UVB than BC1-6 (*Msh2*$^{+/+}$) at 20 to 50 J/m^2 (Figure 17). The LD50 of UVB for MS5-7 cells was approximately 32 J/m^2, whereas that of BC1-6 cells was approximately 26 J/m^2.

MEFs deficient in Msh2 undergo less post-UVB apoptosis than those that express Msh2. In order to determine whether Msh2 is involved in the activation of apoptosis in response to UVB DNA damage, both primary and transformed MEFs were irradiated with UVB and early apoptosis levels were measured using FACScan analysis. Cells were stained with Annexin V, a polypeptide that recognizes and binds to apoptotic membrane marker phosphatidylserine, conjugated to FITC, a fluorescent dye that enables detection of Annexin V-bound cells by FACScan. Vital dye propidium iodide (PI), which intercalates DNA, was used as a counterstain to indicate the integrity of the cell membrane. Therefore, cells that stain negative for both Annexin V and PI are intact and non-apoptotic (Figure 18, bottom left quadrant of each plot); cells that are in early apoptosis stain positive for Annexin V and negative for PI (bottom right quadrant); cells that are in late apoptosis or those that are already dead stain

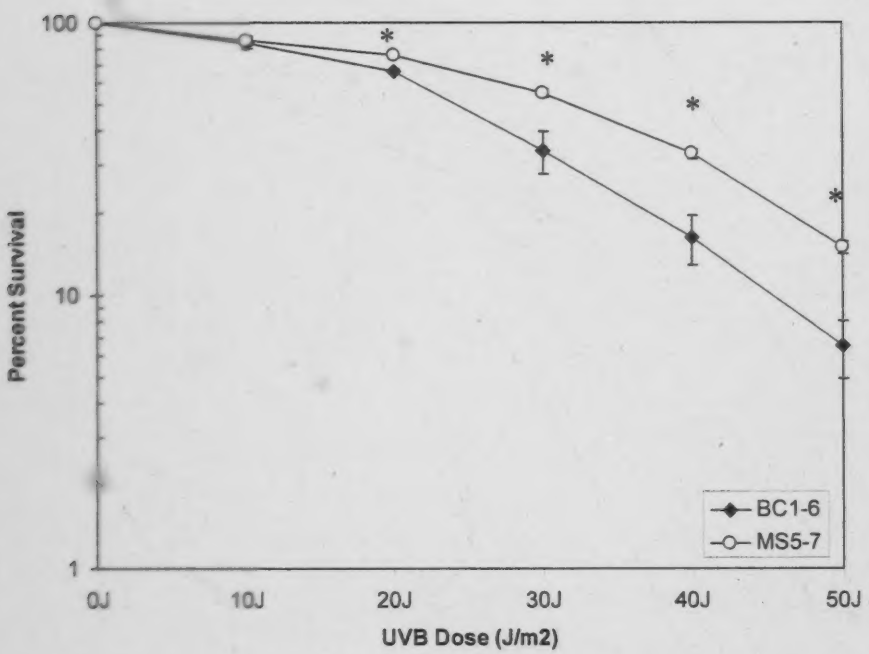

Figure 17. The absence of Msh2 in transformed MEFs enhances post-UVB clonogenic survival. Transformed MEFs were seeded, irradiated with 0-50 J/m^2 UVB, and allowed to grow for 7 days. Plates were stained with crystal violet and colonies with >50 cells were scored. Data, mean ± SE. Standard error bars for MS5-7 are hidden by the data point symbols. Data represents at least 3 independent experiments of 3 plates per dose. Comparisons between BC1-6 and MS5-7 were made using the unpaired Student *t* test. * $P<0.05$.

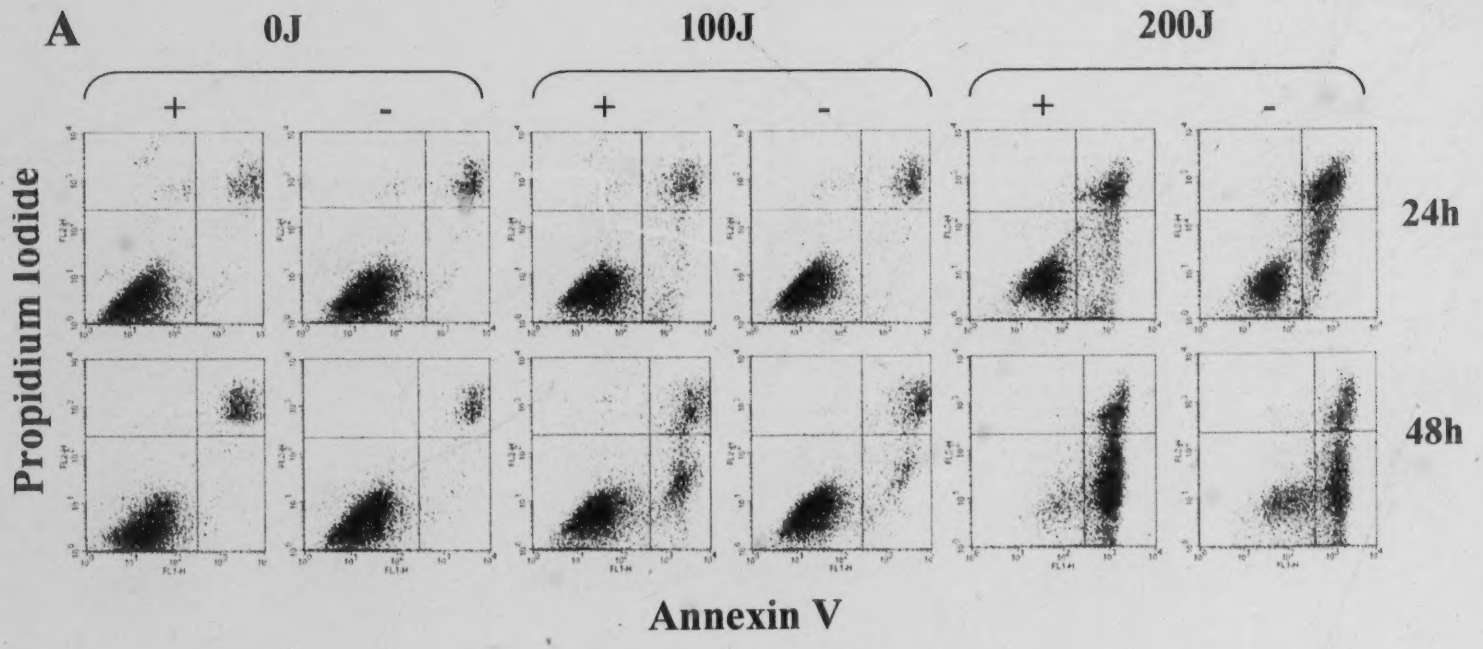

Figure 18. Msh2-deficient primary MEFs undergo less apoptosis than wild-type. FACScan plots (representative of 3 experiments) of fluorescence of PI (y-axis) vs. Annexin V (x-axis). Annexin V-/PI- represent viable cells; Annexin V+/PI- represent early apoptotic cells; Annexin V+/PI+ represent late apoptotic or necrotic cells. For each genotype (+ and – represent Msh2 status) plots are shown for 24 and 48 hours after 0, 100, and 250 J/m^2 UVB.

positive for Annexin V and positive for PI (top right quadrant). My data analyses focused largely on the early apoptotic population of cells (bottom right quadrant). Figure 18 shows the FACScan plots of cellular fluorescence of primary MEFs treated with 0, 100, and 250 J/m^2 UVB sampled after 24 and 48 hours. The doses for the experiments were chosen because comparisons between the apoptotic response of *Msh2*$^{+/+}$ and *Msh2*$^{-/-}$ primary cells were desired for at least two doses that induced different apoptotic kinetics. The cells that underwent a mock UV treatment displayed less than 2% apoptosis after 24 hours and less than 3% apoptosis after 48 hours in both genotypes, confirming a low basal amount of apoptosis under normal culture conditions (Figure 19). 100 J/m^2 represents the dose at which a moderate amount of apoptosis occurs at 24 hours (16.9 ± 1.3% in wild-type and 10.2 ± 1.0% in *Msh2*$^{-/-}$), while after 48 hours most of the cell population is still viable. In contrast, 250 J/m^2 represents a dose at which a large amount of apoptosis occurs at 24 hours (33.62 ± 3.87% in wild-type and 24.22 ± 6.38% in *Msh2*$^{-/-}$) and at 48 hours the cell population in early apoptosis represents the majority (78.13 ± 3.53% in wild-type and 67.94 ± 11.29% in *Msh2*$^{-/-}$). At doses higher than 250 J/m^2, the prominent response was necrosis and the cells could not be stained for analysis. Significantly fewer *Msh2*$^{-/-}$ primary MEFs underwent apoptosis post-UVB at both 100 and 250 J/m^2 than wild-type MEFs ($P<0.05$) (Figure 18 and 19). A UVB dose response was observed with more apoptosis occurring at 250 J/m^2 than at 100 J/m^2 in both *Msh2*$^{+/+}$ and *Msh2*$^{-/-}$ MEFs, but the percentage of post-UVB apoptotic cells in the population at all time points was lower in the absence of Msh2.

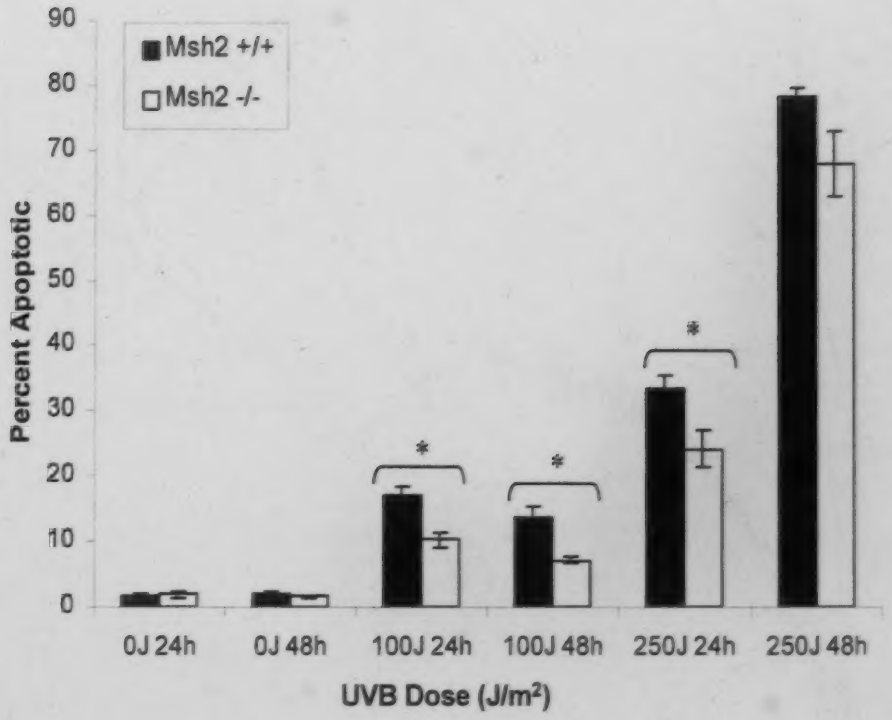

Figure 19. Msh2-deficiency confers significant resistance to UVB-induced apoptosis. A) Percent early apoptosis (Annexin V +/PI -) of wild-type and Msh2-deficient primary MEFs at 0, 100, and 250J/m^2 after 24 hours of recovery. Data, mean ± SE. Data represents at least three independent experiments. Comparisons between Msh2+/+ and Msh2-/- were made using the unpaired Student *t* test. *, $P<0.05$.

To confirm the effect of Msh2-deficiency on post-UVB apoptosis in a different cell type, and for possible insight into the role of p53 in MMR-mediated apoptosis, I utilized TAg-transformed MEFs, in which p53 is bound and inactive, to compare the apoptotic response of wild-type versus Msh2-deficient MEFs. Figure 20 shows the FACScan plots of cellular fluorescence of transformed MEFs treated with 0, 50, 100, 150, and 200 J/m^2 UVB sampled after 24 and 48 hours. The doses for the experiment were chosen because they all displayed unique characteristics with regards to the percentage apoptotic cells at each time point. The samples subjected to mock UV treatment underwent a low basal amount of apoptosis, at less than 1% after 24 hours and less than 3% after 48 hours for both genotypes (Figure 21). At 50 J/m^2 the apoptotic response was less than 10% after 24 hours, and decreased after 48 hours. At 100 J/m^2 the apoptotic response increased to 41 ± 3.34% for BC1-6 and 29.22 ± 2.80% for MS5-7 at 24 hours, the maximum percentage of apoptosis of all doses at 24 hours. Indeed, the UVB-dose response seems to be saturated at 100 J/m^2 for the transformed MEFs, and at doses above 100 J/m^2, the Msh2-deficient MEFs become increasingly resistant to UVB. At 150 and 200 J/m^2 apoptosis actually decreased compared to 100 J/m^2 at 24 hours; for example, in MS5-7 cells apoptosis at 150 and 200 J/m^2 underwent a 0.56 and 0.46 times decrease respectively.

By 48 hours the transformed MEFs treated with 100 J/m^2 or more were almost completely early or late apoptotic; indeed, the apoptotic response at 48 hours was not analyzed for statistical significance in the transformed MEFs because the large majority of cells were in stages of early or late apoptosis,

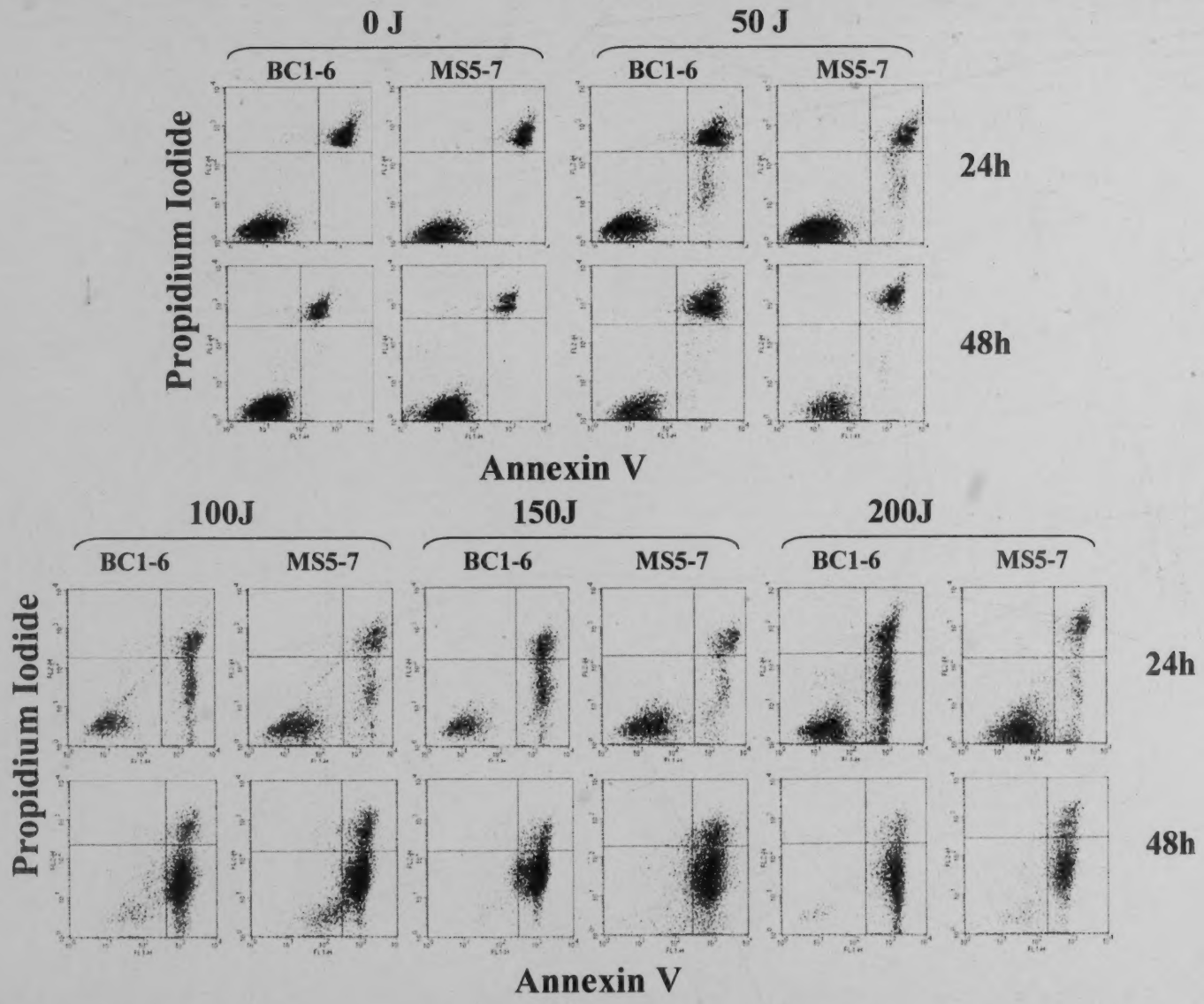

Figure 20. Msh2-deficient transformed MEFs undergo less apoptosis than wild-type. FACScan plots as described in Figure 18. For each genotype plots are shown for 24 and 48 hours after 0, 50, 100, 150, and 200 J/m^2 UVB.

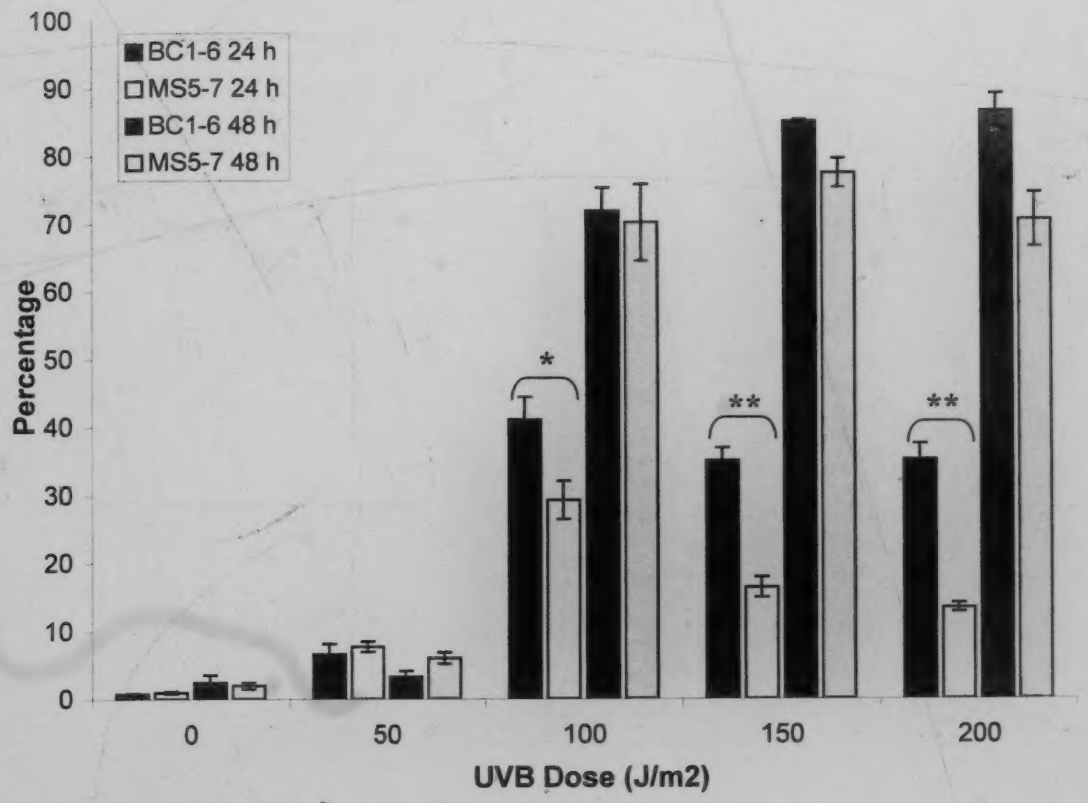

Figure 21. Msh2-deficiency confers significant resistance to UVB-induced apoptosis. Percent early apoptosis (Annexin V +/PI -) of transformed MEFs BC1-6 and MS5-7 at 0, 50, 100, 150, and 200 J/m^2 after 24 and 48 hours of recovery. Data, mean ± SE. Data represents at least three independent experiments. Comparisons between Msh2+/+ and Msh2-/- were made using the unpaired Student *t* test. *, $P<0.05$; **, $P<0.01$.

making the quadrants difficult to resolve and the data less accurate. However, the anticipated dose response was more apparent after 48 hours, with the percentage early apoptotic cells increasing from approximately 70% at 100 J/m^2 to 85% (BC1-6) and 77.5% (MS5-7) at 150 J/m^2, and increasing further in BC1-6 cells to 86.6% at 200J/m^2, whereas a decrease to 70.5% at 200 J/m^2 occurred in MS5-7 cells.

At 50 J/m^2 the percentage of apoptosis in both Msh2-deficient (MS5-7) and wild-type (BC1-6) transformed MEFs was very small and there was no detectable difference between the two cell lines. The percentage of apoptosis in Msh2-deficient transformed MEFs (MS5-7) at all higher doses was significantly less than that of wild-type (BC1-6) ($P<0.05$) after 24 hours (Figure 21). MS5-7 cells also displayed less apoptosis than BC1-6 after 48 hours with doses of 150 and 200 J/m^2.

Interestingly, the transformed MEFs were sensitized to apoptosis at 100 J/m^2 compared to primary MEFs; the proportion of primary MEFs that underwent apoptosis at 24 hours was 16.9 ± 1.3% in wild-type and 10.2 ± 1.0% in *Msh2*$^{-/-}$ cells (Figure 19), whereas in transformed MEFs apoptosis increased to 41.0 ± 3.3% in wild-type and 29.2 ± 2.8% in *Msh2*$^{-/-}$ cells (Figure 21), approximately a 2.4 to 2.9 times increase in UVB-induced apoptosis respectively. Furthermore, the amount of early apoptotic cells declined at 48 hours in primary MEFs, whereas an increase was seen in that of the transformed MEFs. However, doses of 150 and 200 J/m^2 induced approximately the same amount of apoptosis in transformed wild-type as 250 J/m^2 did in primary wild-type MEFs.

That wild-type MEFs consistently underwent significantly more UVB-induced apoptosis than *Msh2*$^{-/-}$ MEFs indicates that Msh2 is required to optimize apoptosis induced by UVB.

Msh2-deficient primary and transformed MEFs display less caspase 3 and PARP cleavage than Msh2-proficient MEFs. In order to confirm that the results obtained with FACScan analysis indeed represent differences in apoptotic cell death among genotypes, I examined levels of cleavage of caspase 3, a late effector of apoptosis (Figure 3), and poly(ADP-ribose) polymerase-1 (PARP), a target for cleavage by the active caspase 3 cleavage product, using Western blot. Levels of both cleaved caspase 3 and cleaved PARP are commonly interpreted quantitatively to indicate levels of apoptosis. Wild-type primary MEFs treated with 200 J/m^2 UVB, a dose that induced considerable levels of apoptosis according to Annexin V-FITC experiments (Figure 19), exhibited cleavage of caspase 3 at 24 hours post-UVB; in contrast, a reduced amount of both 20 and 17 kDa cleavage products was observed in the Msh2-deficient cells (Figure 22A). At 32 hours the amount of cleaved caspase 3 in wild-type cells increased while that of Msh2-deficient cells declined, intensifying the difference (Figure 22A). A similar pattern was observed in transformed MEFs irradiated with 200 J/m^2: Msh2-deficient cells exhibit less cleavage of caspase 3 than wild-type at 24 hours post-UVB (Figure 22B).

Furthermore wild-type transformed MEFs showed more cleavage of PARP than did those deficient in Msh2 24 hours after 200 J/m^2 UVB (Figure

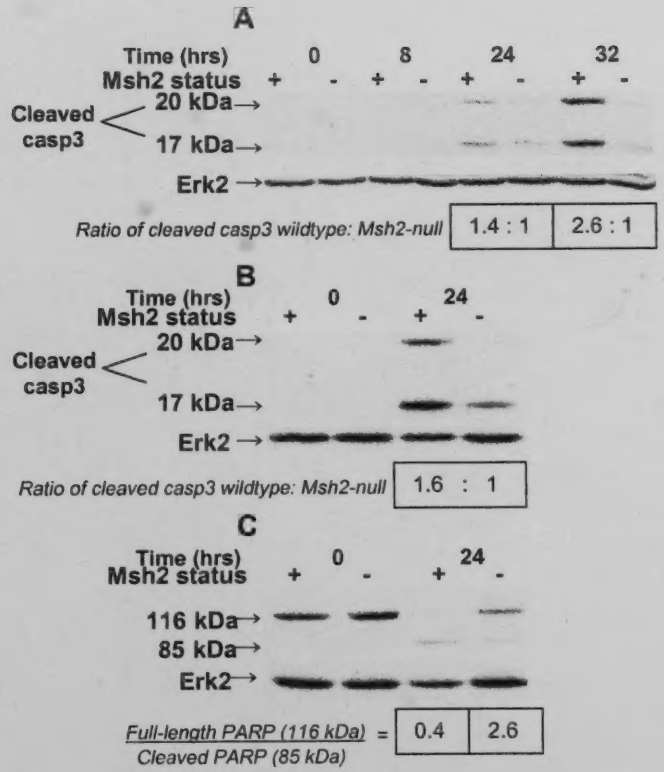

Figure 22. Msh2-deficient MEFs express less cleaved caspase 3 and less cleaved PARP than wild-type. Primary and transformed MEFs were treated with 200 J/m^2 UVB as described and harvested at the indicated time points. Whole cell lysates of floating and attached cells were separated on 13% or 7.5% SDS-PAGE gels and subjected to Western blot analysis with an antibody specific to cleaved caspase 3 or PARP. Equal loading was confirmed by probing the same blot with Erk2-specific antibody and by staining the blot with amido black. Data are respresentative of at least two independent experiments. A) Caspase 3 cleavage in Msh2 proficient (+) or deficient (-) primary MEFs treated with 200 J/m^2 UVB. B) Caspase 3 cleavage in transformed MEFs BC1-6 (+) and MS5-7 (-) treated with 200 J/m^2 UVB. C) PARP cleavage in transformed MEFs BC1-6 (+) and MS5-7 (-) treated with 200 J/m^2 UVB.

22C), following the same pattern as cleavage of caspase 3. Unfortunately, I was unable to detect the PARP cleavage product in primary MEFs possibly due to a low level of expression.

Therefore analysis of levels of caspase 3 and PARP cleavage confirms the results from the apoptosis experiments using Annexin V: in response to UVB irradiation, transformed and primary MEFs deficient in Msh2 display a reduced or impaired apoptotic response.

P53 activated by phosphorylation at serine 18 is more abundant in the presence than in the absence of Msh2. An important part of substantiating the role of MMR in the facilitation of apoptosis post-UVB is the elucidation of a molecular mechanism involved in the pathway of apoptosis. To determine the possible role of p53 in UV-induced apoptosis with respect to Msh2, I investigated its level of both expression and phosphorylation on serine 18 (corresponding to human serine 15). I preferred to examine p53 expression and phosphorylation at a dose of UVB that induced a stress response but did not induce a dramatic apoptotic response so that a time course could be followed while the majority of cells maintained viability. For the primary MEFs the desired effect was found at 100 J/m^2. After exposure to 100 J/m^2 UVB, p53 expression increased in response to UVB, but its expression levels appeared to be the same in the presence or absence of Msh2 (Figure 23B). In contrast, Msh2-deficient primary MEFs showed a diminished ability to phosphorylate p53 at ser15 at 8 hours and 24 hours post-UVB, but the levels seem to equilibrate by 32 hours (Figure 23B). This difference

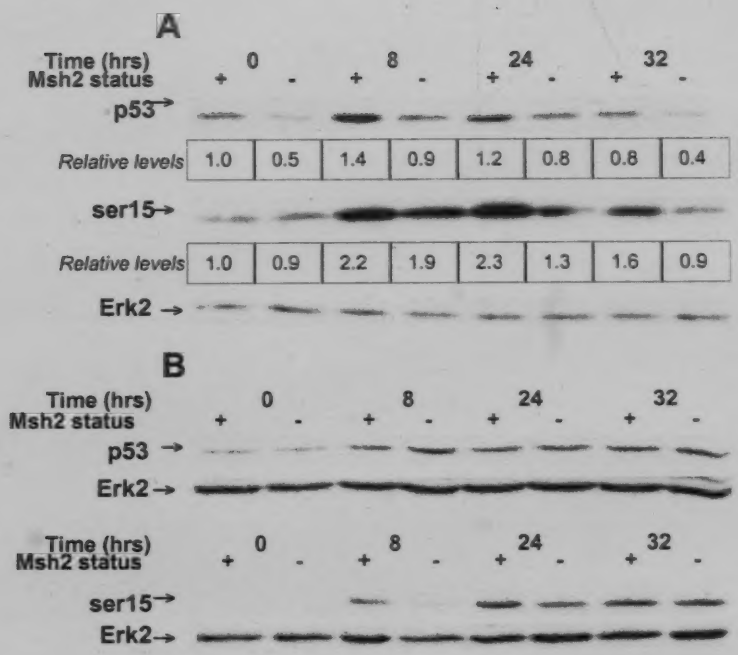

Figure 23. P53 expression and activation by phosphorylation of ser15 in primary and transformed MEFs post-UVB. Primary and transformed MEFs were treated with UVB as previously described and whole cell lysates were separated on 7.5%-13% SDS-PAGE gels and subjected to Western blot analysis using antibodies against p53 and serine 15- phosphorylated p53. A) P53 expression and phosphorylation in transformed MEFs BC1-6 (+) and MS5-7 (-) treated with 100 J/m^2 UVB. B) p53 expression and phosphorylation in primary MEFs proficient (+) and deficient (-) in Msh2 treated with 200 J/m^2 UVB.

was also observed at 200 J/m^2 but the contrast was less apparent (data not shown). In the case of transformed MEFs, I detected a basal level of phosphorylated p53 even at an uninduced state, perhaps simply because TAg-bound p53 has a longer half-life and there was an abundant amount of substrate for the kinase that phosphorylates it. Unlike the primary MEFs, p53 was more abundant in wild-type than *Msh2*$^{-/-}$ transformed MEFs both pre- and post-UVB at all time points (Figure 23A). Moreover, Msh2-deficient transformed MEFs MS5-7 showed strikingly less p53 phosphorylated on ser 15 than wild-type at all time points after UVB (Figure 23A).

P21 accumulated less in Msh2-deficient primary MEFs: In order to examine possible effects of the lowered levels of activated p53 in Msh2-deficient MEFs, and to confirm the inactivation of p53 transactivational activity in transformed MEFs, I examined the expression levels of p21$^{waf1/cip1}$, a transcriptional target of p53. p21 was upregulated by 8 hours in response to UVB at both 100 and 200 J/m^2 to slightly higher levels in wild-type than Msh2-deficient primary MEFs (Figure 24 A, B). However, in transformed Msh2 MEFs the response was significantly different. As expected, p21 transactivation was not nearly as efficient or long-lasting in wild-type transformed cells compared to primary MEFs (Figure 24 C,D). With 100 J/m^2 UVB, p21 expression increased at 8 hours in wild-type transformed MEFs but decreased to a low level at 24 and 32 hours post-UVB, and with 200 J/m^2 UVB, it increased gradually until a peak at 24 hours with a gradual decline by 32 hours (Figure 24 C,D). In contrast, Msh2-

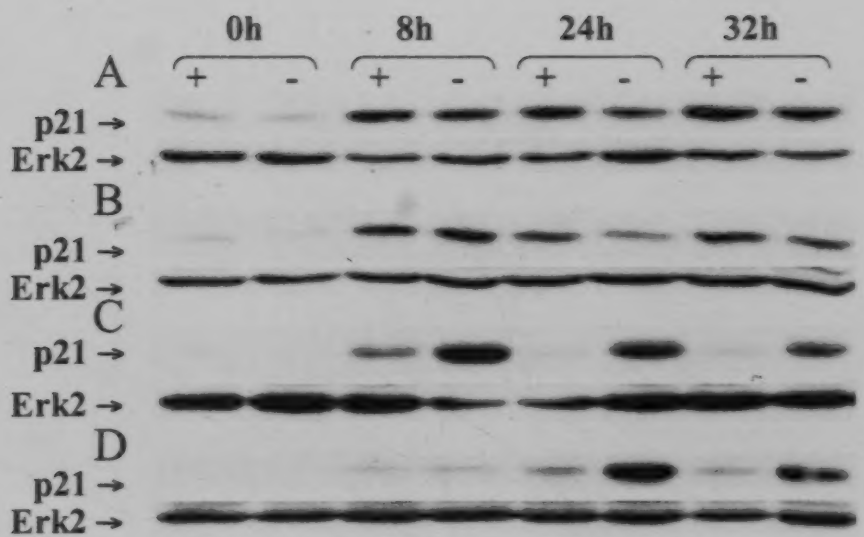

Figure 24. P21 expression in primary and transformed MEFs. Primary and transformed MEFs were treated with UVB as previously described and whole cell lysates were separated on 12-15% SDS-PAGE gels and subjected to Western blot analysis with p21-specific primary antibody. Membranes were probed subsequently or simultaneously with Erk2 primary antibody as a loading control. A) p21 expression in primary MEFs treated with 100 J/m^2; B) primary MEFs treated with 200 J/m^2; C) transformed MEFs treated with 100J/m^2; and D) transformed MEFs treated with 200 J/m^2. Western blot data is representative of at least two independent experiments.

deficient transformed MEFs reacted to 100 J/m^2 UVB with a dramatic upregulation of p21 by 8 hours that held steady for at least 32 hours (Figure 24 C,D). Similarly, after 200 J/m^2 UVB Msh2-deficient transformed MEFs displayed the same low level of p21 upregulation as wild-type cells, but by 24 hours post-UVB a dramatic increase in p21 expression occurred and remained for at least 8 more hours (Figure 24 C,D).

Msh2-deficient mice develop UVB-induced skin tumours more quickly than wild-type mice. To determine whether Msh2 deficiency has an *in vivo* effect on tumorigenesis, and to generate tumour tissue for further analysis on the molecular pathogenesis involved, I participated in a study that involved chronic exposure of *Msh2*$^{+/+}$ and *Msh2*$^{-/-}$ mice with shaven backs to UVB in order to compare their rate of skin tumourigenesis. A total of 29 *Msh2*$^{+/+}$ mice were irradiated, all of which developed skin tumours within the 37 weeks allocated; 27 *Msh2*$^{-/-}$ mice were irradiated, and only 8 developed skin tumours because many died of thymic lymphomas before completion of the study. A Kaplan-Meier survival curve was generated by Dr. Leah C. Young, postdoctoral fellow (Figure 25); the survival curves for both genotypes horizontally track the cumulative dose of UVB, dropping vertically each time a mouse developed a skin tumour. The deaths or treatment withdrawals unrelated to skin tumorigenesis were marked with a vertical stroke at the point corresponding to the total UVB dose incurred. The Kaplan-Meier curve clearly demonstrates an increased propensity for skin tumour development in *Msh2*$^{-/-}$ mice. Statistical analysis, performed by Dr. Leah

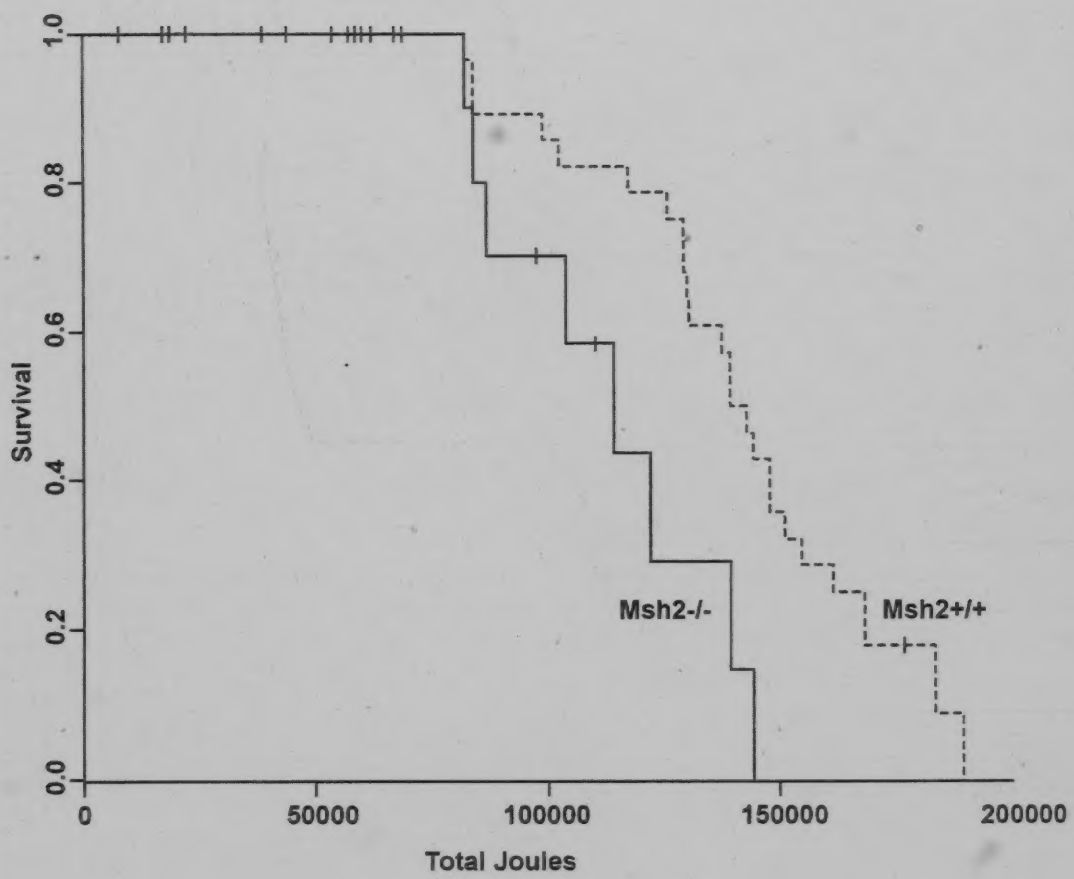

Figure 25. Kaplan-Meier survival curve showing skin tumour development for *Msh2*$^{+/+}$ and *Msh2*$^{-/-}$ mice after chronic doses of UVB (Dr. Leah C. Young). The survival curve descends vertically to demarcate the time at which a skin tumour developed. Vertical strokes in the survival curve indicate a death without development of a skin tumour.

C. Young, indicates that the difference in the rate of skin tumour development is statistically significant (P=0.0134). Histological analyses of the skin tumours are in progress and beyond the scope and timeframe of my thesis and therefore will not be reported here.

Discussion

An increasingly broad spectrum of DNA adducts have been shown to activate a MMR-dependent pathway of apoptosis; indeed, a proposed role of MMR is as a putatively universal DNA damage sensor (Bellacosa, 2001). With respect to DNA damage induced by UV light, MutSα specifically binds CPDs and 6-4PP (Mu et al., 1997; Wang et al., 1999) but may not be involved in their repair (Rochette et al., 2002). Therefore it is reasonable to hypothesize that the repertoire of MMR as damage sensor extends to UV-induced DNA adducts. Previous studies have implicated MMR in cellular responses to UV-induced DNA damage, however no direct link between MMR and UV-induced apoptosis has yet been shown. My study provides evidence that the MMR proteins Msh2 and Msh6 respond to UVB-induced DNA damage. More specifically, Msh2-deficient MEFs show increased survival and a reduced capacity for apoptosis in response to UVB, thus supporting a role for MMR in mediating the apoptotic response to UVB-induced DNA damage. My data also implicates Msh2 in facilitating p53 activation by phosphorylation on serine 15 in response to UVB, further supporting the importance of MMR in the post-UVB cellular response and placing Msh2 upstream of p53, in addition to its known position downstream as a transcriptional target of p53 activation. Finally, this study demonstrates that Msh2 is involved in prevention of murine skin tumourigenesis; given that Msh2 may not be involved in repair of photoproducts, this result supports the hypothesis that Msh2 is

important for other post-UVB cellular responses such as apoptosis, which contribute to tumorigenesis.

Expression of the MMR proteins Msh2 and Msh6 gradually increased with time in UVB-treated primary MEFs (Figure 14), particularly after treatment with 100 J/m^2, demonstrating their responsiveness to UVB-irradiation and implying their involvement in a cellular response to the DNA damage incurred. However, the induction of Msh2 in response to UVB, particularly at 100 J/m^2, was not as pronounced in the transformed MEFs (Figure 14C) with inactive p53, as in the primary MEFs (Figure 14A), therefore Msh2 may require p53 for its complete upregulation in response to UVB. Similarly, Msh6 also accumulated in response to UVB more in primary MEFs than in transformed MEFs (Figure 14 A to D).

Msh2 has been previously reported to be upregulated *in vivo* in the murine epidermis within 30-60 minutes of UV irradiation and to remain elevated for at least 48 hours (Lu et al., 1999). Msh2 contains a p53 response element in its promoter (Warnick et al., 2001) and has been previously demonstrated in human cells to be transcriptionally activated in response to 50-100 J/m^2 UVB irradiation in a p53- and c-jun-dependent manner (Scherer et al., 2001). Induction of Msh2 in transformed MEFs was not expected because the SV40 TAg-bound p53 is presumably incapable of transactivation (Mietz et al., 1992; Segawa et al., 1993). In contrast, the hMSH6 promoter, unlike that of hMSH2, is not transcriptionally stress-inducible and does not contain a p53 response element (Szadkowski and Jiricny, 2002); instead, the heterodimerization of Msh6 with Msh2 determines the stability of Msh6, thus an upregulation in Msh6 would be expected to require a

concomitant upregulation in Msh2. Indeed, Msh2-deficient MEFs, both transformed and primary, do not exhibit any protein expression of Msh6, even after UVB irradiation (Figure 14C,D).

In light of the observation that Msh2 and Msh6 protein levels increase in response to UVB, investigation of the mRNA response of Msh2 and Msh6 is pertinent to determine whether murine Msh2 and Msh6 are transcriptionally induced in response to UVB and whether this mechanism is p53-dependent. Accumulation of Msh2 and Msh6 via post-translational mechanisms that promote increased protein stability is also a consideration in light of compelling recent evidence that in response to alkylation, hMSH2 and hMSH6 accumulation does not involve increased gene activity, but rather translocation to the nucleus with concomitant increase in mismatch binding activity due to phosphorylation by PKC and casein kinase II (Christmann and Kaina, 2000; Christmann et al., 2002).

Although Msh2 and Msh6 in primary MEFs seemed to be more inducible with UVB than in transformed MEFs, both Msh2 and Msh6 proteins were much more abundant in the transformed than the primary MEFs, as shown at 24 hours post-UVB (Figure 14A). This phenomenon was noted with all proteins detected by Western blot in this study and may therefore be a result of the greatly increased growth rate in transformed cells. In contrast, others have noted abrogation of MMR activity with SV40 transformation of a human prostatic epithelial cell line, but a mechanism was not identified (Yeh et al., 2001).

One explanation for an increase in levels of Msh2 and Msh6 in response to UVB would involve an accessory role for MMR in the repair of CPDs and 6-

4PPs, given that MMR is primarily known as a DNA repair system. However, time course experiments detecting post-UVB CPDs by DNA slot blot southWestern blot probed with a DNA adduct-specific antibody demonstrated that both primary and transformed Msh2-deficient MEFs were capable of CPD removal at approximately the same rate as their wild-type counterparts (Figure 15). Because the assay used measured only bulk levels of DNA damage in cells that remained adherent after UVB treatment, the results from three repetitions were considerably variable, presumably because considerations such as growth and death rate were not corrected. Therefore, precise comparisons between rate of repair between cell types was not possible with this assay. However, in all DNA repair experiments performed, the Msh2-deficient cells repaired photoproducts at approximately the same rate as wild-type. These results support previous observations that murine TCR may not require MMR (Sonneveld et al., 2001). Although a more stringent assay, such as those used in previously discussed studies, would be required to detect any subtle differences between *Msh2*$^{+/+}$ and *Msh2*$^{-/-}$ cells, my results allowed me to assess other cellular processes affected by MMR knowing that repair was occurring in all cell types.

Cells that are known to be deficient in TCR due to the absence of one of several proteins essential for TCR, including XPA, XPB, CSA, and CSB, are markedly more sensitive to cell death in response to UV irradiation than wild-type cells or cells lacking proteins essential for GGR but not TCR, such as XPC (McKay et al., 2001). This sensitivity in the absence of TCR correlates with a massive induction of apoptosis and a reduced ability to recover mRNA synthesis

post-UV (McKay et al., 2001). Therefore, an increase in cell death, or a decrease in clonal survival, in MMR-deficient cells compared to wild-type in response to UVB irradiation would be an indication of a role for MMR in the repair of CPDs and 6-4PPs through NER. In contrast to TCR-deficient cells, I found that Msh2-deficient cells exhibited tolerance to UVB-induced DNA damage, supporting the current contention that MMR may not be required for repair of UV-induced DNA adducts. Indeed, in this study Msh2-deficient MEFs exhibited a significant ($P<0.05$) increase in survival post-UVB, both in terms of general survival, as demonstrated using primary MEFs (Figure 16), and in terms of clonogenic survival, as demonstrated using transformed MEFs (Figure 17).

The survival assay performed using primary MEFs (Figure 16) measures post-UVB viability by quantifying only the cells that remain attached to the culture plate 48 hours after UVB treatment. The assay demonstrated that fewer *Msh2*$^{-/-}$ MEFs react to UVB treatment by necrosis or apoptosis than *Msh2*$^{+/+}$ MEFs, with significant differences at UVB doses of 100, 150, and 200 J/m^2, supporting a role for Msh2 in post-UVB survival. However, this quantification does not differentiate between the remaining attached cells that presumably include viable growing cells and viable growth-arrested cells. Therefore, the assay does not correct for the possibility that rather than a difference in the number of *Msh2*$^{-/-}$ cells that escape necrosis or apoptosis, more *Msh2*$^{-/-}$ cells may be capable of reproductive cell growth or fewer *Msh2*$^{-/-}$ cells may have undergone cell cycle arrest. The differences in reproductive cell growth would be addressed using a clonogenic survival assay; although primary MEFs are difficult to grow in

colonies and the assay was not attempted in this study, the experiment would be possible to perform in a semi-solid media. Furthermore, the differences in post-UVB cell cycle arrest were not considered in this study, but MMR-deficiency has been shown to affect either G_1/S or G_2/M checkpoints in response to other DNA adducts (Table 1), therefore cell cycle responses should be considered in response to UVB in future experiments.

The y-axis for the survival curves in Figure 16 is linear, plotting percentage viability. The resulting survival curves are straight after 50 J/m^2, but they do seem to level off at about 15% viability; this leveling is more apparent with the data from the wild-type MEFs, probably because they approach 15% viability at a lower dose than the Msh2-deficient cells. This leveling property of the survival curves may be an artifact of the way the experiment was conducted; although an empty plate stained with crystal violet was included when the plates were scanned, and the density of the empty plate was subtracted from all other values, perhaps this negative control has different staining properties than a culture plate that has grown cells and has incubated for at least 36 hours. Higher UVB doses could be tested to confirm that the curve does not descend further.

The transformed MEFs are capable of clonogenic cell growth, therefore they were subjected to the more traditional method of evaluating cellular response to DNA damaging agents, the clonogenic survival assay. *Msh2*$^{-/-}$ MEFs were significantly more capable of clonogenic cell growth after 20-50 J/m^2 UVB than *Msh2*$^{+/+}$ MEFs (Figure 17). In contrast to the cell viability assay performed using the primary MEFs, the clonogenic survival assay does differentiate surviving cells

that are viable but growth arrested from those capable of cell division, in that it only quantifies the latter. Therefore, this experiment demonstrates that Msh2-deficient cells are less likely to respond to UVB treatment by undergoing apoptosis or growth arrest than Msh2-proficient cells, thus they exhibit slight tolerance to UVB. Therefore, the effect of Msh2-deficiency on clonogenic survival in response to UVB is comparable to the effect observed in response to most of the DNA damaging agents for which a role for MMR in apoptosis has been observed (Table 1).

The y-axis of the graph used to illustrate the results of the clonogenic survival assay is numbered on a log scale, in agreement with many previous similar studies (Figure 17). Using a log scale the survival curves for both genotypes are essentially straight lines at doses higher than 20 J/m^2, substantiating the validity of the data.

Unfortunately, the clonogenic survival of the transformed MEFs and the survival of the primary MEFs cannot be compared directly to determine the possible effects of TAg expression on cell viability due to the substantially different nature of the two experiments. It may have been appropriate to subject the transformed MEFs to a cell survival assay; however, their extraordinarily rapid growth characteristics and their propensity to lift off the culture plate during rinsing made the cell survival assay impossible to perform accurately.

The small number of studies that have done clonogenic survival experiments using similar Msh2-deficient cell types have found inconsistent results. MS5-7 and BC1-6 have been used in one previous study that compared

their cytotoxicity responses to various agents. Using UVC, Fritzell et al. (1997) reported low-level sensitivity of MMR-deficient immortalized MEFs MS5-7, but they did report low-level resistance to IR and complete resistance to alkylating damage, characteristics that have been confirmed by studies in other MMR-deficient cell lines (DeWeese et al., 1998; Kat et al., 1993). Reitmair et al. (1997) similarly found conflicting results with respect to UVC sensitivity: Msh2-deficient MEFs immortalized with E7/Ras were slightly more sensitive than wild-type, whereas Msh2-deficient spontaneously immortalized MEFs were slightly resistant to UVC compared to wild-type. Studies performed in human cancer cell lines have also produced conflicting results: Mellon et al. (1996) reported a slight increase in UVC sensitivity in cell deficient in hMSH2 or hMLH1, whereas Leadon et al. (1997) reported no effect of deficiency in either hMSH2 or hMLH1 on UVC sensitivity using the same cell lines. Interestingly, these two studies did agree that hMSH2 and hMLH1 facilitated the efficiency of TCR and therefore both expected to see sensitivity to UVC in cells lacking MMR. Therefore sensitivity to UVC does not seem to be a reproducible characteristic of MMR-deficient mammalian cells, perhaps resulting from variations in UVC treatment techniques.

Although most of the studies regarding UV sensitivity in MMR-deficient cells used UVC, I investigated the clonogenic response of MMR-deficient cells to UVB radiation, the UV range most responsible for the sun's carcinogenic effects (Li and Ho, 1998). The biological effects of UVB and UVC cannot necessarily be directly compared. Several studies have shown differences in biological responses

to UVC *versus* UVB, including differential gene transactivation by p53 (Pedeux et al., 2002) and a lower ratio of CPDs to oxidized purines (Kulunesics et al., 1999), both of which may affect the role of MMR in cell survival. Rochette et al. (2002) recently surveyed the clonogenic survival of human cancer cell lines to both UVB and UVC irradiation; they found that MMR-deficient cells were significantly more resistant to both UVB and UVC than MMR-proficient cells, although the difference was more pronounced in response to UVB, supporting the results attained in my study. They also found no effect of MMR-deficiency on TCR or recovery of mRNA synthesis in response to UVB, thus providing comprehensive evidence that MMR plays no role in TCR. As discussed previously, I also demonstrated that the Msh2-deficient MEFs were capable of CPD removal using a DNA slot blot southWestern blot probing with DNA adduct-specific antibody, confirming observations that murine NER may not require MMR (Sonneveld et al., 2001). Therefore I conclude that MMR-deficiency does cause increased clonal resistance to UVB, despite conflicting literature on its resistance to UVC, and that the effects of MMR-deficiency in cellular responses to UVB radiation may not be attributed to defective DNA repair.

What function of MMR can account for the increased survival of MMR-deficient cells in response to UVB? An increase in clonogenic survival post-UVB in the absence of functional MMR may indicate a decrease in cell death through apoptosis. I decided to test the hypothesis that MMR deficiency may alter the cells' apoptotic response to UVB. Indeed, I demonstrated that the absence of

Msh2 does confer a significant reduction in the apoptotic response post-UVB in primary and transformed MEFs, supporting a role for Msh2 as a facilitator of apoptosis in the UVB DNA damage response (Figures 18 - 21). As this and other previous studies have established, DNA repair by NER is competent in both MMR-proficient and –deficient cells irradiated with UVB. However, apoptosis is activated in order to avoid excessive DNA damage and to prevent propagation of mutated cells. Thus, without MMR post-UVB apoptosis is reduced, clonogenic survival is increased, and mutagenesis presumably occurs in the increased number of surviving cells.

Several lines of evidence support the assertion that MMR may facilitate UVB-induced apoptosis; as discussed in the introduction, MMR protects from UV-induced tumorigenesis as well as mutagenesis in the absence of NER, but does not play a role in the repair of these adducts. The MMR system is becoming recognized for its role in facilitating apoptosis in response to a growing number of DNA damaging agents, including alkylating agents, oxidative agents, cisplatin, and 5FU (see Table 1). Many of the adducts produced by these agents that induce a MMR-dependent pathway of apoptosis have been shown to be specifically recognized and bound by MutSα (Table 2), as have CPDs and 6-4PPs (Mu et al., 1997; Wang et al., 1999); because MMR is not the primary mechanism for the repair of any of these adducts, their recognition by MutSα may be explained by its sensing their presence and facilitating apoptosis when their repair mechanisms are overwhelmed.

Figures 18 and 20 show the FACScan dot plots of Annexin V/PI assays for primary and transformed MEFs respectively. Although effective at identifying early apoptosis, the Annexin V assay does not necessarily distinguish between cells that have undergone necrosis from those that have undergone apoptosis; however, a time course experiment allows the tracking of a population of cells from early apoptosis to late apoptosis (bottom to top right quadrant), whereas necrotic cells would directly enter the upper right quadrant (BD Pharmingen™ Technical Data Sheet). Indeed, all of the time course experiments done in both primary and transformed MEFs (except mock treated cells) show an increase in both the lower and upper right quadrants of the dot plots from 24 to 48 hours, indicating that a portion of the cell population are undergoing apoptosis. Because the upper right quadrant includes both necrotic and late apoptotic cells, my comparison of the portion of Msh2-deficient and –proficient cell populations undergoing apoptosis focuses on the lower right quadrant, representing only cells in early apoptosis. As the graphs that correspond to FACScan studies of each cell type illustrate, considerably more *Msh2*$^{+/+}$ MEFs apoptose in response to UVB irradiation than MEFs lacking Msh2 expression (Figures 19 and 21).

Primary MEFs were subjected to 100 and 250 J/m^2 UVB, and both wild-type and Msh2-deficient cells exhibited a dose response at 24 hours post-treatment, such that 250 J/m^2 elicited a stronger apoptotic response than 100 J/m^2 (Figure 19). The responses to these two different doses displayed different kinetics: after 100 J/m^2, the percentage of early apoptotic cells peaked at 24 hours and declined by 48 hours, whereas after 250 J/m^2, the percentage of early

apoptotic cells rose from 24 hours to 48 hours. Theoretically, at any genotoxic dose, the amount of genotoxicity is such that a certain number of cells undergo rapid apoptosis, another portion arrest and attempt to repair but eventually opt to apoptose, and the rest successfully repair or tolerate the damage. Perhaps at the lower dose a limited portion of cells undergo apoptosis at different rates and at 48 hours some have progressed to late apoptosis, thereby decreasing the number of cells in early apoptosis. In contrast, at 250 J/m^2 the genotoxic dose may be such that a threshold is reached whereby almost every cell in the population is destined to undergo apoptosis or necrosis; thus at 24 hours many cells are starting the process of apoptosis and by 48 hours the vast majority of the original cells are proceeding with apoptosis or are already dead and no longer included in the analysis. Ideally more time points would have been included in this assay to better distinguish the effects of Msh2 deficiency to differentiate between a difference in rate of apoptosis and a difference in the proportion of apoptotic cells, as this distinction becomes important with therapeutic applications (Steel, 2001). Nevertheless, all time points exhibited a diminished proportion or rate of apoptosis in Msh2-deficient cells, with all differences being significant except 250J 48 hours, signifying a role for Msh2 in facilitating UVB-induced apoptosis. Interestingly, similar differences in the levels of apoptosis were found when Msh6-proficient and –deficient primary MEFs were subjected to the same experiment, indicating that both components of MutSα are important in facilitating apoptosis post-UVB (Young, submitted).

Transformed MEFs were treated with more doses of UVB, including 0, 50, 100, 150, and 200 J/m^2, simply because they were easier to culture and grew more quickly than primary MEFs, thus making them more versatile for experimentation. Similar to primary MEFs, the MMR-deficient transformed MEFs were less susceptible to UVB-induced apoptosis than wild type (Figure 21). However, several differences between the pattern of the levels of apoptosis in primary and transformed MEFs arose. First of all, whereas the primary MEFs exhibited a dose response to UVB, the apoptotic response of transformed MEFs did not fully increase with increasing dose; the amount of early apoptosis at 24 hours post-UVB did increase from 50 to 100 J/m^2, but at doses higher than 100 J/m^2 the apoptotic response decreased in both genotypes. This result is counterintuitive to the idea that more DNA damage is more likely to escape the abilities of the DNA repair system, and therefore to activate more apoptosis. However, the amount of apoptosis that occurred in response to 100 – 200 J/m^2 at 48 hours post-UVB increased to over 70% in both genotypes; the amount of apoptosis at 48 hours actually does follow a dose response in the wild-type MEFs, and all but the response at 200 J/m^2 follows a dose response in the Msh2-deficient MEFs.

Several possibilities exist to explain the relatively lower level of apoptotic response at higher doses. For example, perhaps somehow the cells react to 100 J/m^2 with more apoptosis that is executed quickly, whereas higher doses induce a response that begins with less apoptosis but progresses to a higher amount by 48 hours. It is conceivable that because the cell uses several mechanisms to induce

apoptosis, some doses of UVB activate a stronger reaction for some pathways than others. Perhaps 100 J/m^2 represents an ideal dose for the induction of Fas-mediated apoptosis, for example, accentuating the apoptotic response at this dose more so than other doses. Alternatively, it is also possible that the doses higher than 100 J/m^2 induced a significantly larger amount of necrosis that eliminated a larger number of cells from the assay (due to the eventual disintegration of dead cells) that would have been vulnerable to apoptosis before 24 hours.

Furthermore, the apoptotic response of transformed MEFs 24 hours after 100 J/m^2 UVB is also considerably higher than that of primary MEFs (Figure 19). Indeed, the primary MEFs underwent an average of 16.9 ± 1.3% with and 10.2 ± 1.04% without Msh2, whereas the transformed MEFs underwent an average of 41.0 ± 3.34% with and 29.2 ± 2.80% without Msh2 (Figures 19 and 21), constituting an increase in the amount of UVB-induced apoptosis of 2.4 – 2.9 times for BC1-6 and MS5-7 respectively compared to primary MEFs. In contrast, although none of the other doses performed in the two different experiments are the same, a dose of 250 J/m^2 at 24 hours in primary MEFs induced an average of 33.6% (*Msh2*$^{+/+}$) and 24.2% (*Msh2*$^{-/-}$) apoptotic cells, and a relatively comparable dose of 200 J/m^2 at 24 hours in transformed MEFs induced an average of 35.1% (*Msh2* $^{+/+}$) and 13.4% (*Msh2*$^{-/-}$) apoptotic cells. Therefore, although the effects of Msh2-deficiency may be different in transformed and primary MEFs, resulting in different levels of apoptosis, the wild type primary and transformed MEFs exhibit a very similar level of apoptosis, again emphasizing the uniqueness of the reaction of transformed MEFs to a dose of 100 J/m^2 UVB.

It should also be appreciated that the time course to 48 hours resulted in a large majority of cells residing in the upper and lower right quadrants of the FACScan dot plots (Figure 20); because Annexin V data is derived from the recognition of patterns of dots representing cells and placing the line separating the four quadrants appropriately, the calculated percentages of cells in each quadrant becomes inaccurate when two of the four populations are barely present, as is the case in 100 – 200 J/m^2 at 48 hours (Figure 21). However, the Annexin V/PI assay is more effective as a time course, and as a single point in time the data does not lend itself well to analysis, and therefore the 48 hours time points were included.

A final pattern that emerged from the Annexin V apoptosis assay in transformed MEFs that differed from results obtained in primary MEFs is a more dramatic difference between the amounts of apoptosis in Msh2-deficient *versus* – proficient cells. In the Annexin V/PI experiment with primary MEFs, the most substantial (statistically significant) difference between the average amount of apoptotic cells of each genotype was 9.4%, which occurred at 250 J/m^2 24 hours post-UVB (Figure 19). In contrast, in the experiment with transformed cells the largest (statistically significant) difference between the average amounts of apoptotic cells of each genotype was 21.8% (Figure 21). The reasons for the more substantial effect of Msh2 deficiency in transformed MEFs are speculative, but may be a consequence of the changes in protein expression resulting from cellular transformation with the expression of TAg, many of which are not fully understood, as discussed in paragraphs below. The expression of Msh2 was

shown to be more substantial in transformed MEFs than primary MEFs in Figure 14A; therefore given that Msh2 plays a role in post-UVB apoptosis, the effect of Msh2 deficiency may theoretically be more pronounced in a system in which it is more highly expressed.

My observation that MMR deficiency did not completely abolish apoptosis indicates that Msh2 does not play an exclusive role in facilitating apoptosis in response to UVB. Other DNA damage sensors may be activating intrinsic pathways of UV-induced apoptosis that remain intact without functional MMR, and apoptosis via extrinsic pathways, such as that involving cell death receptor Fas, is also occurring. Although MMR-deficiency results in complete tolerance to alkylation corresponding to a complete abolishment of apoptosis (Hickman and Samson, 1999; Zhang et al., 1999), other adducts show a mere reduction in apoptosis without MMR (Table 1). Because tolerance of MMR-deficient cells to alkylating agents is usually regarded in cells also deficient in MGMT (Hickman and Samson, 1999), the enzyme primarily responsible for removing DNA methylation, tolerant cells additionally lack the primary repair mechanism for alkylation-induced damage, and thus rely on MMR to repair the mismatches that occur after DNA replication. Therefore a deficiency in MMR confers a complete loss of repair and the facilitation of apoptosis. In contrast, both cisplatin- and UV-induced DNA adducts, for example, rely on NER as a primary repair system; cells deficient in MMR lack the pathway of MMR-facilitated apoptosis, but they maintain an intact NER pathway, thus DNA repair may occur. Perhaps when cells that undergo MMR-facilitated apoptosis lack both MMR and

another DNA repair pathway responsible for repair of the particular type of damage being assessed they completely lose their apoptotic response, but when cells lack MMR with functional DNA repair the apoptotic effect is partial, due to successful repair in some cells.

DNA damaging agents that induce more than one type of DNA adduct, such as UV and IR, presumably activate more than one pathway of apoptosis (Bellacosa, 2001). For example, the induction of apoptosis in response to IR is thought to result from a p53-dependent pathway in response to single- and double-strand breaks, as well as a MMR-dependent pathway in response to 8-oxo-G (Bellacosa, 2001; Hardman et al., 2001). In addition to CPDs and 6-4PPs, UVB also induces the formation of ROS, and the pathway of apoptosis activated in response to their induction is distinct and separate from that induced by DNA damage and by Fas (Kulms et al., 2002). Therefore, is it likely that the apoptosis facilitated by MEFs in this study are responding to 8-oxo-G in addition to CPDs and 6-4PPs, a factor that should be taken into consideration in future experiments concerning the signal transduction pathway of MMR-facilitated post-UVB apoptosis.

Although DNA damage is an undisputed stimulant of UV-induced apoptosis, UV does affect other molecular targets that are also capable of inducing apoptosis independent of the nuclear triggers (Kulms and Schwarz, 2002b). For example, UV can directly activate CD95 (Fas, APO-1), a cell death receptor of the tumor necrosis factor receptor superfamily, at the cellular membrane without its natural ligand CD95L (Kulms and Schwarz, 2002b).

Kulms et al. (1999) demonstrated that the almost complete abrogation of UV-induced apoptosis could be shown by abrogating death receptor-mediated apoptosis by irradiating at 4 °C and concurrently enhancing DNA repair with the addition of photolyase. It is possible, therefore, that deficiency of Msh2 in transformed and primary MEFs abrogated the nuclear stimulus for UV-induced apoptosis, but that an independent basal level of death receptor-induced apoptosis occurs equally in both Msh2-proficient and –deficient cells.

To confirm the results from the FACScan apoptosis assay, multiple assays for apoptosis must be performed. I subjected irradiated cells to Western blot using antibodies against proteins commonly used as markers for late-stage apoptosis. Caspases are a large protein family of death proteases that possess an active-site cysteine and cleave substrates at Asp-Xxx bonds, usually resulting in inactivation of their target; caspases are selective in their choice of target proteins, with their distinct substrate specificity being determined by four residues amino-terminal to the cleavage site (Hengartner, 2000). Caspases cause most of the visible changes that characterize apoptosis, and therefore are central to the process; elimination of caspase activity slows down or prevents apoptosis (Hengartner, 2000). Like most proteases, caspases begin as zymogens, containing an N-terminal prodomain, a p20 domain, and a p10 domain (Hengartner, 2000). Downstream caspases, such as caspase 3, a very late effector of apoptosis at the convergence of the mitochondrial and death receptor pathways (Figure 3), are activated by cleavage at Asp-X sites between the p20 and p10 domains by other caspases, as well as between the prodomain and p20 domain (Hengartner, 2000). In the case of

caspase 3, functional cleavage products of 12 kDa and 17 or 19 kDa result (Cell Signaling Technology Datasheet). Therefore the appearance of specific large cleavage products of 19 and 17 kDa in a Western blot signify the activation of procaspase 3, and hence the progression of apoptosis.

Primary MEFs irradiated with 200 J/m^2 UVB displayed a faint trace of 19 and 17 kDa caspase 3 cleavage products by 8 hours post-UVB, and at 24 and 32 hours the cleavage products grew increasingly abundant, with the same amount of 17 kDa as 19 kDa cleavage product (Figure 22A). Indeed, the caspase 3 cleavage products were substantially more abundant in the wild-type than the Msh2-deficient cells at both 24 and 32 hours; overall, this result clearly indicates that apoptosis was diminished without Msh2, coinciding with the conclusion from the evaluation of apoptosis with Annexin V/PI. The densitometric quantification of the signal for both caspase 3 cleavage products indicates that the ratio of cleaved caspase 3 in wild-type to Msh2-null cells is 1.4:1 at 24 hours and 2.6:1 at 32 hours, and the ratio of apoptosis in wild-type to Msh2-null cells (after 250 J/m^2) is 1.4:1 at 24 hours and 1.9:1 at 48 hours (Figure 19), indicating a fairly strong concurrence with Annexin V/PI data, particularly at 24 hours.

However, the pattern of caspase 3 cleavage in primary MEFs does not perfectly match that of Annexin V staining; the amount of caspase 3 cleavage of Msh2-deficient cells appears to have declined from 24 to 32 hours (Figure 22A), whereas the amount of apoptosis measured by FACScan after 250 J/m^2 more than doubled from 24 to 48 hours (Figure 19). This may result from the temporal sequence of apoptotic events, with caspase 3 cleavage being a prelude to the

execution steps, thus expression ends before apoptosis. Furthermore, the comparison of the two experiments assumes many things that are not certain: it assumes that the amount of caspase 3 cleavage is exactly proportional to the amount of apoptosis, that the apoptotic responses of primary MEFs to 200 and 250 J/m^2 UVB are reasonably comparable, and that the amount of apoptosis occurs in a linear fashion so that the level of apoptosis between 24 and 32 hours would be approximately half of that between 24 and 48 hours. Furthermore, since the apoptotic response after 100 J/m^2 actually declined after 24 hours, perhaps the response after 200 J/m^2 does the same; thus the threshold for mounting an apoptotic response that peaked after 24 hours may have occurred between 200 and 250 J/m^2.

The caspase 3 cleavage products were also examined in transformed MEFs irradiated with 200 J/m^2, however, the analysis only included 0 and 24 hours because the integrity of the samples obtained at 32 hours were not of sufficient quality to extract protein for a Western blot (Figure 22B). Thus unfortunately the time line of apoptotic progression examined in the Annexin V experiment cannot be compared to that of caspase 3 cleavage, but the amount of cleavage at 24 hours can be analyzed. In agreement with the FACScan analysis of apoptosis (Figure 21), the Msh2-deficient transformed MEFs exhibited less caspase 3 cleavage than wild-type. Unlike the primary MEFs, however, the transformed MEFs do not express the 17 and 19 kDa cleavage products equally; more 17 kDa than 19 kDa cleaved caspase 3 appears in wild-type MEFs 24 hours after UVB, but in Msh2-deficient MEFs only the 17 kDa cleavage product

appeared, perhaps representing a characteristic of the transformation. The ratio of the 17 kDa cleavage product of caspase 3 in wild-type to Msh2-null cells was approximately 1.6:1, whereas the ratio of percentage early apoptosis in wild-type to Msh2-null cells in the Annexin V assay was 2.6:1 at 24 hours, diminishing to 1.2:1 by 48 hours. Therefore, perhaps the comparison between Annexin V staining and caspase 3 cleavage is not as accurate as the experiment with primary MEFs had suggested, or perhaps differences between primary and transformed cells are exemplified in this case.

Another accepted protein marker for apoptosis is the cleavage of PARP from 116 kDa to 85 kDa, a protease reaction that is carried out by caspase 3; PARP is known to be a DNA repair enzyme that is inactivated by caspase 3 as a late event in apoptosis (Shen and White, 2001). This third experiment comparing the post-UVB apoptotic response of wild-type and Msh2-deficient MEFs was used to confirm the results of the Annexin V assay and the Western blot detecting caspase 3 cleavage. Also because PARP is one of the cleavage targets of activated caspase 3, a Western blot detecting PARP cleavage was used to confirm the levels of activated caspase 3 detected in Figure 22A and B. Transformed MEFs treated with 200 J/m^2 expressed full- size PARP immediately after irradiation at the same quantity in both genotypes, but 24 hours post-UVB Msh2-deficient MEFs express more PARP than wild-type; however, at 24 hours post-UVB the 85 kDa cleavage product of PARP is more abundant in wild-type than Msh2-deficient cells. The extrapolation of the amount of apoptosis in this analysis involves the ratio of full to cleaved PARP rather than their expression levels, where the cells with the

lower ratio of full-length to cleaved PARP are interpreted to be undergoing more apoptosis; in this experiment the wild-type MEFs clearly display a lower ratio of full-length to cleaved PARP, confirming the data from previous experiments.

Unfortunately, the detection of PARP in primary MEFs was not attained, even 32 and 48 hours after 200 J/m^2 of UVB; this inconsistency was unlikely to be caused by a difference in binding properties of the anti-PARP antibody, since two different antibody clones were tested. Perhaps primary MEFs simply express a low amount of PARP.

Having now established that cells that lack Msh2 undergo impaired UVB-induced apoptosis, elucidating molecules that respond differently to UVB in the absence of Msh2 may indicate the molecular signaling pathway involved and may clarify the specific role of MMR. p53 is a well-studied tumor suppressor protein that is pivotal to several DNA damage response pathways and therefore is an obvious candidate for a signal transducer or effector in the apoptotic pathway in which MMR may be the sensor. The role of p53 as a tumour suppressor is two-fold: first it prevents mutated cells from progressing through the cell cycle, and second, it initiates apoptosis in response to DNA damage (Shen and White, 2001). The decision between the two functions, aside from its dependence on cell type and environment, relates to the level of p53 expression, with low levels being correlated to cell cycle arrest, and high levels being correlated to apoptosis (Latonen et al., 2001). Moreover, overexpression of p53 directly stimulates apoptosis (Janus et al., 1999). p53 is best known as a transcriptional regulator, with capabilities of transcriptional activation and repression. Transcriptional

targets of p53 include *p21* and *14-3-3σ* for cell cycle arrest, *bak* and *bax* for mitochondrial-mediated apoptosis, and *Fas* and *DR5/KILLER* for membrane-mediated apoptosis; its transcriptional repression repertoire includes *Bcl-2*, an anti-apoptotic protein (Shen and White, 2001). Both transcriptional activation and repression capabilities of p53 are thought to be enabled by its phosphorylation on various amino acid residues (Shen and White, 2001).

The transformed MEFs that I used to demonstrate increased survival post-UVB in the absence of Msh2 have impaired p53 function, and therefore may be used to compare their apoptotic response to primary MEFs with functional p53 for insight into the possible role of p53 in MMR-mediated apoptosis post-UVB. *In vitro* transformation is a common strategy of obtaining rapidly proliferating cells with an extended capacity for division; essentially the cell has progressed toward a cancerous phenotype. One method of transformation is the transfection of viral oncogenes into the genome of a cell. Because viral propagation depends on DNA replication, several viruses have evolved methods for removing the control of the cell cycle and for inhibiting apoptosis (Roulston et al., 1999). Simian virus 40 (SV40) expresses a powerful oncoprotein called large T antigen (TAg), which is capable of transforming many cell types and inducing tumors in several animal models (Ali and DeCaprio, 2001). Its mechanism of transformation involves the binding and inactivation of key tumor suppressors including the retinoblastoma family of proteins (pRb, p107, and p130), which negatively regulates the G_1/S cell cycle checkpoint, transcriptional co-activators CBP and p300, which are important for transcription, and the transcription factor p53, which induces

apoptosis and cell cycle arrest (Ali and DeCaprio, 2001). The binding of p53 by TAg increases the stability and the steady-state levels of an inactive p53, perhaps by binding the p300/mdm2/p53 complex that targets p53 for degradation (Ali and DeCaprio, 2001). TAg complexes with p53 in its DNA-binding domain, preventing its transactivation activity, and consequently its ability to suppress homologous recombination (Mekeel et al., 1997), to regulate G_1 cell cycle progression (Bernstein et al., 2002), and to induce apoptosis (McCarthy et al., 1994; Roulston et al., 1999). Thus, using otherwise genetically identical primary and transformed cells lines can provide some initial clues as to the involvement of proteins such as p53 in cellular processes.

It is important to emphasize, however, that because TAg inactivates other molecules essential for cell cycle regulation, such as pRb and CBP/p300, the transformed cells have deficiencies other than p53. Because TAg also randomly integrates into the genome, the transformed cells may have additional anomalies that could also potentially complicate the experimental outcome. Furthermore, despite my efforts to maintain low passage, the MMR-deficient cells do accumulate post-replicative mutations with every division, thus they have an increased chance of incurring additional genetic changes, especially in combination with transformation. Therefore, SV40-transformed MEFs are not an ideal model to evaluate the role of p53 in cellular responses, but because they have used as such in many previous studies, initial clues as to the function of p53 in MMR-facilitated apoptosis will be discussed. Further experiments in cells with genetic deficiencies in both Msh2 and p53 are required to make a definitive

statement about the role of p53 in MMR-mediated apoptosis post-UVB; these experiments are underway.

I utilized an Msh2-deficient MEF cell line immortalized with SV40 TAg to ask whether p53 collaborates with Msh2 in the facilitation of UVB-induced DNA damage. If p53 were involved in the pathway of MMR-facilitated apoptosis, transformed MEFs would exhibit lower levels of apoptosis than primary MEFs, and Msh2-deficient transformed cells would exhibit still lower levels of UV-induced apoptosis than wild-type transformed MEFs if p53 acts downstream of Msh2 in the pathway. Surprisingly, transformation actually induced an increase in the amount of UVB-induced apoptosis of 2.4 – 2.9 times for BC1-6 and MS5-7 respectively compared to primary MEFs 24 hours after $100J/m^2$, which is the only dose that is directly comparable between the two cell types (Figures 19 and 21). Therefore it seems possible, at first glance, that MMR-facilitated apoptosis induced by UVB is p53 independent since post-UVB apoptosis in transformed cells was not impaired; however, TAg actually increased the sensitivity of MEFs to UVB at a certain dose, confounding this conclusion about the role of p53.

Although TAg was thought to inhibit p53-mediated apoptosis, some studies show that TAg-immortalized cells remain capable of p53-dependent apoptosis. p53 may require transactivation activity to induce apoptosis (Chao et al., 2000), but newly synthesized p53 does not associate efficiently with TAg, suggesting that rapid transport of p53 to the nucleus after UVB treatment may allow p53 to activate apoptosis before being bound by TAg (Cole and Tevethia, 2002). The transactivation domain of p53, responsible for sequence specific

transcriptional activation and repression, is followed by a poly-proline domain that is required for apoptosis and transrepression, but not for transactivation, suggesting that the transrepression activity of p53 mediates apoptosis (Shen and White, 2001). However, a substantial p53-mediated apoptosis response occurs in the absence of transcription and translocation, confirming the existence of p53-mediated apoptosis independent of sequence-specific transactivation (Shen and White, 2001).

In this study, not only did transformation not debilitate apoptosis, it actually increased the cells' apoptotic response to UVB; however, this effect of TAg is not a novel observation. A recent study by Cole et al. (2002) found sensitization of TAg-immortalilzed rat embryo fibroblasts in response to 5-FU, but this sensitization, surprisingly, did not depend on the ability of TAg to bind to p53, Rb, or p300, but rather on the integrity of the J domain of TAg, which facilitates binding of Rb; these cells also remained capable of p53-dependent apoptosis despite being bound by TAg. Thus it is possible that the apoptosis activation function of p53 is not affected by TAg and that sensitization occurred as a result of an extraneous function of TAg. Similarly, McKay et al. (1999) showed that in human cells, both p53 genetic deficiency and p53 inactivation by human papilloma virus (HPV) 16 protein E6 caused hypersensitivity to apoptosis induced by UV light, correlating to a diminished capacity to recover transcription in p53-deficient cells. This phenomenon may result from the possibility for a direct role of p53 in NER of UV photoproducts (Li and Ho, 1998). Therefore, the fact that p53 is known to play several roles in the cellular response to UV, and the

fact that the functions of p53 inactivated by TAg are not fully known or understood, makes analysis of the role of p53 in my experimental system difficult. Thus no conclusions can be made at this point about the involvement of p53 in a putative pathway of MMR-facilitated apoptosis in response to UVB; I conclude that MMR facilitates UV-induced apoptosis both in primary MEFs and transformed MEFs, which are relevant to the study because they can be likened to cells on the pathway to cancer.

Nevertheless, the involvement of p53 in MMR-mediated post-UVB apoptosis cannot be ruled out. To determine the possible role of p53 in UV-induced apoptosis with respect to Msh2, I investigated its level of expression of p53 as well as its phosphorylation on serine 18 (corresponding to human serine 15), considered to be one of the critical signals through which the p53 response to stress such as UV, including the apoptotic response, is regulated (Appella and Anderson, 2001; Unger et al., 1999). In unstressed cells, wild-type p53 is maintained at low levels through targeted degradation, but phosphorylation on serine 15, among other residues, in response to genotoxic stresses such as UVB transiently stabilize it and allow it to accumulate in the nucleus (Appella and Anderson, 2001).

Among other functions, some studies have shown that the phosphorylation of p53 at ser15 is thought to be essential for p53-dependent apoptosis (Unger et al., 1999). Indeed, I found that serine 18 phosphorylation (human ser15) is reduced or delayed in the absence of Msh2 in both primary and transformed MEFs at 100 J/m^2 (Figure 23A,B), in agreement with the lower level of apoptosis

in Msh2-deficient cells, indicating a possible role for p53 in MMR-dependent apoptosis. Based on this result alone, and in the context of apoptosis, it appears that p53 ser18 (ser15) might be a downstream effector in the pathway of mammalian MMR-facilitated apoptosis induced by UVB, because if p53 activation is debilitated without Msh2, it may be activated by Msh2 or a downstream molecule. However, is p53 ser18 (ser15) necessary for MMR-facilitated apoptosis, and furthermore, does p53 ser18 (ser15) act in apoptosis or some other cellular response mechanism such as cell cycle arrest in this experimental system?

In comparing the expression and phosphorylation of p53 between transformed and primary MEFs (Figure 23 A, B), several interesting differences emerged. First, p53 ser18 (ser15) was found to be grossly overabundant in cells expressing TAg, even at a basal state with no stress activation, in agreement with previous studies (Bowman et al., 2000). When transformed MEFs were exposed to 100 J/m^2 UVB, the levels of both total p53 and ser18 (ser15) phosphorylation increased by 8 hours and gradually began to decline by 24 hours (Figure 23A). However, throughout this time course both the p53 expression and the p53 phosphorylation in MMR-deficient cells was significantly less than that in wild-type cells; therefore the peak of p53 expression and activation was presumably lower in MMR-deficient cells. The effect of Msh2 deficiency on p53 expression in transformed cells fits with the result that p53 phosphorylation depends on Msh2, since p53 ser18 (ser15) phosphorylation increases its half-life and thereby facilitates its post-stress accumulation. In contrast, the level of p53 expression in

primary MEFs rose by 8 hours post-UVB and plateaued at least until 32 hours, but the Msh2-deficient and –proficient cells exhibited approximately the same level of expression throughout. On the other hand, the level of ser18 (ser15) in primary MEFs rose from minimal immediately after UVB to a peak at 24 or 32 hours; however, unlike ser18 (ser15) in transformed MEFs, p53 activation in MMR-deficient cells appeared to be delayed rather than diminished, as the levels between the two genotypes appeared to equalize at 32 hours. This discrepancy suggests that p53 activation is controlled differently in primary and transformed MEFs. It is known that p53 can be activated by post-translational modification without changes to its level of expression (Shen and White, 2001). Perhaps the fact that the transformed MEFs had a significantly larger amount of cellular p53 due to the increase in half-life resulting from TAg binding amplified the effect of Msh2 deficiency on p53 phosphorylation making it more pronounced than that in the primary MEFs. Of course it remains possible that the mutator phenotype of *Msh2*$^{-/-}$ cells, an effect that is amplified by transformation, resulted in a secondary mutation that caused a defect in ser18 (ser15) phosphorylation of p53 post-UVB.

UVC-induced phosphorylation of serine 392 of p53 was previously investigated and found to be independent of hMSH6 status, but the role of hMSH2 or hMLH1 had not been considered (Duckett et al., 1999). However, induction of p53 expression and phosphorylation of p53 serines 15 and 392 in response to alkylating agents that induce O^6MeG formation has been found to absolutely require MutSα and MutLα, although the mechanism for this interaction and its significance have not yet been determined (D'Atri et al., 1998; Duckett et

al., 1999; Hickman and Samson, 1999). The correlation between the pattern of diminished p53 induction and phosphorylation with MMR-deficiency resembles that of the transformed MEFs in response to UVB; considering that the studies performed using alkylating agents also used transformed cell lines, this mutual pattern may represent a property of transformed cells. As previously discussed, MMR-deficient cells are fully resistant to apoptosis in response to alkylation, suggesting that p53 ser18 (ser15) is required for apoptosis and is downstream of MMR in the putative pathway. However, the phosphorylation of p53 was not required for MMR-facilitated apoptosis in response to O^6meG in the same systems that require MMR for such phosphorylation; this result was demonstrated by expressing HPV16 E6 in normal and *Msh2*$^{-/-}$ cells and observing no difference in apoptotic response (Duckett et al., 1999; Toft et al., 1999). Furthermore, in response to other DNA adducts, p53 has been shown to be essential for some but not all pathways of MMR-facilitated apoptosis (Hickman and Samson, 1999; Li, 1999; Wu et al., 1999). Therefore, MMR seems to conduct both early p53-dependent pathways and late p53-independent pathways of apoptosis, some requiring MMR for p53 phosphorylation and some not (Toft et al., 1999). Thus p53 does seem to have a role in MMR-facilitated apoptosis in response to DNA damage, but its role seems neither clearly defined nor essential.

How can one reconcile the dependence on MMR for p53 phosphorylation and the apparent lack of dependence on p53 for apoptosis? A. Bellacosa (2001) proposed that given that p53 plays two separate roles in the cellular response to DNA damage, namely regulation of cell cycle arrest and apoptosis, the

phosphorylations of ser-15 and -392 in response to alkylating agents may be initiated by MMR proteins as part of a signal transduction pathway that results in cell cycle arrest, but not apoptosis (Figure 12). He further argued that phosphorylation on ser-46 of p53 instead is pivotal to p53-mediated apoptosis (Bellacosa, 2001). p53-regulated apoptosis-inducing protein 1 (p53-AIP1) has been shown to be transactivated after phosphorylation of ser46 and to be necessary for apoptosis after UV-induced damage (Oda et al., 2000). In support of this hypothesis, p53 modifications and its pattern of induction have been shown to be highly dependent on UV dose: low doses induced quick p53 accumulation that declined by 24 hours, high amounts of ser15 and ser33, and cell cycle arrest; high doses induced p53 after a delay but high levels maintained after 24 hours, delayed phosphorylation of ser15 and ser33, and apoptosis (Latonen et al., 2001). Accordingly, in the context of my study using UVB irradiation, the decrease in p53 phosphorylated on ser18 (ser15) in the Msh2-deficient MEFs (Figure 21) may not be indicative of the debilitated apoptotic pathway shown by other experiments, but rather indicative of a decrease in the ability of p53 to signal cell cycle arrest. This hypothesis is supported by the observation that the phosphorylation of ser18 (ser15) is less equal between Msh2-proficient and – deficient primary MEFs at 100 J/m^2 than at 200 J/m^2 (data not shown), the former being more likely than the latter to induce an effective cell cycle arrest that enables cells to repair their damaged DNA. The same pattern occurs in ser18 (ser15) phosphorylation of transformed MEFs, with more contrast between genotypes occurring at 100 J/m^2 than at 200 J/m^2; however, the Annexin V/PI

assay revealed that more apoptosis occurred at 100 than 200 J/m^2 at 24 hours, but whether the DNA damage stress response was higher at 100 than at 200 J/m^2 is not known. Perhaps the induction and phosphorylation of p53 should have also been tested in transformed MEFs using 50 J/m^2, a dose that does not induce substantial apoptosis, to determine whether a cell cycle arrest-inducing dose displays different kinetics.

Induction of p21$^{waf1/cip1}$, a well known transcriptional target of p53 that effects G_1 cell cycle arrest in response to genotoxic stress with its potent cyclin-dependent kinase inhibitor activity (Li and Ho, 1998), was compared in *Msh2*$^{-/-}$ and *Msh2*$^{+/+}$ primary MEFs in light of the pattern of p53 ser15 phosphorylation (Figure 24 A,B). p21 induction has been shown to require p53 ser15, and thus in the case of alkylation, requires MutSα for its induction (D'Atri et al., 1998). Similar to the pattern of p53 activation and expression, in response to UV, p21 has been found to be rapidly induced in response to low but not high doses of UV, a pattern opposite to that of apoptosis-activating gene *Bax* (Latonen et al., 2001). Experiments to confirm a decrease in G_1 cell cycle arrest in the absence of MMR and its potential dependence on p53 would therefore be pertinent to the study of the role of MMR in post-UVB genotoxic stress.

Primary MEFs exhibit an increase in p21 expression by 8 hours post-UVB with treatment of both 100 and 200 J/m^2, but the difference between Msh2-deficient and wild-type cells is almost negligible. Interestingly, the induction of p21, a known effector of cell cycle arrest, is slightly less substantial at 200 J/m^2 than at 100 J/m^2, possibly supporting the suggestion made earlier that the reason

the difference in p53 activation was more apparent at 100 J/m^2 was that it may be more involved in cell cycle arrest than apoptosis. p21 expression in transformed cells was examined in order to analyze the effects of SV40 transformation on p53 transactivation. Being a known direct transcriptional target of p53, one might assume that p21 expression would be abrogated in cells transformed with SV40 TAg (Ali and DeCaprio, 2001). Indeed, *Msh2*$^{+/+}$ transformed MEFs exhibit a low level of expression of p21 even after UVB irradiation of 100 or 200 J/m^2 (Figure 24 C, D), aside from a brief increase in p21 expression 8 hours after 100 J/m^2 UVB, possibly due to *de novo* p53 not yet bound by TAg (Cole and Tevethia, 2002). However, *Msh2*$^{-/-}$ transformed MEFs show extremely high expression of p21 post-UVB, 8 hours after 100 J/m^2 and 24 hours after 200 J/m^2, despite the fact that p53 expression in *Msh2*$^{-/-}$ cells is less than that of *Msh2*$^{+/+}$ cells (Figure 24 C, D). Thus in transformed MEFs, the p21 induction does not seem to depend on the function of MMR, but rather seems to depend on the absence of Msh2. With no known previous data on possible regulatory interactions between Msh2 and p21, this anomaly may only be explained by either an acquired mutation in the promoter region of the *p21* gene, or a mutation in a regulatory protein of p21. Whether this extraordinary expression of p21 in the absence of Msh2 has an actual effect on cell cycle arrest or even cell survival awaits further experiments specifically assaying cell cycle arrest.

My experiments suggest that in response to UVB, Msh2 facilitates apoptosis as well as ser15 phosphorylation and stabilization of p53 in transformed MEFs, supporting the proposed model of MMR as a DNA damage sensor

initiating signal transduction pathways of either cell cycle arrest or apoptosis, depending on the severity of DNA damage (Figure 12). Why the putative pathway is different in primary MEFs is unclear. However, the transducers and effectors of this proposed pathway have yet to be clarified in detail, and this information is pertinent if the properties of MMR as damage sensor are to be applied to the clinical setting. The role of p53 in executing MMR-facilitated cell cycle arrest is hypothetical and its confirmation awaits analysis of post-UVB apoptosis using MMR and p53 genetically mutant cells rather than the ambiguous inactivation of p53 by TAg expression. It does remain possible, therefore, that p53 does play a role in post-UVB apoptosis facilitated by MMR, although probably not an obligatory role, and that the reduction of p53 phosphorylation in MMR-deficient cells results in the reduction of the post-UVB apoptotic response.

AT-related kinases ATM or ATR are responsible for phosphorylation of p53 on serine 15 in response to mainly IR and UV respectively (Tibbetts et al., 1999), thus a possible signaling pathway for MMR-mediated post-UVB apoptosis may involve activation of ATM or ATR followed by p53 or a yet unidentified effector. Although ATM has been found to physically interact with hMSH2 and hMSH6 (Wang et al., 2000), no such association between ATR and MMR have yet been identified.

Having established that MMR plays a role in the apoptotic response to UV radiation, an important direction to pursue with experimentation was a possible role for MMR in UVB-induced tumorigenesis. Comparison of the rate of skin tumorigenesis in wild-type and Msh2-deficient mice treated with chronic doses of

UVB indicated that Msh2-deficiency significantly accelerated UV-induced tumorigenesis (Figure 25). Indeed, this result agrees with previously discussed reports of increased propensity of Msh2-deficient mice to skin tumorigenesis; this propensity increased further on a background of NER-deficiency, indicating that the role of Msh2 in the cellular response to UVB is unrelated to DNA repair, and that its role in apoptosis may be involved (Meira et al., 2002; Meira et al., 2001; Yoshino et al., 2002). Furthermore, the Msh2-deficient mice used in these studies are a different strain background than the mice in my study, emphasizing the consistency of the effect of Msh2 in post-UVB cellular responses. Therefore, the role of Msh2 in UV-induced apoptosis identified *in vitro* is indeed relevant *in vivo* in skin tumorigenesis, indicating a possible relationship to NMSC and application to diagnosis and management of skin cancer.

In summary, Msh2-deficiency debilitates the cellular response to UVB radiation conferring increased survival due to a reduction in apoptosis and diminished activation of p53. Msh2 may therefore play an important role in mediating the apoptotic response to DNA damage induced by UV light, an environmental carcinogen of increasing global concern, suggesting that Msh2 may play an important role in preventing UV-induced skin cancer without being directly involved in repair. This evidence, compounded with the role of MMR in apoptosis in response to other DNA adducts, supports the proposed role for MMR as a versatile DNA damage sensor and multi-dimensional tumor suppressor. Furthermore, the impending elucidation of mechanisms by which MMR communicates the presence of DNA damage to effectors of signal transmission

promises monumental insight into the importance of the MMR system in tumor suppression and benefits to the prevention and treatment of skin cancer.

Future Directions

As is the case with many scientific studies, while the results of the experiments performed in this study provided possible answers to questions posed as a hypothesis, many more questions become pertinent as a result. The following are ideas for future experiments to follow up on the results obtained in this study:

1. Perform the same experiments in *Msh2*$^{+/+}$ and *Msh2*$^{-/-}$ keratinocytes to determine whether mismatch repair plays a role in the apoptotic response of the more physiologically relevant keratinocytes to UVB.

2. Determine whether other components of the MMR machinery, such as Mlh1 and Pms2, are involved in the post-UVB cellular response.

3. Compare the cell cycle responses of wild-type and Msh2-deficient cells post-UVB.

   i. Do the cell cycle results correlate to the diminished p21 induction in Msh2-deficient primary MEFs and the unexpected grossly increased induction in Msh2-deficient transformed MEFs?

   ii. Does MMR facilitate both cell cycle arrest and apoptosis, thereby functioning as a damage sensor that determines the type of cellular response to DNA damage?

4. Genetically abrogate the function of p53 to firmly determine the role of p53 in UVB-induced apoptosis and the interaction of p53 and Msh2 in the post-UVB apoptotic pathway.

5. Compare the induction of sunburn cells *in vivo* in the epidermis of wild-type and Msh2-deficient mice given acute doses of UVB in order to follow up the UV-induced tumorigenesis study by asking whether the increased rate of skin tumorigenesis in the absence of Msh2 is due to the abrogation of the apoptotic response.

6. Inhibit other pathways of UVB-induced apoptosis, in particular that induced by CD95 or ROS, to determine whether MMR-mediated apoptosis in response to DNA photoproducts is the only apoptotic pathway induced by DNA photoproducts. In so doing, one could determine whether the decreased apoptotic response in MMR-deficient cells represented a complete abrogation of the pathways activated by DNA photoproducts.

7. Analyze skin tumours, both mouse and human, for MSI and MMR activity, as well as secondary mutations possibly precipitated from a deficiency in MMR, in order to help delineate the mechanism or signaling pathway by which MMR facilitates UVB-induced apoptosis.

8. Investigate the effect of MMR-deficiency on other molecules that may be involved in UVB-induced apoptosis in order to understand the mechanism or signaling pathway involved.

i. Use specific kinase inhibitors for ATM and ATR to determine whether they are involved in MMR-facilitated apoptosis post-UVB.

ii. p73, or other members of its protein family, which is known to be involved in MMR-mediated apoptosis in response to cisplatin.

iii. Kinases that activate MMR in response to other forms of DNA damage, such as PKC.

9. Investigate how the molecules involved in NER that are also known to collaborate with p53 in the activation of apoptosis in response to UVB (XPB and XPD) are affected by MMR-deficiency.

References

(2001). National Cancer Institute of Canada: Canadian Cancer Statistics 2001 (Toronto, Canada).

Adimoolam, S., Lin, C. X., and Ford, J. M. (2001). The p53-Regulated Cyclin-Dependent Kinase Inhibitor, p21 (cip1, waf1, sdi1), is not required for Global Genomic and Transcription-Coupled Nucleotide Excision Repair of UV-Induced DNA Photoproducts. J Biol Chem.

Ali, S. H., and DeCaprio, J. A. (2001). Cellular transformation by SV40 large T antigen: interaction with host proteins. Semin Cancer Biol *11*, 15-23.

Andrew, S. E., Reitmair, A. H., Fox, J., Hsiao, L., Francis, A., McKinnon, M., Mak, T. W., and Jirik, F. R. (1997). Base transitions dominate the mutational spectrum of a transgenic reporter gene in MSH2 deficient mice. Oncogene *15*, 123-129.

Appella, E., and Anderson, C. W. (2001). Post-translational modifications and activation of p53 by genotoxic stresses. Eur J Biochem *268*, 2764-2772.

Ashcroft, M., and Vousden, K. H. (1999). Regulation of p53 stability. Oncogene *18*, 7637-7643.

Bellacosa, A. (2001). Functional interactions and signaling properties of mammalian DNA mismatch repair proteins. Cell Death Differ *8*, 1076-1092.

Bernerd, F., Asselineau, D., Vioux, C., Chevallier-Lagente, P., Bouadjar, B., Sarasin, A., Magnaldo, T. (2001). Clues to epidermal cancer proneness revealed by reconstruction of DNA repair-deficient xeroderma pigmentosum skin in vitro. Proc Natl Acad Sci USA *98*, 7817-7822.

Bernstein, C., Bernstein, H., Payne, C. M., and Garewal, H. (2002). DNA repair/pro-apoptotic dual-role proteins in five major DNA repair pathways: fail-safe protection against carcinogenesis. Mutat Res *511*, 145-178.

Berry, S. E., Davis, T. W., Schupp, J. E., Hwang, H. S., de Wind, N., and Kinsella, T. J. (2000). Selective radiosensitization of drug-resistant MutS homologue-2 (MSH2) mismatch repair-deficient cells by halogenated thymidine (dThd) analogues: Msh2 mediates dThd analogue DNA levels and the differential cytotoxicity and cell cycle effects of the dThd analogues and 6-thioguanine. Cancer Res *60*, 5773-5780.

Bertrand, P., Tishkoff, D. X., Filosi, N., Dasgupta, R., and Kolodner, R. D. (1998). Physical interaction between components of DNA mismatch repair and nucleotide excision repair. Proc Natl Acad Sci USA *95*, 14278-14283.

Bocker, T., Ruschoff, J., and Fishel, R. (1999). Molecular diagnostics of cancer predisposition: hereditary non-polyposis colorectal carcinoma and mismatch repair defects. Biochim Biophys Acta *1423*, O1-O10.

Bowman, K. K., Sicard, D. M., Ford, J. M., and Hanawalt, P. C. (2000). Reduced global genomic repair of ultraviolet light-induced cyclobutane pyrimidine dimers in simian virus 40-transformed human cells. Mol Carcinog *29*, 17-24.

Brash, D. E., Wikonkal, N. M., Remenyik, E., van der Horst, G. T., Friedberg, E. C., Cheo, D. L., van Steeg, H., Westerman, A., and van Kranen, H. J. (2001). The DNA damage signal for Mdm2 regulation, Trp53 induction, and sunburn cell formation in vivo originates from actively transcribed genes. J Invest Dermatol *117*, 1234-1240.

Buermeyer, A. B., Deschenes, S. M., Baker, S. M., and Liskay, R. M. (1999). Mammalian DNA mismatch repair. Annu Rev Genet *33*, 533-564.

Chao, C., Saito, S., Kang, J., Anderson, C. W., Appella, E., and Xu, Y. (2000). p53 transcriptional activity is essential for p53-dependent apoptosis following DNA damage. Embo J *19*, 4967-4975.

Christmann, M., and Kaina, B. (2000). Nuclear translocation of mismatch repair proteins MSH2 and MSH6 as a response of cells to alkylating agents. J Biol Chem *275*, 36256-36262.

Christmann, M., Tomicic, M. T., and Kaina, B. (2002). Phosphorylation of mismatch repair proteins MSH2 and MSH6 affecting MutSalpha mismatch-binding activity. Nucleic Acids Res *30*, 1959-1966.

Cole, S. L., and Tevethia, M. J. (2002). Simian Virus 40 Large T Antigen and Two Independent T-Antigen Segments Sensitize Cells to Apoptosis following Genotoxic Damage. J Virol *76*, 8420-8432.

D'Atri, S., Tentori, L., Lacal, P. M., Graziani, G., Pagani, E., Benincasa, E., Zambruno, G., Bonmassar, E., and Jiricny, J. (1998). Involvement of the mismatch repair system in temozolomide-induced apoptosis. Mol Pharmacol *54*, 334-341.

Davis, T. W., Wilson-Van Patten, C., Meyers, M., Kunugi, K. A., Cuthill, S., Reznikoff, C., Garces, C., Boland, C. R., Kinsella, T. J., Fishel, R., and Boothman, D. A. (1998). Defective expression of the DNA mismatch repair protein, MLH1, alters G2-M cell cycle checkpoint arrest following ionizing radiation. Cancer Res *58*, 767-778.

de Boer, J., and Hoeijmakers, J. H. (2000). Nucleotide excision repair and human syndromes. Carcinogenesis *21*, 453-460.

de Wind, N., Dekker, M., Berns, A., Radman, M., and te, R. H. (1995). Inactivation of the mouse Msh2 gene results in mismatch repair deficiency, methylation tolerance, hyperrecombination, and predisposition to cancer. Cell *82*, 321-330.

de Wind, N., Dekker, M., Claij, N., Jansen, L., van Klink, Y., Radman, M., Riggins, G., van, d., V, van't Wout, K., and te, R. H. (1999). HNPCC-like cancer predisposition in mice through simultaneous loss of Msh3 and Msh6 mismatch-repair protein functions. Nat Genet *23*, 359-362.

DeWeese, T. L., Shipman, J. M., Larrier, N. A., Buckley, N. M., Kidd, L. R., Groopman, J. D., Cutler, R. G., te, R. H., and Nelson, W. G. (1998). Mouse embryonic stem cells carrying one or two defective Msh2 alleles respond abnormally to oxidative stress inflicted by low-level radiation. Proc Natl Acad Sci USA *95*, 11915-11920.

Duc, R., and Leong-Morgenthaler, P. M. (2001). Heterocyclic amine induced apoptotic response in the human lymphoblastoid cell line TK6 is linked to mismatch repair status. Mutat Res *486*, 155-164.

Duckett, D. R., Bronstein, S. M., Taya, Y., and Modrich, P. (1999). hMutSalpha- and hMutLalpha-dependent phosphorylation of p53 in response to DNA methylator damage. Proc Natl Acad Sci USA *96*, 12384-12388.

Duckett, D. R., Drummond, J. T., Murchie, A. I., Reardon, J. T., Sancar, A., Lilley, D. M., and Modrich, P. (1996). Human MutSalpha recognizes damaged DNA base pairs containing O6-methylguanine, O4-methylthymine, or the cisplatin-d(GpG) adduct. Proc Natl Acad Sci U S A *93*, 6443-6447.

Fink, D., Aebi, S., and Howell, S. B. (1998). The Role of DNA Mismatch Repair in Drug Resistance. Clinical Cancer Research *4*, 1-6.

Fink, D., Nebel, S., Aebi, S., Zheng, H., Cenni, B., Nehme, A., Christen, R. D., and Howell, S. B. (1996). The role of DNA mismatch repair in platinum drug resistance. Cancer Res *56*, 4881-4886.

Friedberg, E. C. (2001). How nucleotide excision repair protects against cancer. Nature Rev Cancer *1*, 22-33.

Friedman, H. S., Johnson, S. P., Dong, Q., Schold, S. C., Rasheed, B. K., Bigner, S. H., Ali-Osman, F., Dolan, E., Colvin, O. M., Houghton, P., *et al.* (1997). Methylator resistance mediated by mismatch repair deficiency in a glioblastoma multiforme xenograft. Cancer Res *57*, 2933-2936.

Fritzell, J. A., Narayanan, L., Baker, S. M., Bronner, C. E., Andrew, S. E., Prolla, T. A., Bradley, A., Jirik, F. R., Liskay, R. M., and Glazer, P. M. (1997). Role of DNA mismatch repair in the cytotoxicity of ionizing radiation. Cancer Res *57*, 5143-5147.

Frouin, I., Prosperi, E., Denegri, M., Negri, C., Donzelli, M., Rossi, L., Riva, F., Stefanini, M., and Scovassi, A. I. (2001). Different effects of methotrexate on DNA mismatch repair proficient and deficient cells. Eur J Cancer *37*, 1173-1180.

Gartner, L. P., Hiatt, James L., and Hiatt, J. L. (2001). Color Textbook of Histology, 2nd edn (Philadelphia, Pennsylvania, W.B. Saunders Company).

Gobé, G. a. H., Brian (2000). Apoptosis: Morphological Criteria and Other Assays. In: Encyclopedia of Life Sciences. (London, Nature Publishing Group. http://www.els.net/).

Gong, J. G., Costanzo, A., Yang, H. Q., Melino, G., Kaelin, W. G., Jr., Levrero, M., and Wang, J. Y. (1999). The tyrosine kinase c-Abl regulates p73 in apoptotic response to cisplatin-induced DNA damage. Nature *399*, 806-809.

Hardman, R. A., Afshari, C. A., and Barrett, J. C. (2001). Involvement of mammalian MLH1 in the apoptotic response to peroxide- induced oxidative stress. Cancer Res *61*, 1392-1397.

Hawn, M. T., Umar, A., Carethers, J. M., Marra, G., Kunkel, T. A., Boland, C. R., and Koi, M. (1995). Evidence for a connection between the mismatch repair system and the G2 cell cycle checkpoint. Cancer Res *55*, 3721-3725.

Hengartner, M. O. (2000). The biochemistry of apoptosis. Nature *407*, 770-776.

Hickman, M. J., and Samson, L. D. (1999). Role of DNA mismatch repair and p53 in signaling induction of apoptosis by alkylating agents. Proc Natl Acad Sci USA *96*, 10764-10769.

Humbert, O., Hermine, T., Hernandez, H., Bouget, T., Selves, J., Laurent, G., Salles, B., and Lautier, D. (2002). Implication of protein kinase C in the regulation of DNA mismatch repair protein expression and function. J Biol Chem *277*, 18061-18068.

Jacob, S., Aguado, M., Fallik, D., and Praz, F. (2001). The role of the DNA mismatch repair system in the cytotoxicity of the topoisomerase inhibitors camptothecin and etoposide to human colorectal cancer cells. Cancer Res *61*, 6555-6562.

Janus, F., Albrechtsen, N., Dornreiter, I., Wiesmuller, L., Grosse, F., and Deppert, W. (1999). The dual role model for p53 in maintaining genomic integrity. Cell Mol Life Sci *55*, 12-27.

Jiricny, J. (1998). Replication errors: cha(lle)nging the genome. EMBO J *17*, 6427-6436.

Johnson, K. A., Mierzwa, M. L., Fink, S. P., and Marnett, L. J. (1999). MutS recognition of exocyclic DNA adducts that are endogenous products of lipid oxidation. J Biol Chem *274*, 27112-27118.

Jost, M., Gasparro, F. P., Jensen, P. J., and Rodeck, U. (2001). Keratinocyte apoptosis induced by ultraviolet B radiation and CD95 ligation -- differential protection through epidermal growth factor receptor activation and Bcl-x(L) expression. J Invest Dermatol *116*, 860-866.

Kat, A., Thilly, W. G., Fang, W. H., Longley, M. J., Li, G. M., and Modrich, P. (1993). An alkylation-tolerant, mutator human cell line is deficient in strand-specific mismatch repair. Proc Natl Acad Sci U S A *90*, 6424-6428.

Kawate, H., Sakumi, K., Tsuzuki, T., Nakatsuru, Y., Ishikawa, T., Takahashi, S., Takano, H., Noda, T., and Sekiguchi, M. (1998). Separation of killing and tumorigenic effects of an alkylating agent in mice defective in two of the DNA repair genes. Proc Natl Acad Sci USA *95*, 5116-5120.

Koi, M., Umar, A., Chauhan, D. P., Cherian, S. P., Carethers, J. M., Kunkel, T. A., and Boland, C. R. (1994). Human chromosome 3 corrects mismatch repair deficiency and microsatellite instability and reduces N-methyl-N'-nitro-N-nitrosoguanidine tolerance in colon tumor cells with homozygous hMLH1 mutation. Cancer Res *54*, 4308-4312.

Kulms, D., Poppelmann, B., Yarosh, D., Luger, T. A., Krutmann, J., and Schwarz, T. (1999). Nuclear and cell membrane effects contribute independently to the induction of apoptosis in human cells exposed to UVB radiation. Proc Natl Acad Sci U S A *96*, 7974-7979.

Kulms, D., and Schwarz, T. (2002a). Independent contribution of three different pathways to ultraviolet-B-induced apoptosis. Biochem Pharmacol *64*, 837-841.

Kulms, D., and Schwarz, T. (2002b). Mechanisms of UV-induced signal transduction. J Dermatol *29*, 189-196.

Kulms, D., Zeise, E., Poppelmann, B., and Schwarz, T. (2002). DNA damage, death receptor activation and reactive oxygen species contribute to ultraviolet radiation-induced apoptosis in an essential and independent way. Oncogene *21*, 5844-5851.

Kuluncsics, Z., Perdiz, D., Brulay, E., Muel, B., and Sage, E. (1999). Wavelength dependence of ultraviolet-induced DNA damage distribution: involvement of direct or indirect mechanisms and possible artefacts. J Photochem Photobiol B *49*, 71-80.

Lage, H., and Dietel, M. (1999). Involvement of the DNA mismatch repair system in antineoplastic drug resistance. J Cancer Res Clin Oncol *125*, 156-165.

Lan, Z., Sever-Chroneos, Z., Strobeck, M. W., Park, C. H., Baskaran, R., Edelmann, W., Leone, G., and Knudsen, E. S. (2002). DNA damage invokes mismatch repair-dependent cyclin D1 attenuation and retinoblastoma signaling pathways to inhibit CDK2. J Biol Chem *277*, 8372-8381.

Latonen, L., Taya, Y., and Laiho, M. (2001). UV-radiation induces dose-dependent regulation of p53 response and modulates p53-HDM2 interaction in human fibroblasts. Oncogene *20*, 6784-6793.

Leadon, S. A., and Avrutskaya, A. V. (1997). Differential involvement of the human mismatch repair proteins, hMLH1 and hMSH2, in transcription-coupled repair. Cancer Res *57*, 3784-3791.

Li, G., and Ho, V. C. (1998). p53-dependent DNA repair and apoptosis respond differently to high- and low-dose ultraviolet radiation. Br J Dermatol *139*, 3-10.

Li, G., Mitchell, D. L., Ho, V. C., Reed, J. C., and Tron, V. A. (1996a). Decreased DNA repair but normal apoptosis in ultraviolet-irradiated skin of p53-transgenic mice. Am J Pathol *148*, 1113-1123.

Li, G., Tron, V., and Ho, V. (1998). Induction of squamous cell carcinoma in p53-deficient mice after ultraviolet irradiation. J Invest Dermatol *110*, 72-75.

Li, G. M. (1999). The role of mismatch repair in DNA damage-induced apoptosis. Oncol Res *11*, 393-400.

Li, G. M., Wang, H., and Romano, L. J. (1996b). Human MutSalpha specifically binds to DNA containing aminofluorene and acetylaminofluorene adducts. J Biol Chem *271*, 24084-24088.

Liang, S. B., Furihata, M., Takeuchi, T., Sonobe, H., and Ohtsuki, Y. (2001). Reduced human mismatch repair protein expression in the development of precancerous skin lesions to squamous cell carcinoma. Virchows Arch *439*, 622-627.

Lu, Y. P., Lou, Y. R., Yen, P., Mitchell, D., Huang, M. T., and Conney, A. H. (1999). Time course for early adaptive responses to ultraviolet B light in the epidermis of SKH-1 mice. Cancer Res *59*, 4591-4602.

Maeda, T., Chua, P. P., Chong, M. T., Sim, A. B., Nikaido, O., and Tron, V. A. (2001). Nucleotide excision repair genes are upregulated by low-dose artificial ultraviolet B: evidence of a photoprotective SOS response? J Invest Dermatol *117*, 1490-1497.

Marti, T. M., Kunz, C., and Fleck, O. (2002). DNA mismatch repair and mutation avoidance pathways. J Cell Physiol *191*, 28-41.

Mazurek, A., Berardini, M., and Fishel, R. (2002). Activation of human MutS homologs by 8-oxo-guanine DNA damage. J Biol Chem *277*, 8260-8266.

McCarthy, S. A., Symonds, H. S., and Van Dyke, T. (1994). Regulation of apoptosis in transgenic mice by simian virus 40 T antigen-mediated inactivation of p53. Proc Natl Acad Sci USA *91*, 3979-3983.

McKay, B. C., Becerril, C., and Ljungman, M. (2001). P53 plays a protective role against UV- and cisplatin-induced apoptosis in transcription-coupled repair proficient fibroblasts. Oncogene *20*, 6805-6808.

McKay, B. C., and Ljungman, M. (1999). Role for p53 in the recovery of transcription and protection against apoptosis induced by ultraviolet light. Neoplasia *1*, 276-284.

Meira, L. B., Cheo, D. L., Reis, A. M., Claij, N., Burns, D. K., Riele, H., and Friedberg, E. C. (2002). Mice defective in the mismatch repair gene Msh2 show increased predisposition to UVB radiation-induced skin cancer. DNA Repair (Amst) *1*, 929-934.

Meira, L. B., Reis, A. M., Cheo, D. L., Nahari, D., Burns, D. K., and Friedberg, E. C. (2001). Cancer predisposition in mutant mice defective in multiple genetic pathways: uncovering important genetic interactions. Mutat Res *477*, 51-58.

Mekeel, K. L., Tang, W., Kachnic, L. A., Luo, C. M., DeFrank, J. S., and Powell, S. N. (1997). Inactivation of p53 results in high rates of homologous recombination. Oncogene *14*, 1847-1857.

Mellon, I., and Champe, G. N. (1996). Products of DNA mismatch repair genes mutS and mutL are required for transcription-coupled nucleotide-excision repair of the lactose operon in Escherichia coli. Proc Natl Acad Sci USA *93*, 1292-1297.

Mellon, I., Rajpal, D. K., Koi, M., Boland, C. R., and Champe, G. N. (1996). Transcription-coupled repair deficiency and mutations in human mismatch repair genes. Science *272*, 557-560.

Meyers, M., Wagner, M. W., Hwang, H. S., Kinsella, T. J., and Boothman, D. A. (2001). Role of the hMLH1 DNA mismatch repair protein in fluoropyrimidine-mediated cell death and cell cycle responses. Cancer Res *61*, 5193-5201.

Mietz, J. A., Unger, T., Huibregtse, J. M., and Howley, P. M. (1992). The transcriptional transactivation function of wild-type p53 is inhibited by SV40 large T-antigen and by HPV-16 E6 oncoprotein. Embo J *11*, 5013-5020.

Mu, D., Tursun, M., Duckett, D. R., Drummond, J. T., Modrich, P., and Sancar, A. (1997). Recognition and repair of compound DNA lesions (base damage and mismatch) by human mismatch repair and excision repair systems. MolCell Biol *17*, 760-769.

Murphy, G., Young, A. R., Wulf, H. C., Kulms, D., and Schwarz, T. (2001). The molecular determinants of sunburn cell formation. Exp Dermatol *10*, 155-160.

Myeroff, L. L., Parsons, R., Kim, S.-J., Hedrick, L., Cho, K.R., Orth, K., Mathis, M., Kinzler, K.W., Lutterbaugh, J., Park, K., Bang, Y.-J., Lee, H.Y., Park, J.-G., Lynch, H.T., Roberts, A.B., Vogelstein, B., Markowitz, S.D. (1995). A transforming growth factor type II gene mutation common in colon and gastric but rare in endometrial cancers. Cancer Res *55*, 5545-5547.

Nara, K., Nagashima, F., and Yasui, A. (2001). Highly elevated ultraviolet-induced mutation frequency in isolated Chinese hamster cell lines defective in nucleotide excision repair and mismatch repair proteins. Cancer Res *61*, 50-52.

Narayanan, L., Fritzell, J. A., Baker, S. M., Liskay, R. M., and Glazer, P. M. (1997). Elevated levels of mutation in multiple tissues of mice deficient in the DNA mismatch repair gene Pms2. Proc Natl Acad Sci USA *94*, 3122-3127.

Ni, T. T., Marsischky, G. T., and Kolodner, R. D. (1999). MSH2 and MSH6 are required for removal of adenine misincorporated opposite 8-oxo-guanine in S. cerevisiae. Mol Cell *4*, 439-444.

Ochs, K., and Kaina, B. (2000). Apoptosis induced by DNA damage O6-methylguanine is Bcl-2 and caspase- 9/3 regulated and Fas/caspase-8 independent. Cancer Res *60*, 5815-5824.

Oda, K., Arakawa, H., Tanaka, T., Matsuda, K., Tanikawa, C., Mori, T., Nishimori, H., Tamai, K., Tokino, T., Nakamura, Y., and Taya, Y. (2000). p53AIP1, a potential mediator of p53-dependent apoptosis, and its regulation by Ser-46-phosphorylated p53. Cell *102*, 849-862.

Otto, C., Almqvist, E, Hayden, MR, Andrew, SE (2001). The 'flap' endonuclease gene FEN1 is excluded as a candidate gene implicated in the CAG repeat expansion underlying Huntington disease. Clinical Genetics *59*, 122-127.

Pedeux, R., Lefort, K., Cuenin, C., Cortes, U., Kellner, K., Dore, J. F., and Nakazawa, H. (2002). Specific induction of gadd45 in human melanocytes and melanoma cells after UVB irradiation. Int J Cancer *98*, 811-816.

Peltomaki, P. (2001). DNA mismatch repair and cancer. Mutation Research *488*, 77-85.

Reitmair, A. H., Redston, M., Cai, J. C., Chuang, T. C., Bjerknes, M., Cheng, H., Hay, K., Gallinger, S., Bapat, B., and Mak, T. W. (1996). Spontaneous intestinal carcinomas and skin neoplasms in Msh2-deficient mice. Cancer Res *56*, 3842-3849.

Reitmair, A. H., Risley, R., Bristow, R. G., Wilson, T., Ganesh, A., Jang, A., Peacock, J., Benchimol, S., Hill, R. P., Mak, T. W., *et al.* (1997). Mutator phenotype in Msh2-deficient murine embryonic fibroblasts. Cancer Res *57*, 3765-3771.

Reitmair, A. H., Schmits, R., Ewel, A., Bapat, B., Redston, M., Mitri, A., Waterhouse, P., Mittrucker, H. W., Wakeham, A., Liu, B., and . (1995). MSH2 deficient mice are viable and susceptible to lymphoid tumours. Nat Genet *11*, 64-70.

Rich, T., Allen, R. L., and Wyllie, A. H. (2000). Defying death after DNA damage. Nature *407*, 777-783.

Rochette, P. J., Bastien, N., McKay, B. C., Therrien, J. P., Drobetsky, E. A., and Drouin, R. (2002). Human cells bearing homozygous mutations in the DNA

mismatch repair genes hMLH1 or hMSH2 are fully proficient in transcription-coupled nucleotide excision repair. Oncogene *21*, 5743-5752.

Roulston, A., Marcellus, R. C., and Branton, P. E. (1999). Viruses and apoptosis. Annu Rev Microbiol *53*, 577-628.

Scherer, S. J., Maier, S. M., Seifert, M., Hanselmann, R. G., Zang, K. D., MÅller-Hermelink, H. K., Angel, P., Welter, C., and Schartl, M. (2001). p53 and c-Jun functionally synergize in the regulation of the DNA repair gene hMSH2 in response to UV. J Biol Chem *275*, 37469-37473.

Segawa, K., Minowa, A., Sugasawa, K., Takano, T., and Hanaoka, F. (1993). Abrogation of p53-mediated transactivation by SV40 large T antigen. Oncogene *8*, 543-548.

Shen, Y., and White, E. (2001). p53-dependent apoptosis pathways. Adv Cancer Res *82*, 55-84.

Shin, C. Y., Mellon, I., and Turker, M. S. (2002). Multiple mutations are common at mouse Aprt in genotoxin-exposed mismatch repair deficient cells. Oncogene *21*, 1768-1776.

Sonneveld, E., Vrieling, H., Mullenders, L. H., and van Hoffen, A. (2001). Mouse mismatch repair gene Msh2 is not essential for transcription- coupled repair of UV-induced cyclobutane pyrimidine dimers. Oncogene *20*, 538-541.

Steel, G. G. (2001). The case against apoptosis. Acta Oncol *40*, 968-975.

Stratton, S. P., Dorr, R. T., and Alberts, D. S. (2000). The state-of-the-art in chemoprevention of skin cancer. Eur J Cancer *36*, 1292-1297.

Swann, P. F., Waters, T. R., Moulton, D. C., Xu, Y. Z., Zheng, Q., Edwards, M., and Mace, R. (1996). Role of postreplicative DNA mismatch repair in the cytotoxic action of thioguanine. Science *273*, 1109-1111.

Sweder, K. S., Verhage, R. A., Crowley, D. J., Crouse, G. F., Brouwer, J., and Hanawalt, P. C. (1996). Mismatch repair mutants in yeast are not defective in transcription- coupled DNA repair of UV-induced DNA damage. Genetics *143*, 1127-1135.

Szadkowski, M., and Jiricny, J. (2002). Identification and functional characterization of the promoter region of the human MSH6 gene. Genes Chromosomes Cancer *33*, 36-46.

Tanaka, K., Kamiuchi, S., Ren, Y., Yonemasu, R., Ichikawa, M., Murai, H., Yoshino, M., Takeuchi, S., Saijo, M., Nakatsu, Y., *et al.* (2001). UV-induced skin carcinogenesis in xeroderma pigmentosum group A (XPA) gene-knockout mice with nucleotide excision repair-deficiency. Mutat Res *477*, 31-40.

Therrien, J. P., Loignon, M., Drouin, R., and Drobetsky, E. A. (2001). Ablation of p21waf1cip1 expression enhances the capacity of p53- deficient human tumor cells to repair UVB-induced DNA damage. Cancer Res *61*, 3781-3786.

Tibbetts, R. S., Brumbaugh, K. M., Williams, J. M., Sarkaria, J. N., Cliby, W. A., Shieh, S. Y., Taya, Y., Prives, C., and Abraham, R. T. (1999). A role for ATR in the DNA damage-induced phosphorylation of p53. Genes Dev *13*, 152-157.

Toft, N. J., Winton, D. J., Kelly, J., Howard, L. A., Dekker, M., te, R. H., Arends, M. J., Wyllie, A. H., Margison, G. P., and Clarke, A. R. (1999). Msh2 status modulates both apoptosis and mutation frequency in the murine small intestine. Proc Natl Acad Sci USA *96*, 3911-3915.

Tominaga, Y., Tsuzuki, T., Shiraishi, A., Kawate, H., and Sekiguchi, M. (1997). Alkylation-induced apoptosis of embryonic stem cells in which the gene for DNA-repair, methyltransferase, had been disrupted by gene targeting. Carcinogenesis *18*, 889-896.

Tron, V. A., Trotter, M. J., Tang, L., Krajewska, M., Reed, J. C., Ho, V. C., and Li, G. (1998). p53-regulated apoptosis is differentiation dependent in ultraviolet B-irradiated mouse keratinocytes. Am J Pathol *153*, 579-585.

Unger, T., Sionov, R., Moallem, E., Yee, C., Howley, P., Oren, M., and Haupt, Y. (1999). Mutations in p53 serines 15 and 20 impair its apoptotic activity. Oncogene *18*, 3205-3212.

Wang, H., Lawrence, C. W., Li, G. M., and Hays, J. B. (1999). Specific binding of human MSH2.MSH6 mismatch-repair protein heterodimers to DNA incorporating thymine- or uracil-containing UV light photoproducts opposite mismatched bases. J Biol Chem *274*, 16894-16900.

Wang, Y., Cortez, D., Yazdi, P., Neff, N., Elledge, S. J., and Qin, J. (2000). BASC, a super complex of BRCA1-associated proteins involved in the recognition and repair of aberrant DNA structures. Genes Dev *14*, 927-939.

Warnick, C. T., Dabbas, B., Ford, C. D., and Strait, K. A. (2001). Identification of a p53 response element in the promoter region of the hMSH2 gene, required for expression in A2780 ovarian cancer cells. J Biol Chem *276*, 27363-27370.

Wikonkal, N. M., and Brash, D. E. (1999). Ultraviolet radiation induced signature mutations in photocarcinogenesis. J Investig Dermatol Symp Proc *4*, 6-10.

Wu, J., Gu, L., Wang, H., Geacintov, N. E., and Li, G. M. (1999). Mismatch repair processing of carcinogen-DNA adducts triggers apoptosis. Mol Cell Biol *19*, 8292-8301.

Wu, M., Ding, Han-Fei, Fisher, David, E (1999). Apoptosis: Molecular Mechanisms. In: Encyclopedia of Life Sciences (London, Nature Publishing Group. http://www.els.net/).

Yamada, M., O'Regan, E., Brown, R., and Karran, P. (1997). Selective recognition of a cisplatin-DNA adduct by human mismatch repair proteins. Nucleic Acids Res *25*, 491-496.

Yeh, C. C., Lee, C., Huang, M. C., and Dahiya, R. (2001). Loss of mismatch repair activity in simian virus 40 large T antigen-immortalized BPH-1 human prostatic epithelial cell line. Mol Carcinog *31*, 145-151.

Yoshino, M., Nakatsu, Y., Riele, H., Hirota, S., Kitamura, Y., and Tanaka, K. (2002). Additive roles of XPA and MSH2 genes in UVB-induced skin tumorigenesis in mice. DNA Repair (Amst) *1*, 935-940.

Young, L. C., Peters, A.C., Maeda, T., Edelmann, W., Kucherlapati, R., Tron, V.A., Andrew, S.E. (submitted). DNA mismatch repair protein Msh6 is required for optimal levels of UVB-induced apoptosis in primary mouse fibroblasts. J Invest Dermatol.

Zeng, M., Narayanan, L., Xu, X. S., Prolla, T. A., Liskay, R. M., and Glazer, P. M. (2000). Ionizing radiation-induced apoptosis via separate Pms2- and p53-dependent pathways. Cancer Res *60*, 4889-4893.

Zhang, H., Richards, B., Wilson, T., Lloyd, M., Cranston, A., Thorburn, A., Fishel, R., and Meuth, M. (1999). Apoptosis induced by overexpression of hMSH2 or hMLH1. Cancer Res *59*, 3021-3027.

Zhou, B. B., and Elledge, S. J. (2000). The DNA damage response: putting checkpoints in perspective. Nature *408*, 433-439.

Ziegler, A., Jonason, A. S., Leffell, D. J., Simon, J. A., Sharma, H. W., Kimmelman, J., Remington, L., Jacks, T., and Brash, D. E. (1994). Sunburn and p53 in the onset of skin cancer. Nature *372*, 773-776.